

**Investigation of Neutral Lipid Production in
Desmodesmus armatus and *Synechocystis* sp
PCC6803**

By

ADNAN ABDULAH HAMAD AL-MOUSAWI

BSc, in Biology, University of Basrah, Iraq, 2001

MSc, in Biotechnology, University of Baghdad, Iraq, 2004



**The
University
Of
Sheffield.**

**Thesis submitted in part fulfilment of the requirement
For the degree of Doctor of Philosophy**

**Department of Molecular Biology and Biotechnology
The University of Sheffield, UK**

September 2017

Declaration

I hereby declare that this thesis is my own work and effort. Where other sources of information have been used, they have been acknowledged.

Signed:

By Adnan Al-Mousawi

Dedication

To

My beloved country (IRAQ)

&

MY Father (Dr. ABDULLAH AL-MOUSAWI)

My Cousins: Naofal (Abo Sharar) & Mujtaba

(May Allah have mercy them)

Abstract

Microalgae has been introduced in the last decades to be an optimum source for biofuel production that can be utilised efficiently to replace the conventional fossil fuels as a source of energy. In our study, a local strain of green microalgae was isolated from the Weston Park pond (Sheffield, UK) and identified, using different molecular markers including 18S rDNA, ITS1, ITS2, and 5.8S rDNA, as *Desmodesmus armatus*. The neutral lipid content (as the basis of renewable biodiesel production) of both *D. armatus* and the model cyanobacterium *Synechocystis* sp. was measured using the lipophilic fluorescent dye Nile Red. The two strains were grown in normal BG11 medium and under stress conditions including high salinity (0.2, 0.4 M NaCl), different concentrations of sodium nitrate in the BG11 media (10% NaNO₃, N-free), and different sources of nitrogen (NH₄Cl, urea). The results showed that N-free BG11 medium was the best stress conditions in both strains for inducing a significant ($p < 0.05$) increase in neutral lipid content.

Further work concentrated on *D. armatus* and the Fatty Acid Methyl Esters (FAME) conversion yield was examined using a direct transesterification method and the composition of fatty acids was investigated using GC-MS. *Desmodesmus armatus* grown in N-free BG11 medium showed the highest yield and the contents of C16 and C18 fatty acids (useful for biodiesel production) increased significantly under this stress condition. Further analysis of *D. armatus* lipid content was conducted using ¹H NMR and the results confirmed that the fatty acid content is much higher in the N free grown cells.

The final set of experiments focused on random mutation of *D. armatus* cells using Ultra Violet light (254 nm) to generate new strains with high neutral lipid content. The high lipid containing cells were isolated using Nile Red staining and automated fluorescence assisted cell sorting (FACS) flow cytometry technique. A mutant strain was isolated with 5 times greater yield of neutral lipid than the wild type strain based on the median of the Nile Red fluorescence of the wild type and the mutant cells. This significant increase in the lipid yield using UV-induced random mutation, Nile Red staining and FACS has

paved the way for further investigation of the molecular and genetic approaches to identify the key genes that control neutral lipid biosynthesis in microalgae.

Acknowledgement

The supreme thanks belong to Allah, the Almighty, the creator, without his care I could not imagine who to finish my hard four years work.

I am massively grateful my gorgeous supervisor Dr. James Gilmour for his excessive support, infinite patience, calm resolve, and huge experience that help me to overcome all the obstacles that I have suffered during my project.

I would like to thank my sponsor The Higher Education Committee of Education development in Iraq -Iraqi Prime minister office (HCED) who has offered me an opportunity to finish my PhD in the United Kingdom and for their financial and emotional support for me during my project. Also, I would like to thank the Ministry of Higher Education and Scientific Research-Republic of Iraq, University of Basrah, College of Science-Department of Biology, who provide me all the official documents that help me to achieve the scholarship.

My great thank to the University of Sheffield, and the Department of Molecular Biology and Biotechnology, for their marvellous efforts to facilitate all the requirements that I require to finish my study.

I could not find an appropriate word to express my immensely grateful to my close friends Murtakab Al-Hejjaj, Ehssan Al-Bermayn, Naer AlKabbawi, Yasir Alabdali, and all my Iraqi colleagues in Sheffield for their support, help, and love that help me to continue my work.

A huge thanks to all my previous and current members of Gilmour's lab Richard Smith, Adel Almutairi, Abdullah AlTemaimi, Hatice Burak, Halima Alhani, Gloria Padmaperuma Tom Burns, and Fawzia for their scientific and emotional support during my study.

Also I would to thank staff members in the university of Sheffield which have helped me in many experiment, including Simon Thorpe (Chemistry) for GC-MASS assistance, Professor Mike Williamson for processing NMR samples, Flow cytometry group

(Medical school) for flow cytometry running. And my colleague Ibrahim Yaseen(MBB) for analysing the flow cytometry results.

Finally, I have a deep grateful and thank to my beloved wife, my children Reema, Abdulah, and Deema for their endless patience and emotional support and love that have offered to me during these four years. Also, I would like to thank my beloved mum, brother, sisters and my relatives especially my uncle Fakhir Al-Mousawi and his family for their hugely support, prayer, to help me finish this project.

Table of Contents

Abstract	III
Acknowledgement	V
List of Figures	X
List of Tables	XIII
Abbreviation	XIV
Chapter One Literature Review	15
1.1 Introduction	16
1.1.1 Global warming and fossil fuel	16
1.1.2 Renewable energy	18
1.1.3 Biofuels	20
1.1.4 Biodiesel	27
1.1.5 Microalgae.....	28
1.1.6 Microalgal Lipid	29
1.1.7 Algal lipid biosynthesis	30
1.1.8 Microalgal cultivation	32
1.1.9 Strategies to induce lipid synthesis in microalgae.....	36
1.2 Aims of the project	42
Chapter Two Materials and Methods	43
2.1 Cleaning and Sterile Techniques	44
2.2 BG11 Medium	44
2.2.1 Modified BG11 Media	45
2.3 Collection of Samples	46
2.4 Cell Density Evaluation	48
2.4.1 Spectrophotometer	48
2.4.2 Cell Counting and Growth Curve Determination.....	48
2.5 Microscopic Examination of the Pond Samples	49
2.6 Assessing Bacterial Contamination and Purification Methods	49
2.6.1 Percoll™ Treatment	50
2.6.2 Centrifuge Washing Technique (Purification of Algal Samples)	50
2.7 Molecular Identification of the Strains	51
2.7.1 Extraction of DNA	51
2.7.2 Gel Electrophoresis.....	54
2.7.3 Polymerase Chain Reaction amplification	54
2.7.4 PCR Purification	58
2.7.5 DNA Quantification	58
2.7.6 DNA Sequencing	59
2.7.7 Phylogenetic tree construction of pond water samples.....	59
2.8 Relationship between Cell count versus OD₅₉₅ nm for <i>Synechocystis</i> PCC6803 and <i>Desmodesmus armatus</i> cells	59
2.9 Lipid Extraction and Determination	60

2.9.1	Nile Red Fluorescence Microscopy.....	60
2.9.2	Neutral Lipid Quantification using Nile Red dye.....	61
2.10	Relationship between OD and Dry Weight.....	70
2.11	Nuclear Magnetic Resonance (NMR) determination of neutral lipid	71
2.12	Analysis and Quantification of Fatty Acid Composition	72
2.12.1	Transesterification of Algal Cells	72
2.13	Flow Cytometry Analysis of Neutral Lipid Content	77
2.13.1	Determination of DMSO Concentration	77
2.13.2	Optimising Nile Red Concentration	78
2.13.3	Flow Cytometry Analysis	79
2.14	Random Mutation of <i>D.armatus</i> Cells.....	79
2.14.1	UV Mutant Cells Sorting	80
2.14.2	Selection of Mutated Cells	81
2.14.3	Nile Red determination of the wild type and UV exposed <i>D.armatus</i> . neutral lipid	82
2.15	statistical analysis	82
Chapter Three Isolation and Identification of Pond Water Isolate and		
<i>Synechocystis</i> sp. PCC6803		
3.1	Introduction	84
3.2	Results	86
3.2.1	Growth of strains.....	86
3.2.2	Molecular Identification of <i>Synechocystis</i> sp. and pond water isolate	88
3.2.3	Phylogenetic tree construction	96
3.2.4	Growth curve of <i>Desmodesmus armatus</i> and <i>Synechocystis</i> PCC 6803	97
3.2.5	Relationship between cell count versus OD ₅₉₅	99
3.3	Discussion	100
3.3.1	Identification and characterisation of Pond Water Isolate <i>and Synechocystis</i> sp.	100
Chapter Four Determination and Quantification of Neutral Lipid.....		
4.1	Introduction	105
4.2	Results	109
4.2.1	Fluorescence microscopy for visualisation of lipid droplets.....	109
4.2.2	Determination of Neutral Lipid Using Nile Red	110
4.2.3	Effect of Salinity on the growth of <i>D. armatus</i> and <i>Synechocystis</i> cells	114
4.2.4	Effect of nitrogen depletion	116
4.2.5	Effect of Different Nitrogen Sources	118
4.2.6	Triolein calibration curve.....	120
4.2.7	Relation between OD and Cell Dry weight.	122
4.2.8	The lipid content of <i>D. armatus</i> and <i>Synechocystis</i> cells.....	123
4.2.9	Fatty Acid profile of N free BG11 stressed <i>D. armatus</i> cells.....	129
4.2.10	Determination of lipid content using NMR	130
4.3	Discussion	132
4.3.1	Influence of microwaves and solvents on investigation of neutral lipid	132
4.3.2	Influence of algal cell concentration and time of staining	133

4.3.3	Influence of Nile Red concentration.....	134
4.3.4	Influence of Salinity on the neutral lipid accumulation.....	135
4.3.5	Influence of nitrogen depletion.....	136
4.3.6	Influence of different nitrogen sources.....	137
4.3.7	Fatty acid profile of nitrogen starved <i>D. armatus</i> cells	138
4.3.8	¹ H-NMR determination of lipid content	139
Chapter Five Attempts to Enhance the Neutral Lipid Content of <i>Desmodesmus armatus</i>		
armatus		140
5.1	Introduction	141
5.2	Results	144
5.2.1	Determination of the influence of DMSO.....	144
5.2.2	Optimising the concentration of Nile Red	145
5.2.3	Random mutation of <i>D. armatus</i> cells using UV mutagens.....	147
5.2.4	Flow cytometry of UV irradiated <i>D. armatus</i> cells	148
5.2.5	Fluorescence activated cell sorting (FACS) of the UV irradiated <i>D. armatus</i> cells 149	
5.2.6	Screening of the mutated cells.....	150
5.2.7	Determination of the neutral lipid in Wild type and sorted UV exposed <i>D. armatus</i> 151	
5.3	Discussion	152
5.3.1	Flow cytometry for analysis of neutral lipid in <i>D. armatus</i> cells.....	152
5.3.2	Random mutation of <i>D. armatus</i> cells.....	153
5.3.3	Flow cytometry analysis of the UV mutated <i>D. armatus</i>	154
5.3.4	Fluorescence Activated cell sorting (FACS).....	154
5.3.5	Nile Red determination of wild type and UV mutated cells	155
Chapter Six Discussion, Conclusions, and Future Work		157
6.1	Discussion	158
6.2	Conclusions	162
References		164
APPENDIX.....		195
Appendix A.....		195
Appendix B.....		197
Appendix C.....		198
Appendix D		200
Appendix E		202

List of Figures

Figure 1.1 The CO ₂ level in the atmosphere from 1959-2016.....	17
Figure 1.2 The energy sources consumption in the USA in 2016.	17
Figure 1.3 Energy consumption by final sectors from 1965-2035	18
Figure 1.4 Energy consumption by region from 1965-2035	18
Figure 1.5 The top biofuel production countries in 2016.	21
Figure 1.6 The global production in million tonnes (based on regions) of gasoline biofuel between 2006-2016.	22
Figure 1.7 Mechanism of first generation biofuel production. (from https://elodiebrans.files.wordpress.com/2013/08/procesobiocombustibles.gif)	23
Figure 1.8 Schematic of biofuel (bioethanol) production from lignocellulosic biomass.	25
Figure 1.9 Schematic to illustrate fatty acid de novo synthesis of microalgal lipid.)	32
Figure 1.10 Schematic of various types of large scale algal cultivation systems	36
Figure 2.1 Western Park Pond where water samples were collected	47
Figure 2.2 <i>Synechocystis</i> PCC 6803 obtained from Prof Hunter Lab (Department of Molecular Biology and Biotechnology, University of Sheffield)	47
Figure 2.3 Bead bug microtube homogenizer for disruption of algal cells	53
Figure 2.4 96 well plate layout for the optimum concentration of algal cells	64
Figure 2.5 96 well plate layout of the optimum Nile Red concentration with optimum concentration of algal cells.....	67
Figure 2.6 96 well plate layout of different concentrations of triolein mixture for the calibration curve.	69
Figure 2.7 96 well plate layout of different concentrations of DMSO mixture for determination of the best concentration of DMSO that was used in the flow cytometry.....	78
Figure 2.8 High speed flow cytometry BD LSR II Flow cytometry	79
Figure 2.9 BD FACS Aria for sorting of mutant cells.....	81
Figure 3.1 Growth curve comparison of two <i>Synechocystis</i> PCC6803 strains.....	86
Figure 3.2 Extraction of DNA from <i>Synechocystis</i> sp. PCC6803 using CTAB protocol and run in a 1% Agarose gel	88
Figure 3.3 Extraction of DNA from <i>Synechocystis</i> PCC6803 using ZR Microbe Soil kit protocol and run in a 1% Agarose gel.....	89
Figure 3.4 Extraction of DNA from pond water isolate using ZR Microbe Soil kit protocol run in a 1% Agarose gel.	90
Figure 3.5 PCR amplification of <i>Synechocystis</i> PCC 6803 genomic DNA using 16S rRNA primers.....	91
Figure 3.6 PCR amplification of pond water isolate using 18S rRNA Lim & Sheehan primers..	92
Figure 3.7 PCR amplification of the pond water isolate strains using ITS1 primers.	94
Figure 3.8 PCR amplification of the pond water isolate using ITS2 and 5.8S rDNA primers..	95

Figure 3.9 Phylogenetic tree analysis of 18S and ITS region sequences of water pond sample using Maximum likelihood.....	96
Figure 3.10 Growth curve of <i>Desmodesmus armatus</i> cells grown over 26 days cultivation.....	97
Figure 3.11 Growth curve of <i>Synechocystis</i> PCC 6803 after 23 days cultivation.	98
Figure 3.12 Relationship between <i>D. armatus</i> OD ₅₉₅ and cell count	99
Figure 3.13 Relation between <i>Synechocystis</i> sp. OD ₅₉₅ and cell count.	99
Figure 4.1 Number of publications related to the utilisation of NR to evaluate the neutral lipids in different cells from 1995-till May 2016..	107
Figure 4.2 Number of publications related to the utilisation of NR to evaluate the neutral lipids in different cells from 1995-till May 2016..	109
Figure 4.3 Optimization of NR staining time and cell concentration on fluorescence intensity of the green alga <i>D. armatus</i>	110
Figure 4.4 Optimization of NR staining time and cell concentration on fluorescence intensity of the <i>Synechocystis</i> PCC 6803.....	111
Figure 4.5 Optimization of NR staining concentration for the green alga <i>D. armatus</i> cells.....	112
Figure 4.6 Optimization of NR staining concentration for the Cyanobacterium <i>Synechocystis</i> PCC6803 cells.	113
Figure 4.7 Nile Red Fluorescence Intensity measurements of <i>D. armatus</i> cells grown in BG11 media with: zero concentration of NaCl, 0.2 M and 0.4 M NaCl respectively.....	114
Figure 4.8 Nile Red fluorescent intensity measurement of <i>Synechocystis</i> cells grown in BG11 media with: zero concentration of NaCl, 0.2 M NaCl, and 0.4 M NaCl respectively.	115
Figure 4.9 The fluorescent Intensity of <i>D. armatus</i> cells grown under normal BG11, 25% NaNO ₃ , 10% NaNO ₃ and N Free BG11.....	116
Figure 4.10 The fluorescent Intensity of <i>Synechocystis</i> cells grown under Normal BG11, 10% NaNO ₃ , and N Free BG11. NaNO ₃ was used as a source of Nitrogen in the medium.).....	117
Figure 4.11 The fluorescent intensity of <i>D. armatus</i> cells grown under different N sources that are: 10% NaNO ₃ , NH ₄ Cl, and urea.	118
Figure 4.12 The fluorescence intensity of <i>Synechocystis</i> cells grown under different N sources that are: 10% NaNO ₃ , NH ₄ Cl, and urea.....	119
Figure 4.13 Linear correlation between fluorescence intensity and triolein concentration of <i>D armatus</i> cells	120
Figure 4.14 Linear correlation between fluorescence intensity and triolein concentration of <i>Synechocystis</i> cells to allow the conversion of fluorescence readings to triolein equivalents.....	121
Figure 4.15 Linear relation between OD and dry weight of <i>D. armatus</i> cells.....	122
Figure 4.16 Linear relation between OD and cell dry weight of <i>Synechocystis</i> cells	122
Figure 4.17 Fatty acid methyl ester profile of <i>D. armatus</i> cells grown under N Free BG11..	129
Figure 4.18 NMR spectra of <i>D. armatus</i> grown under normal BG11 and N Free BG11.....	130
Figure 5.1 Optimisation of DMSO concentration for use as a stain carrier.	144

Figure 5.2 Flow cytometry analysis of <i>D. armatus</i> cells unstained and stained with different concentrations of Nile Red.....	146
Figure 5.3 The growth of <i>D. armatus</i> cells exposed to UV mutagenesis for different lengths of time.	147
Figure 5.4 FACS analysis of 30 min UV mutated <i>D. armatus</i>.....	149

List of Tables

Table 2.1 Sequence of 16S rRNA , 18S, 5.8S, ITS1, and ITS2 rRNA Primers.....	55
Table 2.2 Contents of Tubes for PCR Amplification.....	56
Table 2.3 PCR Cycling using 16S rRNA Primers	57
Table 2.4 PCR Cycling using 18S rRNA primers	57
Table 2.5 PCR Cycling using ITS1,ITS2,5.8S rDNA primers	57
Table 2.6 Scheme of different algal concentrations for determining the relationship between OD ₅₉₅ and cell count.....	60
Table 2.7 Dilution scheme to produce a range of cell concentrations for Nile Red peak fluorescence test.	62
Table 2.8 Plate reader sitting for the optimum concentration of algal cells.	63
Table 2.9 Serial dilutions of algal cells for the determination of cell concentration for Nile Red experiment	64
Table 2.10 Nile Red concentrations prepared from the 1 mg ml ⁻¹ Nile Red stock.....	66
Table 2.11 Concentrations of triolein mixture for Nile Red fluorescence calibration curve.	68
Table 2.12 Concentrations of <i>D. armatus</i> cells for preparation of Dry weight versus OD.	70
Table 3.1 Significant alignment with initial 18S Forward sequence of Pond water strain.....	93
Table 4.1 Lipid content of <i>D. armatus</i> grown under normal and different salinity concentrations.	123
Table 4.2 Lipid content of <i>Synechocystis</i> PCC6803 grown under normal and different salinity concentrations.....	124
Table 4.3 Lipid content of <i>D. armatus</i> grown under different concentration of NaNO ₃	125
Table 4.4 Lipid content of <i>Synechocystis</i> grown under different concentration of NaNO ₃	126
Table 4.5 Lipid content of <i>D. armatus</i> grown with different Nitrogen sources.....	127
Table 4.6 Lipid content of <i>Synechocystis</i> PCC6803 grown under different Nitrogen sources.	128
Table 4.7 ¹ HNMR chemical shift (ppm) of functional group and values of <i>D. armatus</i> grown under normal medium (BG11) stress N Free BG11.	131
Table 5.1 Flow cytometry analysis of <i>D. armatus</i> cells stained with different concentration of Nile Red.	145
Table 5.2 Flow cytometry analysis of UV irradiated <i>D. armatus</i> cells for different time periods. Each value is the average of three replicates.....	148
Table 5.3 Flow cytometry analysis of neutral lipid content in both a single wild type cell (H5) and 12 single UV mutated sorted cells (A4 to H12).	150
Table 5.4 lipid content of both wild type (H5) and sorted UV mutated (H12) grown under normal and N free BG11 for 18 days.....	151

Abbreviation

ACCase	Acetyl CoA carboxylase
Acetyl CoA	Acetyl coenzyme A
DAG	Diacylglycerol
DEPC	Diethyl pyrocarbonate
DMSO	Dimethyl sulfoxide
EIA	Energy information administration
ER	Endoplasmic reticulum
EU	European Union
FACS	Florescence Activated Cell sorting
FAS	Farming Advisory System
FAT	Fatty acid thioesterase
FC	Flow Cytometry
FSC	Forward Scatter
GC-MASS	Gas Chromatography-Mass spectrophotometry
GHG	Green House Gases
H12	single cell UV exposed FACS sorted <i>D.armatus</i> strain
H5	Single cell wild type <i>D.armatus</i> strain
Malonyl CoA	Malonyl coenzyme A
MAT	Malonyl CoA transacylase
MEGA	Molecular Evolution Genetics Analysis
NMR	Nuclear Magnetic Resonance
NR	Nile Red dye
PBR	Photobioreactor
SCS	Side scatter
TAG	Triacylglycerol
UV	Ultra Violet

Chapter One Literature Review

1.1 Introduction

1.1.1 Global warming and fossil fuel

Throughout the world, humanity faces two crucial catastrophic challenges which are the energy crisis and environmental pollution in which the ongoing threat to life has reached a high risk level (Gupta and Tuohy, 2016). The main causes of these challenges are the continuous burning of coal, gas and diesel oil, which produce Green House Gases (GHG) leading to global warming that is approaching a tipping point (Hansen *et al.*, 2013). The concentration of carbon dioxide (CO₂) which is well known as the main anthropogenically emitted GHG has increased significantly from 316 ppm in 1959 to 404 ppm in late 2016 as shown in Figure 1.1 (Gupta and Tuohy, 2016). Human activities that involve combustion of fossil fuel, the absence of a strategy to make a balance between biofuel burning like wood and planting of new trees play a crucial role in the rapid raise in GHG. The serious concern of the continuous rise in the level of CO₂ in the environment is that it obstructs the passage of thermal infrared radiation from the surface of the earth back into the space and accordingly the temperature of the Earth will rise annually which is known as the global warming phenomenon (BP, 2014). Global warming has many drawbacks that impinge on many life sectors especially food security and malnutrition. Serious environmental changes are expected to result as a reaction to global warming like land degradation and alterations in the hydrological resources, crucial ecosystem services and agricultural yields become more problematic (Easterling *et al.*, 2007). The distribution of diseases like diarrhoea as a result of a shortage of potable water resources are the another potential drawbacks of climate change (Confalonieri *et al.*, 2007).

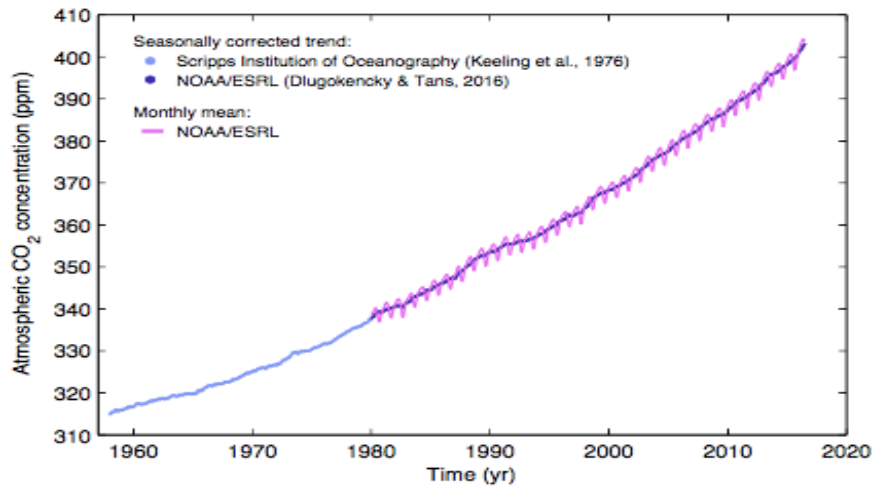


Figure 1.1 The CO₂ level in the atmosphere from 1959-2016. The figure shows clearly a dramatic enhancement in the CO₂ level because of anthropogenic activity (adapted from Gupta and Tuohy, 2016).

Based on the US Energy Information Administration (EIA) figures for 2016, more than 80% of energy in the USA derived from three types of fossil fuel: petroleum 37%, natural gas 29%, and coal 15% (Figure 1-2).

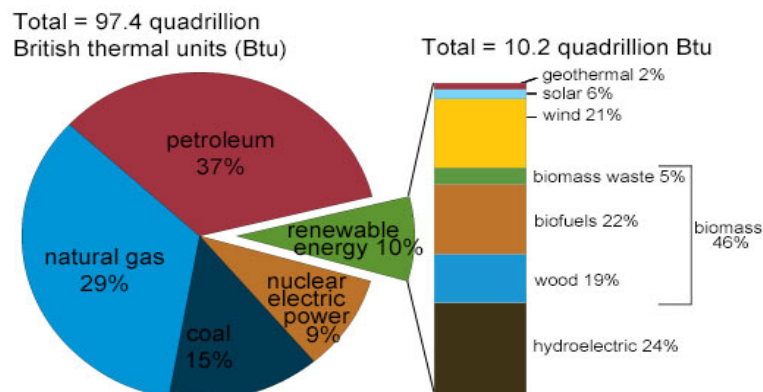


Figure 1.2 The energy sources consumption in the USA in 2016 (EIA, 2016).

The domination of GHG emitting fuels as sources of energy will continue and furthermore, GHG emitting fuels are expected to supply more than three-quarters of the total energy required in 2035. An increase in the population worldwide will

undeniably lead to enhanced demands for energy in different sectors like industry, buildings and transport (Figure 1.3).

In terms of world regions, the need for energy sources is developing and expected to rise in China and India which are considered among the speediest growing economies (Figure 1.4)(BP, 2017a).

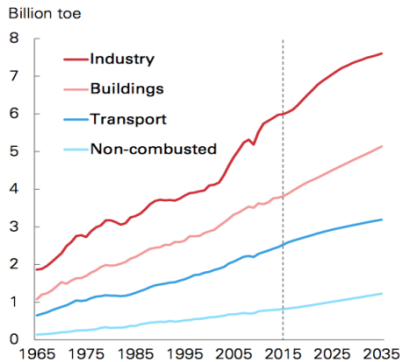


Figure 1.3 Energy consumption by final sectors from 1965-2035 (BP, 2017a)

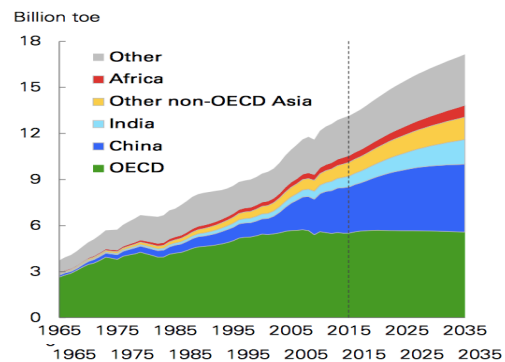


Figure 1.4 Energy consumption by region from 1965-2035 (BP, 2017a)

1.1.2 Renewable energy

In recent years, governments, scientists, and organisations worldwide are expressing growing concerns over challenges to explore a clean, sustainable, environmentally friendly, and renewable source of energy that can effectively mitigate the negative impacts of a total reliance on fossil fuel as a source of energy. In addition to the drawbacks of GHG emissions from conventional energy production, fossil fuel is a finite resource of energy and will be exhausted in the future and consequently cannot be trusted as a productive and economic energy sources for the future (Quintana *et al.*, 2011). To resolve this crucial problem, many countries around the world signed an agreement called the Kyoto Protocol in 1997, in which the industrialised countries agreed to decrease the GHG emissions by 5.2% compared to the 1990 standards. In 2015, 194 countries signed an agreement at the Paris conference on climate change to restrict the temperature globally to 2°C increase (Andresen, 2015). Moreover,

developed countries have attempted to behave cooperatively and prepared USD 100 billion per year by 2020 to fund researches in Renewable energy field in developing nations (OECD, 2016). The EU countries have two main targets to achieve by 2030, 1) reduce the local GHG emissions by 40%, and 2) an efficient increment of renewable sources of energy by about 27% (European Council, 2014).

Renewable energy is simply defined as a source of energy that can be formed from natural resources like solar energy, wind energy, biomass energy, geothermal energy and accordingly cannot be depleted (Rathore and Panwar, 2007). The improvement and efficient utilisation of renewable energy offers significant advantages across the world such as a rise in the renewable energy use that covers national needs and contributes to providing energy with small or zero percentage emissions that significantly mitigate air pollution, improves the standard of life and creates new job opportunities. It can also help with efforts of governments in fulfilling their international agreements that deal with environmental protection (Zakhidov, 2008). Furthermore, the plan to implement renewable resources in rural areas will open the way to resolve social and economic problems and minimize the migration towards urban regions (Bergmann *et al.*, 2008).

Among different renewable resources, (EIA, 2016) reported that biomass is currently considered to have the highest potential as an alternative fuel in comparison with other renewable sources (Figure 1.2) with 46% of total renewable energy being produced from biomass. Also, known as bioenergy, biomass is defined as a renewable source of energy that is generated from organic (biological) materials and not embedded in geological formations (fossilised). Biomass energy can be used either in its original form, or converted to different forms of solid, gaseous, or liquid biofuels. These fuels can be utilised efficiently in various sectors to provide electricity supply, transport, heating, cooling and in a variety of industrial processes.

1.1.3 Biofuels

Biofuels are renewable, environmentally friendly, carbon neutral, alternative sources of energy that are produced from biomass in solid, liquid and gaseous forms. Biofuel can be exploited effectively to address various problems like the need to reduce the environmental impacts of the GHG emissions produced from fossil fuel resources, a rapid enhancement of energy demands, an increment in the conventional fossil fuel prices, and the predicted depletion of the fuel resources (Wang *et al.*, 2011).

Generally, biofuel is divided into two main types: liquid biofuel and gaseous biofuel (biogas). Liquid biofuel is subdivided into biogasoline mainly as bioethanol that is derived from biomass fermentation (carbohydrates) or biomethanol which is derived from oxidation of waste biomass. Biodiesel is the other subdivision of biogasoline which is produced essentially from different types of lipid sources (fats). Biogas is the other type of biofuel that is produced from anaerobic fermentation of biomass sources. Both bioethanol and biodiesel are significantly exploited in the transport sector in which they can be mixed with the conventional fuel or used directly without blending by utilising specialised transport engines. Biogas is mainly used in cooking, heating, but it can also be used in natural gas vehicles (Demirbas, 2008; IEA, 2016).

The production of biofuel globally has increased dramatically from about 20 million tonnes in 2006 to more than 80 million tonnes in 2016. Based on the recent statistics (BP, 2017a) the major biofuel production countries are USA and Brazil which supply about 65% of total biofuel production worldwide. The USA produced 43%, followed by Brazil with 22% (Figure 1.5). Other biofuel producing countries are Germany 3.9%, Argentina 3.4%, Indonesia 3%, France 2.7% and China 2.5%.

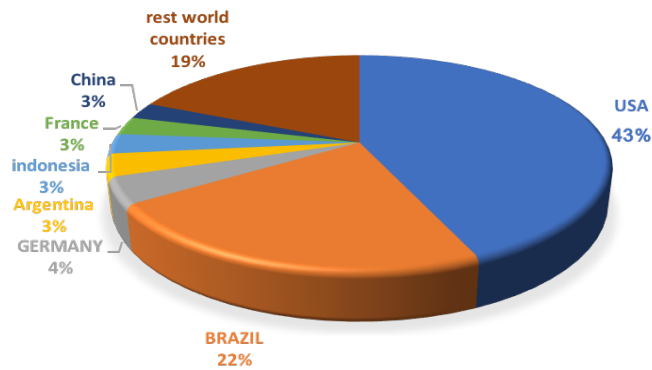


Figure 1.5 The top biofuel production countries in 2016, data adapted from (BP, 2017a).

The production of gasoline biofuel (ethanol and biodiesel) increased significantly over the last decade (BP, 2017b). Figure 1.6 shows clear increment in ethanol production in some areas in which USA (North America) and Brazil (South and Central America) produced the largest volumes of total global production based on utilising sugarcane and corn as a source for ethanol production. In contrast, the production of biodiesel increased quickly around the world especially in Europe and Asia with varied sources of biodiesel production. European countries mainly concentrated on waste, soy, rapeseed and palm as sources for biodiesel production. In contrast, Asian countries based their biofuel production on sugarcane, wheat, and Cassava to produce different types of biofuels. However, the USA produced the highest amount of biodiesel in 2016 with about 5 billion litres (Huenteler and Lee, 2015; Biofuels, 2016; BP, 2017b).

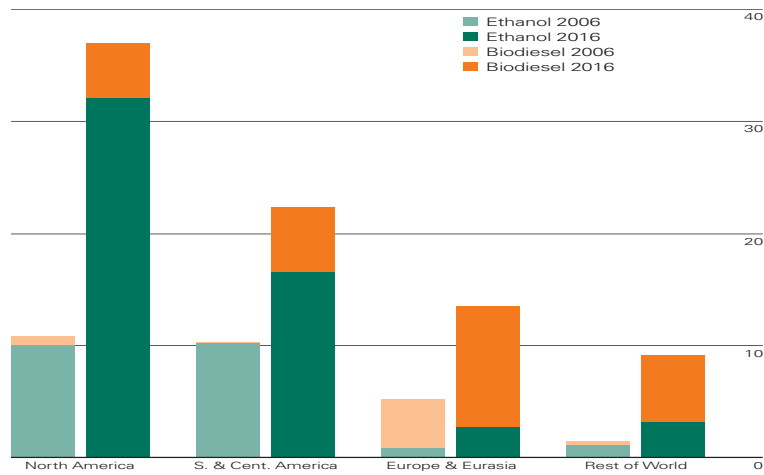


Figure 1.6 The global production in million tonnes (based on regions) of gasoline biofuel between 2006-2016 adapted from (BP, 2017b).

1.1.3.1 Biofuel generations

Various generations of biofuel have emerged based on several parameters (Araujo *et al.*, 2017) which are:

- A) feedstock
- B) technology process,
- C) final product,
- D) and the chemical composition.

1.1.3.1.1 First generation biofuels

The main sources for the production of first generation biofuels are food and food-based crops (Figure 1.7). Ethanol is the common type of biofuel produced essentially from the fermentation of a variety of sugar containing plants or grain crops like sugarcane (Brazil), corn (USA), sugar beet, wheat and potatoes (China and India) (OECD/IEA, 2008; Brower *et al.*, 2014). The conversion of sugar to ethanol requires many steps which start with the harvesting of the crops, followed by the extraction of sugar and dilution to 20%. Then yeast, mainly *Saccharomyces cerevisiae*, is added to convert sugar to ethanol, eventually dried (pure) ethanol is produced by two distillation

steps using other solvents like cyclohexane (Cheng and Timilsina, 2011). In comparison with conventional fossil fuel, bioethanol has distinct features which make it a favoured type of renewable energy that can be used directly or blended with other gasoline oil these include its high octane level and less energy content per volumetric unit, evaporation enthalpy, and faster flame (Balat, 2007).

For biodiesel, vegetable oils (soybean, palm, sunflower, and rapeseed) and animal fats are considered the common sources. The production of biodiesel is based mainly on the transesterification reaction of the oil or the fat with alcohol to generate fatty acid methyl esters (FAMES) which are the precursor for biodiesel which are used directly or blended with conventional oil (Demirbas and Demirbas, 2011).

Several advantages can be achieved from using biomass based biofuel as a source of energy. For example, it is produced worldwide, the production process is easy and without including high cost materials, and it can be stored for a long time period. However, there are some drawbacks of using terrestrial crops for biofuel production because these crops represent the main source of nutrition for some countries and consequently their alternative use has a dramatic effect on the food security by enhancing the cost of food, water shortages, and leading to deforestation (FAO, 2008; Scharlemann and Laurance, 2008).

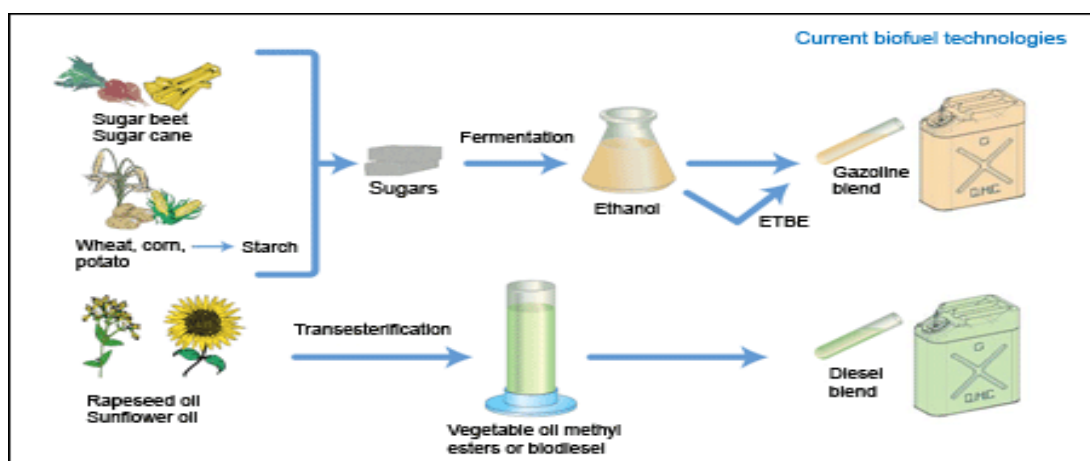


Figure 1.7 Mechanism of first generation biofuel production.

(<https://elodiebrans.files.wordpress.com/2013/08/procesobiocombustibles.gif>)

1.1.3.1.2 Second generation biofuels

Second-generation biofuels are mainly produced from non-edible lignocellulosic biomass whose use can overcome the drawbacks of using agricultural land as source for biofuel production (Murphy and Kendall, 2015). The biomass sources of second generation biofuels are differentiated into three main groups: homogeneous like white wood chips, quasihomogeneous like agricultural and forest residues, and non-homogenous which include lower cost feedstock such as community solid waste (Lavoie *et al.*, 2011). The products of lignocellulosic biomass are mainly generated through two conversion methods: biochemically to produce alcohol fuels like ethanol and butanol, and thermochemically to produce biodiesel.

The production of ethanol is conducted through several steps (Figures 1.8) : pretreatment, saccharification, fermentation and distillation. Pretreatment is the initial step that facilitates the delignification and separation of the three-main carbon based polymers of the lignocellulosic biomass that are cellulose, hemicellulose and lignin. Cellulose is the main constituent of cellulosic biomass and is composed of a crystalline lattice of long chains of glucose monomers. The crystalline feature of cellulose makes its glucose monomers hard to extract. Hemicellulose is a polymer consisting of a range of sugars (C5 and C6 sugars). While lignin is a complex mixed polymer cross linked together and very difficult to break down, (Dashtban *et al.*, 2009)

The main objectives of pretreatment step are to break down the complex lignocellulosic biomass, to induce formation of sugar directly or consequently by hydrolysis process, to inhibit the loss or degradation of the sugar produced, to reduce the foundation of the inhibitory yields, minimise the energy demands, and reduce the total cost of production (Sarkar *et al.*, 2012; Barakat *et al.*, 2014). Various approaches have been used for the pretreatment steps such as steam explosion, pyrolysis, ammonium fibre explosion (AFEX), and hydrogen peroxide-acetic Acid (HPAC) (Mosier *et al.*, 2005; Galbe and Zacchi, 2007; Wi *et al.*, 2015).

Saccharification is the term for the enzymatic hydrolysis used for the conversion of complex lignocellulosic biomass into simple sugars. Enzymatic hydrolysis has distinct features that make it preferable to acid or alkaline hydrolysis i.e. its lower toxicity and

minimum cost. Cellulose is converted by cellulase to glucose while hemicellulose is hydrolysed to several pentoses (C5) and hexoses (C6). Many species of bacteria and fungi produce cellulase enzymes, however, *Trichoderma* is the most powerful cellulase and hemicellulase producing fungal strain that produces a variety of cellobiohydrolases, endoglucanases and endoxylanases (Sandgren *et al.*, 2001; Jørgensen *et al.*, 2003). The main disadvantages of lignocellulose biomass are the absence of effective technologies that help the commercial conversion of the lignocellulosic and forest waste substrate into biofuel product (Tabatabaei *et al.*, 2011)

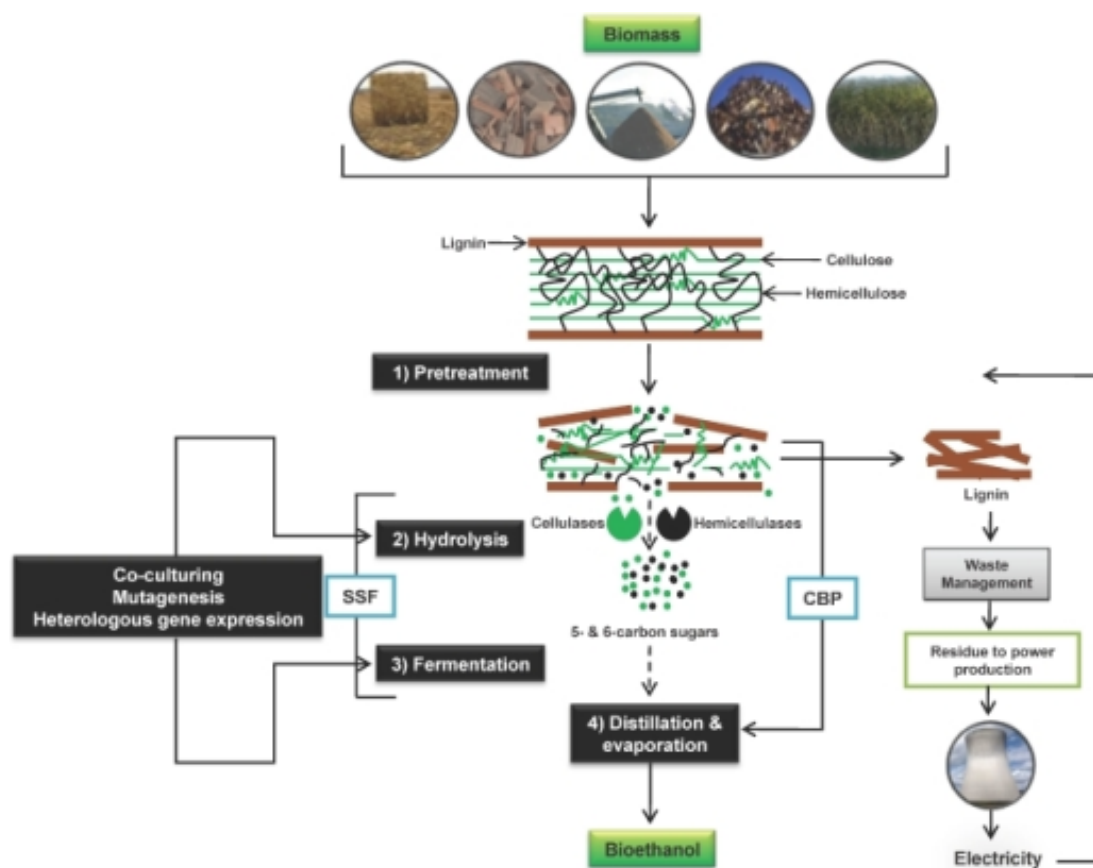


Figure 1.8 Schematic of biofuel (bioethanol) production from lignocellulosic biomass adapted from (Dashtban *et al.*, 2009). SSF = Saccharification and Fermentation, CBP = Consolidated Bioprocessing.

1.1.3.1.3 Third generation biofuels

Microalgae have achieved great attention as an attractive feedstock for renewable biofuel that can overcome the rapid depletion and the potentially catastrophic environmental impacts of fossil fuels as a source of energy (Halim and Webley, 2015). Microalgae have several distinct characteristics that make them a favourable candidate for the biofuel production in comparison to first and second generation biofuels. These characteristics include a rapid growth rate which enhances the biomass yield 10 to 20 times more than other biofuel crops and mitigates the period of time required to produce the biofuel, and the ability to accumulate large amounts of neutral lipids which is the main precursor for biodiesel production (Kocot and Santos, 2009; Rodolfi *et al.*, 2009). Microalgae can be cultivated in various environments like freshwater, wastewater, seawater and marginal lands which avoids the possibility of competing with arable lands used for agriculture purposes, also microalgae can have a positive impact on wastewater treatment through bioremediation processes (Chisti, 2007; Day *et al.*, 2012; Govender *et al.*, 2012).

Moreover, microalgae play a vital role to sequester carbon dioxide and consequently reduce its global warming influence (Wang *et al.*, 2008; Show *et al.*, 2017). One of the most important features of fuel produced by microalgae is that the atmospheric level of CO₂ is potentially decreased to about 78% because the fuel produced from microalgae will not cause an increase in this level (Brown and Zeiler, 1993). Furthermore, microalgae produce some useful bio-products after oil extraction that can be utilised as feed, fertiliser, or other commercial approaches such as proteins (Hirano *et al.*, 1997). Microalgae can produce either biodiesel from the synthesis of high level of lipids (Hu *et al.*, 2008; Harwood and Guschina, 2009), or bioethanol through fermentation of the abundant content of carbohydrates in microalgae. The valuable features of microalgal carbohydrates are that they are rich in sugar and starch, lack lignin and low hemicellulose content that consequently enhances the hydrolysis efficiently and fermentation products (Choi *et al.*, 2012; Li *et al.*, 2014). Microalgae produced biomethane by anaerobic digestion of wastewater derived microalgae (Ward *et al.*, 2014). Furthermore, some microalgal species can be utilised to produce biohydrogen via direct biophotolysis like green algae that include hydrogenase enzyme or by indirect

biophotolysis by utilising Cyanobacteria (blue green algae) species to release H₂ by nitrogen fixation (Eroglu and Melis, 2016)

1.1.4 Biodiesel

Biodiesel is chemically defined as the mono alkyl esters (methyl, propyl, ethyl) of long chain fatty acids originated from the transesterification of biomass sources of neutral lipid (Igbokwe and Nwaiwu, 2013). Transesterification is the common chemical reaction in which one mole of glyceride reacts with three moles of alcohol (mainly ethanol or methanol) to produce three moles of monoalkyl esters and one mole of glycerol that is separated from the ester layer either by decantation or centrifugation (Innocent *et al.*, 2013). Biodiesel can be derived from various renewable edible and nonedible feedstocks including animal fat, waste cooking oil, and plant oil. Biodiesel produced from these sources is nontoxic, highly biodegradable, carbon neutral, can be exploited directly or blended with diesel, and can be easily handled and stored for a long time (Daroch *et al.*, 2013). However, edible and non-edible feedstocks can be exploited commercially because an increase in the demand of fuel, low yield, and the requirement not to compete with the arable lands and freshwater necessary for food and water security. Therefore, carbon neutral biodiesel produced from microalgae is considered to be the optimum feedstock for biodiesel production. Microalgae as a feedstock is considered a promising source for biodiesel production (Gangadhar *et al.*, 2016). The physiochemical characteristics of highly purified biodiesel produced from microalgae are usually assessed through the profile of FAMES and need to be accordance with the values of EN 14214 or ASTM D6751 standards of Europe or USA. The most crucial features of biodiesel that should be evaluated are ester composition, cetane number (CN), density, viscosity, cold filter plugging (CFPP), free and total glycerol, higher heating value and lubricity (Levine *et al.*, 2014).

Various studies state that the properties of biodiesel produced from different microalgal species meet international standards and therefore provide a convenient and valuable source of engine fuel (Mohammad-ghasemnejadmaleki *et al.* 2014; Gangadhar *et al.*, 2016; Bharti *et al.*, 2017). With respect to the biodiesel feedstock, the

production of biodiesel has increased in European countries which represent the largest producer of biodiesel worldwide from about 11 million litres in 2011 to about 12.2 million litres. Germany, France and Spain are the main European countries for biodiesel production in which rapeseed, and palm oil are used as the main feedstocks for biodiesel production (FAS, 2016). The price of biodiesel mainly depends on the type of feedstock used, which represents about 60-70% of the total cost of biodiesel fuel (Canakci and Sanli, 2008).

1.1.5 Microalgae

Microalgae include both prokaryotic (cyanobacteria) and eukaryotic microorganisms that lack roots, stems, and leaves. They can grow rapidly in a variety aquatic and terrestrial environments. Microalgal species are found as unicellular, colonial, and filamentous forms (Lee, 2008). Their growth rate is rapid and varies according to the species with doubling times of 24 hours for green algae, 17 hours for cyanobacteria and 18 hours for other microalgal taxa. However, due to the large diversity of algal species and some can grow very quickly with doubling times of 7-8 hours (Griffiths and Harrison, 2009). They are photosynthetic microorganisms which produce approximately half of the atmospheric oxygen, they can be either autotrophic, heterotrophic, or mixotrophic. If microalgae are autotrophic, they exploit inorganic compound as their sole carbon source. Autotrophic microalgae can be either photoautotrophic in which light is the source of energy, or chemoautotroph that oxidize inorganic compounds for energy. Heterotrophic microalgae oxidise organic compounds for energy and can grow in the absence of light. Mixotrophic microalgae combined aspects of both phototrophs and heterotrophs for energy generation (Lee, 2008). Algal reproduction is generally carried out in two ways: vegetative, asexual, or sexual. Vegetative reproduction is simply performed by binary fission, while asexual reproduction occurs by the formation of several types of spores such as autospores or aplanospores. Sexual reproduction is important for generating new combinations of genetic materials.

Microalgae are able to sequester carbon through their ability of to fix CO₂ efficiently from various sources including atmosphere, industrial exhaust gases and soluble carbonate salts during photosynthesis. Gases exhausted from industrial process that contain up to 15% CO₂ are considered to be a high value source of CO₂ that is a crucial factor for microalgal cultivation and consequently the optimum way to fix CO₂ in comparison with the low percentage of CO₂ in the atmosphere. Moreover, various species of microalgae have distinct features through efficient exploitation of carbonates like Na₂CO₃ and NaHCO₃ necessary for cell growth. The rich extracellular carbonic anhydrase activity of some microalgae helps them to convert carbonate to free CO₂ and then make the CO₂ assimilation quicker(Wang *et al.*, 2008). Microalgae produce a variety of valuable products that are commercially exploited in various fields including human health and food, such as carotenoids, proteins, carbohydrates, anti-oxidant agents, vitamins and sterols (Borowitzka, 2013; Xia *et al.*, 2013; Cuellar-bermudez *et al.*, 2014).

1.1.6 Microalgal Lipid

Microalgal lipids are considered to be a promising source for biodiesel production because their profile is quite analogous with terrestrial crop based biofuels. Lipid is a well-known bioproduct that refers to all organic compounds that are highly soluble in organic solvents and cannot be dissolved in water. Lipid is composed mainly of glycerol head group often attached to a sugar and 12-22 carbon fatty acid chains esterified to the glycerol. Generally, microalgal lipids are separated into two main groups: polar lipids like glycolipids (involve the combination of two fatty acid chains, glycerol, and sugar particle like galactosyldiacylglyceride) occur in the chloroplast membrane. Glycolipids are split into sphingolipid mainly located in animal cells, and glyceroglycolipid that is widely distributed in higher plants, algae and bacteria. Glycolipid is considered to be the main content of thylakoid membrane (80-90%). Phospholipid (including two fatty acids with phosphorus group on glycerol) is the other type of polar lipid that is considered to be a key component of algal cell membranes. The main function of polar lipids (also called structural lipid) are they play a vital role

for exchange of energy, substances, and signals through monitoring the membrane permeability of the algal cells (Kitamoto *et al.*, 2009). The main component of polar lipids is polyunsaturated fatty acids (PUFA) that are synthesized during the aerobic desaturation and chain elongation of fatty acids especially palmitic (C16) and oleic (C18) acids (Erwin, 1973).

Non-polar lipid (neutral lipid) is the other type of algal lipid and is split into monacylglycerol, diacylglycerol, and triacylglycerol (TAG). TAG is the most abundant type of non-polar lipid that can be easily broken down to release metabolic energy. TAG is normally synthesized in the light, accumulated in distinct spherical structures named lipid droplets in the cytosolic bodies, and exploited efficiently for the synthesis of polar lipid during the night. TAG is the key precursor for biodiesel production that can be converted to fatty acid methyl esters (FAME) through transesterification. The fatty acids of TAG are mainly saturated or monosaturated, however some high lipid content microalgal species accumulate long chain poly unsaturated fatty acids (PUFA) (Bigogno *et al.*, 2002). TAG is more favourable as a source of biofuel production in comparison with phospholipid and glycolipid because it is rich in fatty acids and also lack of phosphorus and sulphur in their structure. The occurrence of phosphate in lipids inhibits the transesterification reaction, and because of that the TAG yield is about 99% while for phospholipid it is less than 70% ((Williams and Laurens, 2010).

1.1.7 Algal lipid biosynthesis

The synthesis of fatty acids occurs largely in the chloroplast (Figure 1.9) where glycolysis and pyruvate kinase (PK) catalyse pyruvate to form phosphoenolpyruvate (PEP) that is accordingly altered to acetyl coenzyme A (CoA). Fatty acid biosynthesis is mainly induced through the role of a multifunctional enzyme complex acetyl CoA carboxylase (ACCCase) in which acetyl CoA and bicarbonate is metabolised to malonyl CoA. Acetyl CoA Carboxylase (ACCCase) is one of the key enzymes that play a crucial role in lipid (and thus biofuel) formation. Two catalytic centres biotin carboxylase (BC) and carboxyl transferase (CT) located in ACCCase facilitate the catalysis of irreversible carboxylation of acetyl CoA to generate malonyl CoA (Maity *et al.*, 2014)

Malonyl CoA is then converted into malonyl ACP through the action of malonyl CoA transacylase (MAT). Both acetyl CoA and malonyl ACP are deemed as a template for fatty acid biosynthesis. Firstly, butyryl (C₄)-ACP is synthesized from acetyl(C₂)-CoA and malonyl (C₃)-ACP through serial reactions including condensation, decarboxylation, and reduction of non-malonyl-ACP to form ketoacyl-ACP. The formation of the keto unit was associated with the consumption of molecules like ATP and NADPH that are utilised to elongate the fatty acid molecule by adding C₂-saturated carbon unit in fatty acid biosynthesis. Acyl-ACP is then elongated up to acyl (C_{16 or 18})-ACP. The termination of fatty acid chain elongation is catalysed through different fatty-ACP thioesterases (FAT) that hydrolyse acyl-ACP into free fatty acids (FFAs) (C_{16 or 18}). The fatty acids synthesized on the plastid envelope are excreted to cytosol by association with the route of binding of CoA (Rezanka and Sigler, 2009; Joyard *et al.*, 2010). The fatty acids in the acyl-ACP form can be directly utilised by sequential acylation of glycerol 3-phosphate located in the chloroplast that results in the formation of diacylglycerol (DAG). In some microalgal species e.g. *Chlamydomonas*, DAG can act as a precursor for TAG synthesis in chloroplast (Fan, Andre and Xu, 2011). However, the common pathway for synthesis of TAG is that the FFAs are excreted from the chloroplast to the cytosol, and then the long chain acyl-CoA synthetase (LACS) attach CoA to the FFA and consequently lead to the production of acyl-CoA that can be utilised for elongation and desaturation steps in the endoplasmic reticulum (ER). Many studies have reported that TAG synthesis in green microalgae is carried out in both ER-derived compartments and the chloroplast through the activities of different acyltransferase isoforms (Li-Beisson *et al.*, 2015).

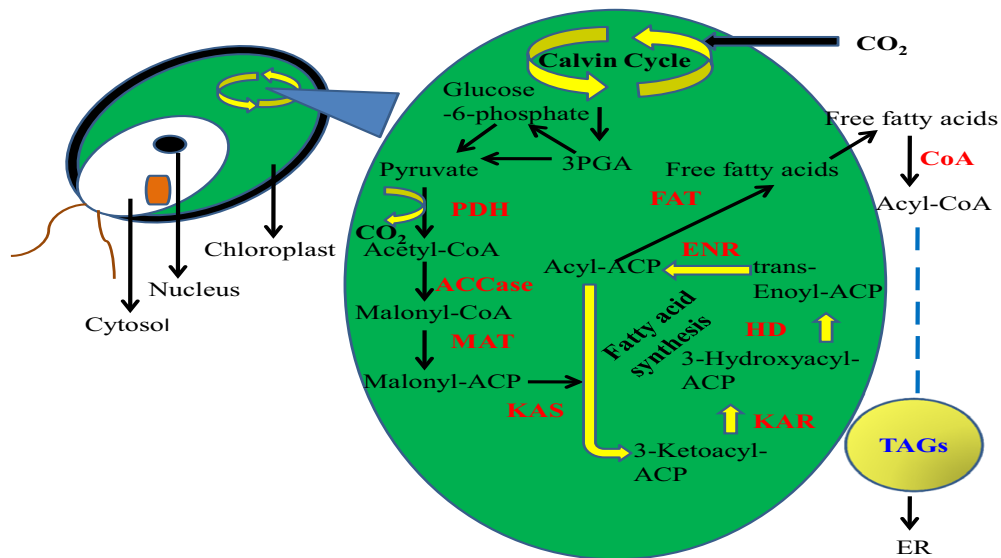


Figure 1.9 Schematic to illustrate fatty acid *de novo* synthesis of microalgal lipid. ACCase acetyl CoA carboxylase, ACP acyl carrier protein, CoA coenzyme A, FAT fatty acyl-ACP thioesterase, PGA phosphoglyceraldehyde, HD 3-hydrocyl-ACP dehydratase, ENR enoyl-ACP reductase, KAR 3-kotoacyl-ACP synthase, MAT malonyl-CoA ACP transacylase, PDH pyruvate dehydrogenase complex, TAG triacylglycerol. Adapted from (Mondal *et al.*, 2017).

1.1.8 Microalgal cultivation

The first attempts at large scale microalgal cultivation were carried out in the 1940s and 1950s when microalgae were grown in open ponds and utilised as a nutritional source during the Second World War and its aftermath. The main goal of algal cultivation for biodiesel production is to maximise lipid productivity (lipid yield) by increasing both the growth rate and lipid yield. In batch cultivation systems, the process of lipid production includes maximising the biomass concentration at the end of the exponential phase and then induce lipid synthesis through various processes mainly through reducing the nutrient content of the medium ((Singh and Sharma, 2012). The common techniques used for algal cultivation include open ponds, and photobioreactors (PBRs). Each technique has its unique features and the two main factors for selecting the cultivation system are the price and reliability.

1.1.8.1 Open ponds

Open ponds are the oldest type of large scale algal cultivation processes and have been commercially established from 1970 ((Borowitzka and and Borowitzka, 1988). Open pond design can either be natural like lakes and ponds, or consist of large artificial like large tanks. The circular design is the conventional type of pond that is widely used in waste water treatment in which the algal culture is circulated around the pond and the pond is equipped with rotating arm that is used to mix the algal culture and avoid any possibility of sedimentation. Circular open ponds are commonly used for large scale cultivation of *Chlorella* sp. in Asia. Generally, the productivity of algal biomass in circular pond varies from 8-21 g m⁻² day⁻¹ ((Benemann and Oswald, 1996; Lee, 2001; Chisti, 2008). Raceway (Figure 1.10) is the other type of open pond design that is the most common artificial type of open pond. The design of raceway ponds involves a container made from concrete, dug into the ground and lined with a plastic membrane to prevent seepage. Most raceway ponds include a paddle wheel, used widely to ensure the flow of liquid and the suspension of algal cells in the medium, which prevents any sedimentation. The depth of a raceway pond should be about 20-50 cm in order to guarantee the penetration of light to the bottom of the culture as light intensity plays a vital role for enhancing the lipid production of algal cells. The algal biomass production in raceway ponds ranged from 60-100 g m⁻² day⁻¹ that make it more commercially viable than the circular pond for algal cultivation (Tredici, 2004).

The main benefits of using open ponds for large scale algal cultivation are the low cost of construction and maintenance, minimal energy requirements, simple system of cultivation in terms of operation, and the fact that they can be constructed in a variety of places including marginal land (Rodolfi *et al.*, 2009; Chisti, 2012). On the other hand, various drawbacks of open ponds are the large area required to scale up, their high susceptibility to contamination and invasion by other microalgae, bacteria and invertebrates. Biomass cultivation in open ponds is also dependent on weather conditions including temperature, and light intensity that are considered among the vital factors that make the productivity of algal cells highly dependent on the season, often spring and summer is when the productivity reaches the maximum yields. Water

evaporation and the diffusion of CO₂ to/from the atmosphere are other common problems with the open pond system ((Osundeko and Pittman, 2014).

1.1.8.2 Closed Photobioreactors

The main reason for using closed photobioreactors is to solve the problems associated with the cultivation of algae using open pond systems. Photobioreactors can be defined as closed or (mostly closed) vessels that offer an ideal system for capturing and exploiting of light, and CO₂ necessary for pilot cultivation of algal cells. A photobioreactor consists of four main systems: solid phase (microalgal cells), liquid phase (medium consisting of nutrients to enhance the growth), gaseous phase (CO₂ and O₂) in which gas exchange filter is used to monitor the transfer and exit of gases, and a source of light in which the illumination should be designed to mitigate mutual shading (Posten, 2009). Various types of photobioreactor have been designed such as the stirred tank, vertical column, horizontal tubular, and flat panel (Figure 1.10). The selection of a specific photobioreactor is mainly dependent on the species to be cultivated, and the properties of the final products (Carvalho *et al.*, 2006). The operation of the photobioreactor can be carried out outdoors using sunlight as a source of light or indoors utilising artificial source of light for illuminating the algal culture. Indoor photobioreactors can also be illuminated by sunlight if placed in a greenhouse for example.

The design of any type of photobioreactor needs to consider the following factors: the reactor must be versatile to allow cultivation of different microalgal strains, the culture must be provided with uniform illumination and an efficient mechanism for transfer of CO₂ and O₂, the evaporation of water loss and CO₂ diffusion must be kept to a minimum and the surface area to volume ratio must be considered with respect to culture illumination and mitigation of dark zones. The design must also take into account the probability of foam being produced, particularly in high density cultures ((Singh and Sharma, 2012).

Each type of photobioreactor has advantages and limitations, the conventional stirred tank bioreactor advantages are good heat and mass transfer, the agitation being carried out very efficiently using a mechanical agitator and the low probability of contamination.

However, the low surface area to volume ratio causes inefficient utilization of light thereby minimising photosynthesis and the high energetic cost of the mechanical agitator requires extra energy consumption (Doran, 2013).

Vertical photobioreactors (Figure 1.10) are mainly divided into bubble column and airlift bioreactors. One of the advantages of this type of photobioreactor is that the agitation of algal cells within the medium is carried out through the air sparger at the bottom of reactor that converts the released gas into tiny bubbles enhancing the mass transfer to release CO₂ and capture O₂. The other advantage is less energy consumption in comparison with the conventional stirred bioreactor. While one drawback is the relatively high cost of vertical photobioreactors, due to the materials that are used for their construction (Posten, 2009; Doran, 2013).

The distinct features of horizontal tubular photobioreactors (Figure 1-10) are the high surface to volume ratio that enhances the exposure of microalgal cells to the light source, the agitation conducted through recirculation by air pumps, low cost construction materials, and can be used outdoors. The main limitation of horizontal photobioreactors are high levels of dissolved O₂ that inhibit the rate of photosynthesis. The high accumulation of O₂ decreases algal productivity which makes the use of this type of bioreactor not economically feasible (Mirón *et al.*, 1999; Doran, 2013).

The flat panel photobioreactor (Figure 1.10) also has a high surface area to volume ratio that allows for efficient exposure to the light. Agitation is carried out through bubbling air from the bottom or the side of the bioreactor and leads to low accumulation of O₂. It is possible to cheaply construct flat panel photobioreactors, but they are difficult to scale up. The other main disadvantages of flat panel photobioreactors are: a) difficulties with temperature regulation and b) aeration causing hydrodynamic stress (Ugwu *et al.*, 2008).

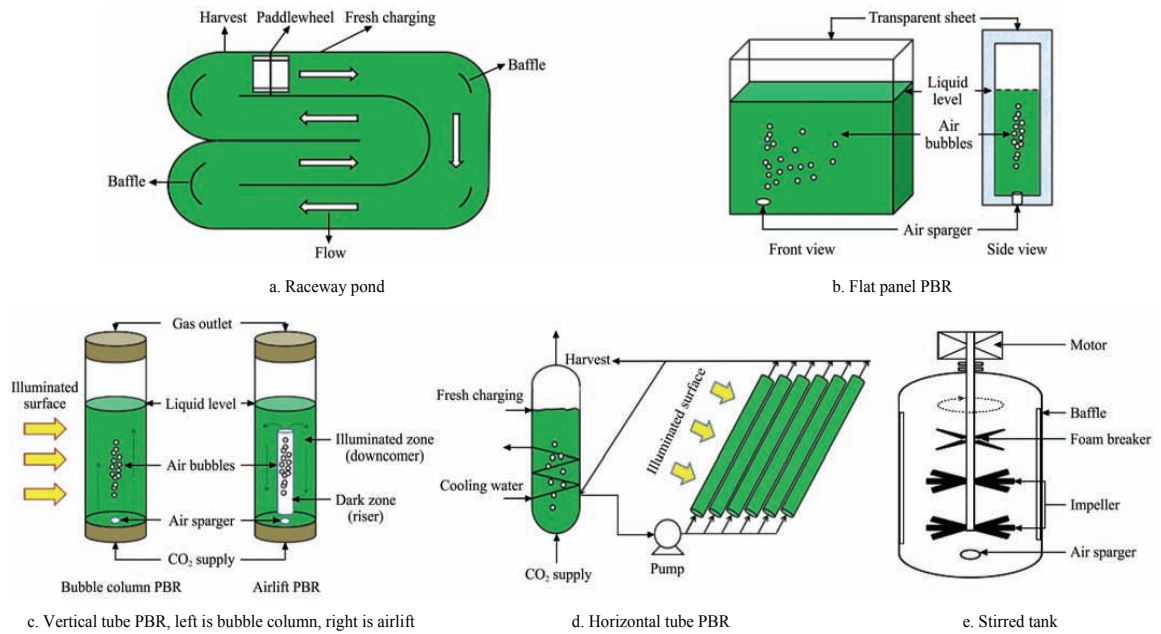


Figure 1.10 Schematic of various types of large scale algal cultivation systems adapted from (Ting et al., 2017)

1.1.9 Strategies to induce lipid synthesis in microalgae

Microalgae produce high value bioproducts including lipid and the synthesis of neutral lipid is highly influenced by various parameters that play an important role in adjusting the growth rate of microalgae. Generally, these parameters are classified into three groups (Mata *et al.*, 2010):

Abiotic factors including light, temperature, carbon dioxide, pH, salinity, and nutrients (carbon, nitrogen, and phosphorus) that are essential for algal growth.

Biotic factors involve bacteria, viruses, fungi and other microalgae and the effects of competition for abiotic growth factors.

Additive factors that have an operational function for microalgal growth, such as stirring speed for mixing and the percentage dilution factor used in fed-batch or continuous cultures.

1.1.9.1 Light

Light is the energy source that drives the conversion of CO₂ to organic compounds (mainly sugars) through photosynthesis. The growth rate of microalgae increases with increasing light intensity until the saturation intensity point is reached where the level of photon absorption surpasses the rate of electron transport and consequently no further increase in photosynthetic activity takes place. Further increasing the light intensity will cause degradation of the photosynthetic apparatus at PS2- this is called photo-inhibition (Chang *et al.*, 2016). In general, the optimum light intensity varies between algal species, for instance, the light saturation intensity point of *Chlorella* sp. was found to be 8000 lux, while it was reported that 10000 lux was the optimum light intensity for *Nannochloropsis* sp. (Cheirsilp and Torpee, 2012). For *Scenedesmus* sp. the optimum light intensity was 6000 lux (Mandotra *et al.*, 2016).

Increasing light intensity maximises lipid content in various microalgae probably because adequate light intensity induces the storage of excess photoassimilates, that can be converted into several chemical products. The highest percentage lipid content (47%) for *Nannochloropsis* sp. was achieved under the high light intensity of 700 $\mu\text{mol photons m}^{-2} \text{ s}^{-1}$ (Pal *et al.*, 2011). The lipid content of *Scenedesmus* sp. enhanced gradually from 21.2 to 33.7% when cultured on increasing light intensity from 3000 to 6000 lux (Mandotra *et al.*, 2016). The level of light intensity can also affect the type of lipid produced. Under low light intensity the algal cells tend to produce large amounts of polar lipids to maximise the synthesis of chloroplast membranes. While an increase in the light intensity induced the algal cells to accumulate neutral lipids without greatly influencing the algal growth rate (Breuer, Lamers, *et al.*, 2013).

1.1.9.2 Temperature

Temperature is the other factor that influences the growth rate and lipid profile of microalgae. Generally, algal biomass production increases with an increase in the temperature until an optimum temperature is reached. Many microalgal cells grow well at temperatures ranging from 25 - 30°C. At higher temperatures, the growth of algal cells is decreased mainly because heat probably denatures functional proteins and

photosynthetic enzymes. Moreover, high temperature causes a drop in the neutral lipid content of microalgae, although the proportion of saturated and monounsaturated fatty acids increase (James *et al.*, 2013). At low temperatures (below 15°C), algal cells production is inhibited due to an increase in the viscosity of the cytoplasm and a decrease in the transport into the cell of essential nutrients. Furthermore, low temperatures lead algal cells to accumulate unsaturated fatty acids that are used to increase the fluidity of the membrane (Chang *et al.*, 2016).

The optimum temperature for lipid synthesis was found to vary depending on the species ((Sibi *et al.*, 2016). An increase in the temperature from 20 to 25°C doubled the lipid content (7.9 to 14.9%) of *Nannochloropsis oculata*. For *Chlorella vulgaris* 25°C was reported as the ideal temperature for lipid production and any change in the temperature led to clear reduction in the lipid yield (Converti *et al.*, 2009). On the other hand, 20°C was found to be the optimum temperature for both *Scenedesmus* sp. and *C. minutissima* to achieve their highest yield of lipid (Xin, Hong-ying and Yu-ping, 2011; Cao *et al.*, 2014).

1.1.9.3 Carbon dioxide

Carbon is a major component of microalgal cells (45-50%) dry weight and the main source of carbon for algal photosynthesis is CO₂ from the atmosphere, or from industrial processes (exhaust or flue gas containing a range of components), and from soluble carbonates (Kumar *et al.*, 2010). To greatly boost algal biomass production and lipid yields, CO₂ is supplied to algal cultures as a gaseous form mixed with air (Amaro, Guedes and Malcata, 2011), or through the supply of waste gases containing a high CO₂ content (15 – 20%).

The optimal concentration of CO₂ varies between different microalgal species, however overdose of CO₂ has negative impacts on the growth of microalgae mainly because the excess CO₂ is converted to carbonic acid (H₃CO₃) that consequently leads to a decreasing the pH of the culture. Microalgal biomass can be grown at atmospheric concentration of CO₂ (0.03%), but increasing the amount of CO₂ normally increases the growth rate at least up to 5% CO₂ (Ying *et al.*, 2014). However, as noted above, industrial flue gas often

contains high concentrations of CO₂ and some microalgal species can grow well at elevated CO₂ levels e.g. the highest lipid productivity in *Chlorella vulgaris* was achieved in cells cultured with 8% CO₂ under nitrogen limited conditions (Montoya *et al.*, 2014). Biomass productivity and lipid yield also increased in *Nannochloropsis* cells after supplementation with 15% CO₂ (Jiang *et al.*, 2011). Another study showed that both *Scenedesmus obliquus* and *Chlorella pyrenoidosa* show their maximum yield of lipid polyunsaturated fatty acids when supplemented with high concentrations of CO₂ (30 - 50%) (Tang *et al.*, 2011).

1.1.9.4 Nutrient limitation

Nutrient starvation or depletion is considered as an efficient and common strategy for increasing the lipid content of algal cells. Microalgae can adapt their cells to various alterations in the environment. Under unfavourable conditions microalgal cells tend to initiate a defence mechanism in which energy is accumulated as neutral lipid mainly in the form of triacylglycerol (TAG) to protect the cells from photo-oxidation (Adams *et al.*, 2013; Sibi *et al.*, 2016).

Nitrogen starvation is the most common approach to significantly increase lipid accumulation. Nitrogen is the second most essential component (1-10%) of algal cells and is mainly provided in growth media as either ammonium, nitrate or urea. In some microalgae ammonia is exploited more effectively and can be converted directly to amino acids (Lv *et al.*, 2010; Xin *et al.*, 2010). Nitrogen starvation stops or dramatically slows down cell division and consequently induces a shift in the biosynthetic pathway of lipid to over synthesise neutral lipid (TAG) instead of membrane lipids essential for the cell membrane formation (Hu, 2004). The lipid content of *Chlorococcum* sp. and *Scenedesmus destricola* improved from 31.6% to 40.7% and from 48% to 54% respectively when they were cultured under nitrogen deficient conditions, (Li *et al.*, 2013). Moreover, N starvation led to a ten-fold increase in the lipid content of *Micractinium pusillum* after 6 days growth (Li *et al.*, 2012).

Phosphorus is another essential nutrient constituting around 1% of algal cell dry weight. Phosphorus plays a crucial role in the growth and metabolic pathways of microalgae as

it is involved in energy transduction and is a vital part of nucleic acid structure (Juneja *et al.*, 2013). Various studies have reported the influence of phosphorus starvation on the induction of neutral lipid synthesis in microalgal cells e.g. the lipid content in *Scenedesmus obliquus* increased from 10% to 29.5% when they were cultured under phosphorus starvation (Mandal and Mallick, 2009).

Sulphur is another crucial nutrient for algal growth and sulphur deprivation has been shown to induce the lipid accumulation in the algal cells through the alteration of the metabolic pathway of carbon from protein to neutral lipid synthesis. Sulphur starvation induced the accumulation of TAG in *Chlamydomonas reinhardtii* cells (Cakmak *et al.*, 2012; Sato *et al.*, 2014) and sulphur deficiency led to enhanced lipid levels (1.2 to 2.4%) for a *Chlorella* sp. (Mizuno *et al.*, 2013).

1.1.9.5 Salinity

Microalgal cells tend to accumulate high lipid yield as a defence mechanism after exposure to salinity stress that enhances the external osmotic pressure. An increment in the salinity of the algal environment has a remarkable influence on the physiological and biochemical properties of the algal cells because of the alteration in the ionic balance inside the cells. In response to a salinity increase, fresh water algal cells release ions through the membrane and adjust the absorption of ions, they also accumulate high lipid products (Talibi *et al.*, 2013). However, excess salinity has a negative effect on algal growth and lipid accumulation due to its inhibitory effect on the photosynthetic activity of the algal cells.

Several studies have investigated the effect of salinity on lipid accumulation in marine or salt tolerant microalgae *Dunaliella* sp. that is a good example of an alga which is tolerant to salinity stress and its lipid content increased remarkably (up to 70%) under high salinity ((Takagi and Yoshida, 2006). *Nanochloropsis salina* lipid yield increased when they were cultivated under high NaCl concentrations (Bartley *et al.*, 2013). Another study stated that high salinity can be exploited as a lipid trigger that enhances the level of various fatty acids in the fresh water species *Chlamydomonas reinhardtii*

that were good precursors for biodiesel production like palmitic acid (C16:0), and linolenic acid (C18:3n3) (Hounslow et al., 2016).

1.1.9.6 Metal stress

Micronutrient metal ions like iron, zinc, copper, manganese and calcium have a crucial role to play in both growth and lipid production in microalgae. These metals are essential for electron transport in photosynthesis and cellular respiration (Huang *et al.*, 2013). Iron (Fe^{+3}) ion affects many genes that regulate the lipid synthesis pathway and consequently enhances the lipid yield in microalgae. *Scenedesmus* sp. growth rate and lipid yield were increased by increasing the concentrations of iron, magnesium, and calcium (Ren *et al.*, 2014). An increase in the lipid content of *Botryococcus* sp. was seen after cultivation in a high iron concentration (Yeesang and Cheirsilp, 2011). Another study described an increase in the growth and lipid content of *Monoraphidium* sp. after adding magnesium to the medium (Huang, et al., 2014). Other metals like zinc and copper have an influence on algal growth and lipid enhancement through their roles as enzyme cofactors (Zhou *et al.*, 2012).

1.2 Aims of the project

The main aims of the work described in this thesis are:

Isolation, molecular identification, and construction of a phylogenetic tree of the fresh water algal strain isolated from Weston Park pond, Sheffield, United Kingdom. (Chapter 3)

Investigate the neutral lipid content in *Desmodesmus armatus* (the strain isolated from Weston Park Pond) and compare it with neutral lipid content of the model strain of cyanobacteria *Synechocystis* sp. PCC 6803 (obtained from Prof. Hunter lab, Department of Molecular Biology and Biotechnology - University of Sheffield-UK) under normal and stress growth conditions (high salinity, nitrogen starvation, and altered source of nitrogen in the medium). Various neutral lipid assessment techniques were used including fluorometric determination in combination with lipophilic Nile Red dye, gas chromatography - mass spectrometry (GC-MS) technique, and nuclear magnetic resonance (NMR). (Chapter 4)

Attempt to increase the neutral lipid yield of *D. armatus* through random mutation using UV-C (254 nm) as mutagen, compare the neutral lipid content between the wild type and the UV exposed cells using flow cytometry in combination with Nile Red dye and fluorescence activated cell sorting (FACS) techniques. (Chapter 5)

Chapter Two

Materials and Methods

2.1 Cleaning and Sterile Techniques

To avoid any contamination, all culture equipment used in experiments was autoclaved. Also, inoculation and sub-culturing were carried out with a flame after cleaning the bench with 70% ethanol. Moreover, the glassware was soaked for 2 hours in concentrated sulphuric acid to ensure that all residual material from previous cultures was removed.

2.2 BG11 Medium

Both water samples (see section 2.3) and *Synechocystis* sp. strain were grown in BG11medium.

BG11 medium was prepared according to ((Xin *et al.*, 2010) using a series of stock solutions that are then combined. The stock solutions were prepared as follows:

Stock solution	Gram per litre
(1)NaNO ₃	15.0

Stock solution	Gram per 500 ml
(2)K ₂ HPO ₄	2.0
(3)MgSO ₄ .7H ₂ O	3.75
(4) CaCl ₂ .2H ₂ O	1.80
(5) Citric acid	0.30
(6) Ammonium ferric citrate green	0.30
(7) EDTANa ₂	0.05
(8) Na ₂ CO ₃	1.00

(9) Trace metal solution	
Stock solution	Gram per litre
H ₃ BO ₃	2.86
MnCl ₂ .4H ₂ O	1.81
Na ₂ MoO ₄ .2H ₂ O	0.39
CuSO ₄ .5H ₂ O	0.08
Co(NO ₃) ₂ .6H ₂ O	0.05

1 litre of medium was prepared by adding 100 ml of stock 1, 10 ml each from stocks (2-8), and 1 ml of stock 9 and the volume was made up to 1 litre by distilled water. The medium was adjusted to pH=7.2 using 1 M HCl or NaOH. The medium was autoclaved at 121°C for 15 to 20 mins.

For agar medium, 15 g of Bacteriological agar (Oxoid L11) was added to the medium prior to autoclaving.

2.2.1 Modified BG11 Media

Different modifications were made to the BG11 medium, to grow the algal samples under stress conditions.

2.2.1.1 High Salinity BG11 Medium

High salinity BG11 media (0.2 M NaCl, 0.4 M NaCl, 0.6 M NaCl , 0.8 M NaCl) were prepared by adding 11.7 g , 23.4 g , 35 g, 47 g of NaCl to 1 litre of BG11, the medium was adjusted to the pH=7.2 using 1 M HCl or NaOH.

2.2.1.2 BG11 Medium Containing Different Concentrations of NaNO₃

To provide different concentrations of nitrogen in the BG11 media, different volumes of stock solution 1 (15 g/l NaNO₃) were added to BG11 media to make 75%, 50%, 25% concentrations of nitrogen in the BG11 media.

2.2.1.3 BG11 Medium Containing Different Nitrogen Sources

To investigate the effect of different nitrogen sources, NH₄Cl and urea were added in place of NaNO₃ in BG11 medium. The same amount of nitrogen in the medium was

maintained by dissolving 9.44 g of NH_4Cl and 5.3 g of urea respectively in separate 1 litre aliquots of BG11 media. Both modified media were adjusted to $\text{pH}=7.2$ using 1 M NaCl or NaOH

2.3 Collection of Samples

Water samples were collected from different locations around the edge of Weston Park pond (Sheffield, UK) using sterile 50 ml Falcon tubes (Figure 2.1), each tube was filled with 50 ml of pond water (after shaking the tube several times to disturb the sediment). Each sample was then aseptically transferred to a sterile 250 ml flask and 50 ml of sterile double strength BG11 medium was added.

The cyanobacterium *Synechocystis* sp. PCC6803 was obtained from Professor Hunter's lab (Department of Molecular Biology and Biotechnology, University of Sheffield) in the form of streaks on agar plates (Figure 2.2). Two types of *Synechocystis* PCC 6803 (Nixon, and Vermass) colonies were subcultured in BG11 medium.

Both water pond samples and *Synechocystis* strains were incubated in the growth room at $25 \pm 1^\circ\text{C}$ with continuous light ($50 - 70 \mu\text{mol m}^{-2} \text{s}^{-1}$) supplied by daylight fluorescent lights. When required, shaking (80 rpm) was provided for flask cultures.

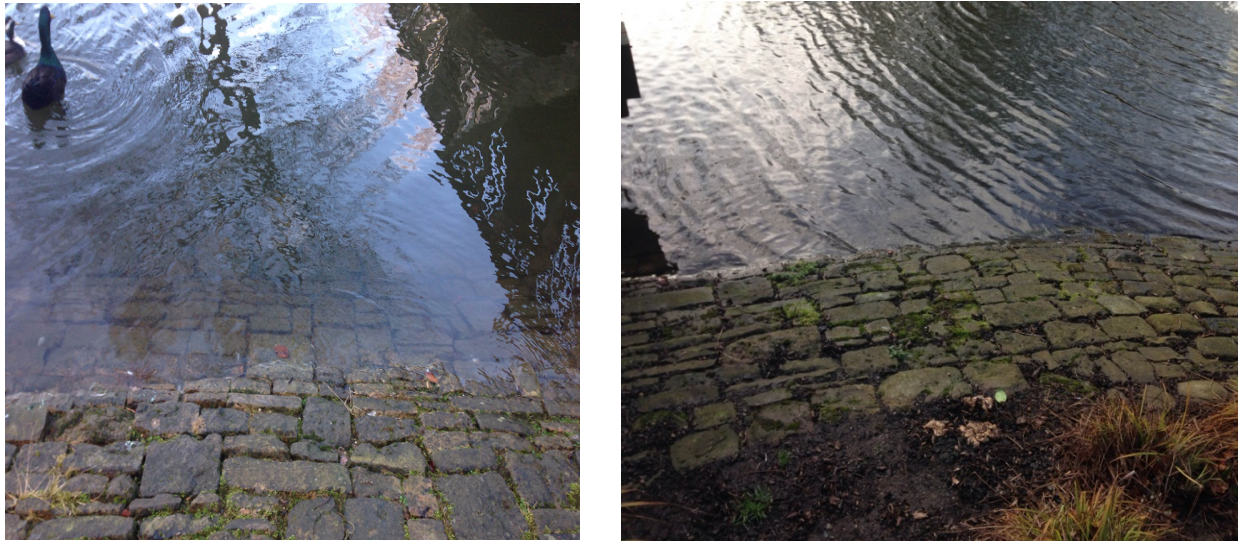


Figure 2.1 Western Park Pond where water samples were collected

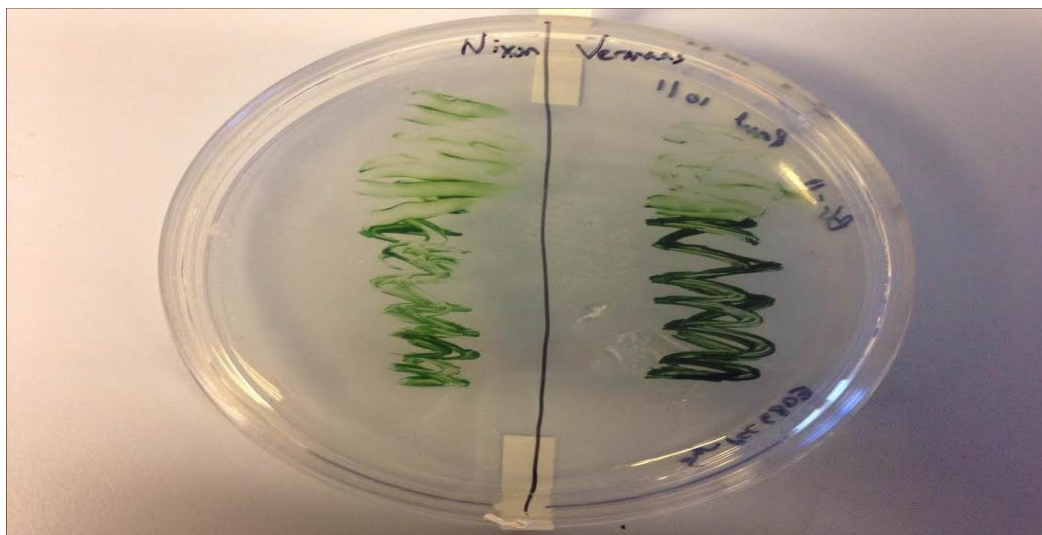


Figure 2.2 Synechocystis PCC 6803 obtained from Prof Hunter Lab (Department of Molecular Biology and Biotechnology, University of Sheffield)

2.4 Cell Density Evaluation

2.4.1 Spectrophotometer

A UV-Vis Unicam Helios α -spectrophotometer (Unicam) was used to assess the optical density (OD). A wavelength of 595 nm was initially used to measure turbidity of both *Synechocystis* and pond water samples.

In general a 1 ml aliquot of culture was aseptically transferred to a 1 ml plastic cuvette (634-0675 Polystyrene, VWR). The cuvette was briefly agitated to ensure homogenous dispersal before being placed into the spectrophotometer for OD measurement. The OD of sterile media and distilled H₂O (dH₂O) did not differ. Consequently, 1 ml of dH₂O was used as a blank in all subsequent experiments to avoid wasting media and potential media contamination. If the optical density of the algae sample was above 0.6 the sample was diluted with dH₂O.

2.4.2 Cell Counting and Growth Curve Determination

Growth curves for both *Synechocystis* and *D. armatus* cells were determined following the protocol described by (Guillard and Sieracki, 2005):

- A suitable inoculum culture of each strain was chosen and the cell number was counted using Helber Counting Chamber and light microscope (Nikon, Japan).
- Exactly 100 ml of BG11 was transferred to pre autoclaved 3*250 ml flasks.
- The flasks were inoculated with each strain separately, and the volume of inoculum was adjusted from the original flask using fresh medium to provide an initial cell density (cells ml⁻¹) of 1*10⁴ for *Scenedesmus* sp. and 1*10⁵ for *Synechocystis* sp. The strains were incubated at 25 ± 1⁰C with continuous light (50 – 70 $\mu\text{mol m}^{-2} \text{s}^{-1}$) supplied by daylight fluorescent lights.
- The strains were counted daily by shaking the flasks and placing 20 μl of the culture within the engraved circle of the Helber Counting Chamber slide, then the cover slip was added using a sliding motion.
- The slide was examined under the appropriate magnification usually x400 phase contrast. The number of small squares counted depended on the

density of the culture, for example the less dense cultures required a count of all the cells within 400 small squares.

- An Excel spreadsheet was prepared between the cell count and the days.

Calculations

Each small square has an area of $1/400$ mm and with the cover slip correctly in the place the depth of liquid is 0.02 mm.

The volume of liquid contained within a single square is

$$= 1/400 \times 0.02 \text{ mm}^2$$

$$= 0.0025 \times 0.02 \text{ mm}^2$$

$$= 5 \times 10^{-5} \text{ cm}^3 \text{ (ml)}$$

If the total count of the 50 Small Squares is Y then:

$$= Y / (50 \times 5 \times 10^{-8}) \text{ ml}^{-1}$$

$$= Y \times 4 \times 10^5 \text{ ml}^{-1}$$

2.5 Microscopic Examination of the Pond Samples

After the water pond samples showed growth in the BG11 medium flasks, serial slides from each culture were prepared and examined using light microscope (Nikon, Japan). Most of the slides contained a mixture of microalgae and bacteria. Therefore, the major population of microalgae strains were purified using different techniques.

2.6 Assessing Bacterial Contamination and Purification Methods

Different methods were used to achieve an axenic (bacteria-free) microalgal strain from water pond samples grown in BG11 medium.

2.6.1 Percoll™ Treatment

This differential centrifugation method was carried out according to Sitz and Schmidt, (1973). Percoll™ standards of 10%, 20%, 30%, 40%, 50%, 60% were made up with autoclaved distilled water in 15 ml Falcon tubes stored on ice. For example 1 ml of 60% standard was prepared by adding 0.6 ml of Percoll™ to 0.4 ml of autoclaved distilled water. A density gradient was obtained in a 15 ml Falcon tube: 1 ml of 60% Percoll followed by 1 ml of each standard in order of decreasing Percoll™ concentration. The standards were added into the Falcon tube at a 40° angle to avoid mixing between layers as much as possible. Using the same technique, 1 ml of a contaminated algae culture (OD_{595} above 1) was transferred to the top of the density gradient. The Falcon tube was centrifuged at 500 *g* for 10 minutes. Immediately after centrifugation the top layer of Percoll™ was discarded. With a fresh pipette tip, the layer of algae cells was carefully extracted and transferred to fresh medium.

2.6.2 Centrifuge Washing Technique (Purification of Algal Samples)

Centrifuge washing technique was adapted from Phang and Chu (1999) and sterile dH₂O was prepared by autoclaving at 121°C for 15 minutes. Microalgal samples (12 ml) were transferred from a well grown culture into 4*15 ml Falcon tubes and centrifuged at 1500 *g* for 15 minutes. After the supernatants were discarded, the cells in each tube were suspended in fresh sterile water using vortex mixing to produce a homogeneous suspension. Centrifugation and washing steps were repeated for six times to exclude most contaminants present in the algal samples and the cells were then streaked on BG11 agar plates.

2.7 Molecular Identification of the Strains

Both *Synechocystis* and the water sample strain were identified using 16S and 18S rDNA primers respectively. The identification procedure included extraction of genomic DNA, PCR amplifications, and sequencing of the PCR product. The water sample strain was initially identified as a species of the genus *Scenedesmus* (subsequently *Desmodesmus armatus*)

2.7.1 Extraction of DNA

Genomic DNA extraction of samples was performed using two protocols:

a) by using the surfactant hexadecyltrimethylammonium bromide (CTAB) or b) by using the ZR Soil Microbe DNA Microprep™ Kit.

2.7.1.1 CTAB Protocol

Genomic DNA extraction for both *Synechocystis* and *D. armatus* cells were carried out based on the protocol described by Li *et al.*, (2002):

- 5-10 ml of algae culture was centrifuged in a 15 ml Falcon tube for 10 min at 3000 *g*.
- Supernatant was discarded and the pellet was resuspended in 500 µl of CTAB (prepared by dissolving 2% CTAB, 2% β-mercaptoethanol, 0.1 M Tris-HCl pH=8.0, 1.4 M NaCl and, 20 mM EDTA), the suspension was then sonicated for 30 s at full power.
- Sample was then incubated at 65°C for 1 hour.
- 500 µl of phenol-chloroform isoamylalcohol (24:25:1) was added to the sample. Sample was then vortexed and centrifuged for 5 min at full speed in a microfuge.
- Carefully, the top layer was removed into a fresh Eppendorf tube and 500 µl of chloroform was added.
- Sample was then centrifuged for 5 min at full speed in a microfuge and the top layer was measured and transferred into a fresh Eppendorf tube.
- 1/10 total volume of 3 M sodium acetate pH 5.2 was added. This was followed by adding 2.5 volumes cold 100% ethanol.

- Sample was then incubated on ice for 10 mins at least, then centrifuged at 6000 *g* for 15 min.
- Supernatant was discarded immediately and 1 ml of 70% ethanol was added.
- Eppendorf tube was then centrifuged for 5 mins at full speed and supernatant was discarded.
- Centrifugation was carried out again for the same time and speed and the remaining of ethanol was pipetted off carefully.
- Air drying was then performed for 10 mins.
- Pellet was resuspended in 50 μ l of sterile MilliQ water.
- DNA pellet was left on bench to resuspend overnight and incubated for 60 mins at 50°C in the morning.

2.7.1.2 DNA Extraction using ZR Soil Microbe DNA Kit

D. armatus genomic DNA was extracted using ZR soil Microbe DNA MicroPrep™ (Zymo Research ,Irvine, CA, USA) kit according to the manufacturer's protocol as follows:

- 20 ml of each sample was centrifuged at 3000 *g* for 10 min, the supernatant was discarded.
- 750 μ l of Lysis solution was added to the pellet and transferred into a ZR Bashingbead™ lysis tube.
- The tubes were then bead beaten using 0.5 mm bead tubes (Bead bug microtube homogenizer, Sigma Aldrich, see Figure 2.3) for 3 min at 3000 *g*.
- The Bashingbead™ Lysis tube was then centrifuged at 10,000 \times *g* for 1 min.
- About 400 μ l of the supernatant was transferred to a Zymo-spin™ filter in a collection tube and centrifuged at 7000 \times *g* for 1 min.
- 1,200 μ l of Soil DNA binding buffer was added to the filtrate in the collection tube from the last step.
- 800 μ l of the mixture from the last step was transferred to a Zymo-spin™ IC Column in a collection tube and centrifuged at 10,000 \times *g* for 1 min.
- The flow through was discarded from the collection tube and the last step was repeated.

- 200 μ l of DNA Pre-wash Buffer was added to the Zymo-spin™ IC Column in a new collection tube and centrifuged at $10,000 \times g$ for 1 min.
- 500 μ l of Soil DNA Wash Buffer was added to the Zymo-spin™ IC Column and centrifuged at $10,000 \times g$ for 1 min.
- The Zymo-spin™ IC Column was transferred to a clean 1.5 ml microcentrifuge tube and 50 μ l of DNA Elution Buffer was added directly to the column matrix. To elute the DNA the column matrix was centrifuged at $10,000 \times g$ for 30 seconds.
- The eluted DNA was left overnight, then incubated for 60 mins at 50°C in the morning.



Figure 2.3 Bead bug microtube homogenizer for disruption of algal cells

2.7.2 Gel Electrophoresis

The presence of genomic DNA in the extracted algal samples was investigated by preparation of 1% agarose gel. 0.6 g of agarose powder (ICN Biomedicals Inc.) was dissolved with 60 ml of distilled water and 1.2 ml of 50x TAE buffer (prepared by dissolving 242 g of Tris, 100 ml of 0.5 M EDTA and 57.1 ml of Glacial acetic acid in 1 litre of distilled water). A 6 µl aliquot of Gel Red was added to the gel mix after heating the mix in a microwave oven at power 6 for 90 seconds. 10 µl of the DNA sample was mixed with 2 µl of 6x DNA loading dye and loaded onto the agarose gel. Also, 6 µl of 1 kb DNA ladder (Thermo Scientific) was loaded onto the agarose gel and the electrophoresis was run at 80 V for 45 min. Bands were visualized with a UV lamp and photographs taken to capture the image.

2.7.3 Polymerase Chain Reaction amplification

PCR amplifications were performed for identification of the pond samples using 18S Lim primers (Lim *et al.*, 2012). For further identification of pond water samples, the internal transcribed spacer (ITS) region were amplified using 5.8S rDNA ITS1, and ITS2 primers. (Nakayama *et al.*, 1996; Hoshina *et al.*, 2004; Hoshina *et al.*, 2005).

Moreover, the standard strain *Synechocystis* PCC 6803 was confirmed using (16S primers) in a MyCycler thermal cycler (Bio-Rad). The sequences of 16S, 18S, 5.8S, ITS1, and ITS2 primers are shown in Table 2.1 and the PCR mixtures are shown in Table 2.2

Table 2.1 Sequence of 16S rRNA , 18S, 5.8S, ITS1, and ITS2 rRNA Primers

Primer	Sequence	Reference
27 F 16S	5-AGA GTT TGA TCC TGG CTCAG -3	Stackebrandt and Goodfellow (1991)
1492 R 16S	5-TACGGCTACCTTGTTACGACTT -3	
18S rRNA For Lim	5-GCGGTAATTCCAGCTCCAATAGC-3	Lim <i>et al.</i>, (2012)
18S rRNA Rev Lim	5 –GACCATACTCTCCCCCGGAACC-3	
18S rRNA For Sheehan	5-AATTGGTTGATCCTGCCAGC -3	
18S rRNA Rev Sheehan	5-TGATTCTGTGCAGGTTCCACC-3	
5.8S rDNA F	5-GTCAGAGGTGAAATTCTTGG-3	Nakayama <i>et al.</i>, (1996)
5.8S rDNA R	5-CAATGATCCTTCCGCAGGTT-3	Hoshina <i>et al.</i>, (2005)
ITS1 F	5-TACCTGGTTGATCCTGCCAG -3	Nakayama <i>et al.</i>, (1996)
ITS1 R	5-TAACTAAGAACGGCCATGCAC -3	Hoshina <i>et al.</i>,(2005)
ITS2 F	5-TGGTGAAGTGTTCCGATTGG -3	Hoshina <i>et al.</i>, (2004)
ITS2 R	5-TCCCAAACAACCCGACTCT-3	Hoshina <i>et al.</i>, (2005)

Table 2.2 Contents of Tubes for PCR Amplification

SAMPLE	16S	18S Lim	Control
Master mix	20	20	20
For primer	4	4	4
Rev primer	4	4	4
Distilled water	17	17	22
Genomic DNA	5	5	0
Total volume is 50 µl for all samples			

The confirmation of *Synechocystis* PCC 6803 using PCR amplification was performed using 16SrDNA primers ((Stackebrandt and Goodfellow, 1991) (Table 2.1) following the protocol described in Table 2.3, while the identification of pond samples was conducted following the protocol shown in Table 2.4.

Table 2.3 PCR Cycling using 16S rRNA Primers

Initial Denature	94 °C	3 min	
Denature	95 °C	1min	} 30 cycles
Anneal	58 °C	1 min	
Elongation	72 °C	1 min	
Final Elongation	72 °C	5 min	

Table 2.4 PCR Cycling using 18S rRNA primers

Initial Denature	94 °C	5 min	
Denature	94 °C	30 sec	} 30 cycles
Anneal	58 °C	30 sec	
Elongation	72 °C	1 min	
Final Elongation	72 °C	10 min	

Table 2.5 PCR Cycling using ITS1,ITS2,5.8S rDNA primers

Initial Denature	94 °C	5 min	
Denature	94°C	30 sec	} 30 cycles
Anneal	55 °C	30 sec	
Elongation	72 °C	1 min	
Final Elongation	72 °C	5 min	

The PCR products were detected using 1% agarose gel (as described in section 2-7-2), and the positive results were purified using an Anachem KeyPrep PCR clean-up kit as follows.

- The volume of the samples was determined and adjusted to 100 µl with sterile distilled water. Five volumes of buffer PCR were added and the samples were mixed thoroughly by vortexing or inverting several times.
- The samples were transferred to a column (max. 1 ml) assembled in a clean collection tube, centrifuged at 10,000 × *g* for 1 min. The flow through was discarded.
- The columns were washed with 750 µl Wash Buffer and centrifuged at 10,000 × *g* for 1 min and the flow through was discarded.
- The columns were centrifuged at 10,000 × *g* for 1 min to remove residual ethanol.
- The columns were placed into clean microcentrifuge tube. About 80 µl of Elution Buffer was added onto column membrane and allowed to stand for 2 min. The eluted DNA was collected by centrifuging the column at 10,000 × *g* for 1 min.

The eluted DNA was confirmed by electrophoresis of the purified DNA and the rest of DNA was stored at 4°C.

2.7.4 PCR Purification

As an alternative to the Anachem Key Prep Kit, some PCR products were purified using QIAquick PCR Purification kit (Qiagen). Moreover, the yield of the purified PCR product was measured in quartz cuvette at 260 nm using a spectrophotometer.

2.7.5 DNA Quantification

DNA was quantified using a Nanodrop spectrophotometer (JENWAY Genova Nano, UK) following the manufacturer's protocol using the wavelength of 260 nm.

For DNA

$$\text{DNA conc (ng } \mu\text{l}^{-1}) = ((62.9 \times (A_{260} - A_{320})) - (36 \times (A_{280} - A_{320}))/0.02$$

Where A_{260} is proportional to DNA & RNA concentration, A_{280} corrects for contamination compounds, A_{320} corrects for turbidity of sample, and 0.02 corrects concentrations for the 0.2 mm light path length.

2.7.6 DNA Sequencing

DNA samples were sent out for sequencing to Eurofins/MWG. The obtained sequences were then compared against sequences in the GenBank nucleotide collection using the Basic Local Alignment Search Tool (BLAST).

2.7.7 Phylogenetic tree construction of pond water samples

After PCR amplification, 18S, 5.8S, ITS1, ITS2 gene sequences of pond water samples were individually investigated with genus specific sequences using National Centre for Biotechnology Information (NCBI) database through basic local alignment tool (Blast). The highest identity scores of genus sequences were selected and with the query sequences retrieved from NCBI GenBank database, Jalview software (Waterhouse, *et al.*, 2009) was used to conduct multiple sequences alignment of the query and retrieved sequences using Muscle method. The phylogenetic tree was then constructed using Molecular Evolutionary Genetics Analysis (MEGA, version 7) using neighbour joining method and Maximum likelihood methods (Kumar *et al.*, 2016).

2.8 Relationship between Cell count versus OD₅₉₅ nm for *Synechocystis* PCC6803 and *Desmodesmus armatus* cells

To investigate the relationship between optical density (OD) measurement and cell count of algal cells, an OD against cell count standard curve was prepared based on the work of (Reed, 1998; Madigan, 2003; Skoog, Holler and Crouch, 2007). 30 ml of well grown microalgal culture was taken and adjusted to OD₅₉₅ =1 using fresh BG11 medium using plastic cuvettes and spectrophotometer (UNICAM Helios Alpha). A serial dilution of the algal culture with fresh BG11 medium was prepared in 15 ml Falcon tubes based on Table 2.6. From each concentration, 1 ml was transferred to the plastic cuvette and the OD at 595 nm was measured using spectrophotometer with fresh BG11 medium as blank. At the same time, 900 µl from each dilution was transferred to an Eppendorf tube

followed by adding 100 µl of iodine and mixing well. Then, 20 µl was placed into the counting chamber of a Neubauer improved haemocytometer and viewed using a Nikon microscope with the x40 objective (x400 magnification). Five replicates were carried out for each dilution, and the number of cells in each dilution was calculated using the calculations shown in section 2.4.2. Then the results of both OD and cell count of each dilution was compiled to give a calibration curve of OD at 595 against cell count.

Table 2.6 Scheme of different algal concentrations for determining the relationship between OD₅₉₅ and cell count.

Tube Number	Conc. (%)	Culture (ml)	Media(ml)
11	5.00	0.25	4.75
10	10.00	0.50	4.50
9	20.00	1.00	4.00
8	30.00	1.50	3.50
7	40.00	2.00	3.00
6	50.00	2.50	2.50
5	60.00	3.00	2.00
4	70.00	3.50	1.50
3	80.00	4.00	1.00
2	90.00	4.50	0.50
1	100.00	5.00	0.00

2.9 Lipid Extraction and Determination

2.9.1 Nile Red Fluorescence Microscopy

The visualising of microalgal neutral lipid in the lipid bodies which appear as oil droplets was examined by staining the *Desmodesmus* cells grown under different stress conditions with Nile Red (NR) based on the work by Cooksey *et al.*, (1987). A well grown *Desmodesmus armatus* culture (OD₅₉₅=1, late stationary phase) was diluted to OD=0.2 at 595 nm using fresh media. 1 ml of culture was added to an Eppendorf tube containing

5 µl of Gram's Iodine, then the tube was shaken to kill the cells and stop their motility. 10 µl of (100 µg/ml) of NR dissolved in DMSO was added to the tube and mixed by inversion, the penetration time of the dye was monitored. 10 µl of the NR stained culture was transferred to a clean microscope slide and a cover slip was added gently. The edges of the slide were then sealed with a nail varnish to avoid any possibility of evaporation. The slide was then placed in the microscope after the varnish was dried. The imaging of the samples was captured using Nikon Eclipse E400 Microscope attached with a Nikon DXM1200 digital camera. Excitation light of the samples was supplied by a Nikon Super High Pressure Mercury Lamp via 450-490 nm monochromatic optical filter. All images were taken using a 100x oil immersion lens after adding a drop of mineral oil onto the cover slip. For each sample, two images were taken, one by white light, and the other by excitation light. The monitoring of white light was carried out using the microscope iris while the fluorescence was monitored by the inbuilt shutter. The acquisition of the images was conducted using LUCIA G software capture settings: Red: 48, Green: 31, Blue: 68, Gain: 25, Gamma: 0.40, Offset: 23, Fine preview: on, Exposure: 72 ms.

2.9.2 Neutral Lipid Quantification using Nile Red dye

Determination of neutral lipid in *Synechocystis* PCC6803 and *D. armatus* were carried out using two protocols as described below:

2.9.2.1 Determination of Neutral Lipid without Microwave-Assistance

The quantification of neutral lipid in both strains was performed based on (Chen *et al.*, 2009; Bertozzini *et al.*, 2011; Pick and Rachutin-zalogin, 2012) using the lipophilic fluorescence Nile Red dye in 96 well plates in combination with a plate reader (Biotek, UK).

2.9.2.1.1 Determination of optimum cell concentration

To quantify the neutral lipid content of microalgae using Nile Red precisely, optimizing the concentration of algal cells was crucial. The cell concentration optimization was carried out as follows:

- 10 ml of well grown culture ($OD_{595}=1$) was transferred into 15 ml Falcon tube.
- The sample was then centrifuged for 5 min at 3000 *g*. The supernatant was discarded and an appropriate volume of fresh medium was added to the sample pellet, mixed well until reach $OD_{595}=1$.
- Serial dilutions of cell concentrations were prepared up to 2ml in Eppendorf tubes using fresh BG11 medium as shown in Table 2.7.

Table 2.7 Dilution scheme to produce a range of cell concentrations for Nile Red peak fluorescence test.

Percentage	100	87.5	75	62.5	50	37.5	25	12.5	Total (ml)
Culture (μ l)	2000	1750	1500	1250	1000	750	500	500	9
Medium (μ l)	0	250	500	750	1000	1250	1500	1500	7

Eppendorf tube was transferred to one of the 12 channels in a multi-pipette reservoir (Thermo Scientific), then using multichannel pipette, 4*200 μ l of each concentration (unstained) were transferred to the 96 well plate (E-H). After that, 200 μ l was withdrawn from each Eppendorf tube to make the final volume of each tube =1 ml. 20 μ l of Nile Red (from 15.9 μ g/ml stock solution dissolved in acetone) was transferred to each Eppendorf tube and the timer started. 800 μ l of each Nile Red stained cell concentration was transferred to another reservoir. 4*200 μ l of each concentration was transferred to the 96 well plate (A-D). The plate was then put in the plate reader after removing the lid of the plate as shown in (Figure 2.4). The settings for the plate reader were based on previous work (Bangert 2013) as shown in Table 2.7. To track the fluorescence, Gen5 2.05 software was used for 30 minutes at 5 minutes intervals.

Table 2.8 Plate reader sitting for the optimum concentration of algal cells.

Procedure sitting	
Plate type	96 well plate
Read	Fluorescence end point
	Full Plate
	Filter set 1
	Excitation :485/20, Emission :580/50
	Optics: Top, Gain:60
	Read speed: Normal

Conc. of Dilution from 1(A) @OD 595 %):(mg/ml)			100	87.5	75	62.5	50	37.5	25	12.5	Empty wells			
			1	2	3	4	5	6	7	8	9	10	11	12
stained Cells	R1	A	200	200	200	200	200	200	200	200	0	0	0	0
	R2	B	200	200	200	200	200	200	200	200	0	0	0	0
	R3	C	200	200	200	200	200	200	200	200	0	0	0	0
	R4	D	200	200	200	200	200	200	200	200	0	0	0	0
Unstained Cells	R1	E	200	200	200	200	200	200	200	200	0	0	0	0
	R2	F	200	200	200	200	200	200	200	200	0	0	0	0
	R3	G	200	200	200	200	200	200	200	200	0	0	0	0
	R4	H	200	200	200	200	200	200	200	200	0	0	0	0

Figure 2.4 96 well plate layout for the optimum concentration of algal cells, R1-R4 are technical replicates from the same concentration

2.9.2.2 Microwave-Facilitated Nile Red Quantification of Microalgal Neutral Lipid

2.9.2.2.1 Determination of the optimum algal cell concentration and peak time.

A series of 8 dilutions were prepared from late log phase of algal cells ($OD_{595}=1$) against dH_2O (Table 2.9). 1 ml of each algal cell dilution was then transferred into an Eppendorf tube, the ODs were measured at 595 nm for each dilution to offer ODs at the concentrations of the given culture.

Table 2.9 Serial dilutions of algal cells for the determination of cell concentration for Nile Red experiment

Percentage	100	87.5	75	62.5	50	37.5	25	12.5	Total(ml)
Culture(μ l)	1000	875	750	625	500	375	250	125	4.5
Medium(μ l)	0	125	250	375	500	625	750	875	3.5

The Eppendorf tubes were then centrifuged at 3000 *g* for 10 minutes, discarded the supernatant, and 20 μl of dH_2O were added to the pellets. 10 μl of resuspended algal pellet was transferred into two 2 ml screw top microfuge tubes, one of them was labelled as stained and the other was unstained. 50 μl of dimethyl sulfoxide (DMSO) were then added to each screw capped microfuge tube. All the tubes were heated in the Matsui microwave for 50 seconds at full power after loosely tightening the lid of the tubes. After the tubes were removed from the microwave, 930 μl of dH_2O were transferred to the stained tubes, and 490 μl of dH_2O were added to the unstained tubes. For the stained tubes, a timer was started at the time that 10 μl of 100 $\mu\text{g}/\text{ml}^{-1}$ (final concentration of NR in the tube is 1 $\mu\text{g}/\text{ml}^{-1}$) fluorescence dye dissolved in DMSO was added. All the stained tubes were microwaved again at full power for 60 seconds. The entire 1 ml of each stained tube was transferred to a multi-pipette reservoir. Using a multi-channel pipette, 200 μl aliquots of each stained tube were transferred to the 96 well plate rows from A to D, offering 4 technical replicates of each concentration. The same step was done for the unstained tubes in rows E to H as shown in Figure 2.4. The plate, after removal of the lid, was put into a 96 well plate reader. To track the fluorescence, Gen5 2.05 software was used for 30 minutes at 5 minutes intervals (Table 2.8).

The readings of the plate reader were then exported to an Excel sheet, then each four technical replicates (stained and unstained) of each concentration were averaged and the standard deviation of each average was then calculated. The values of stained cells were subtracted from the unstained to exclude any cellular background fluorescence. The net fluorescence was normalised and the best concentration of algal cells were then chosen based on the highest values of normalised with low standard deviation of the stained and unstained values and the best time of running.

2.9.2.2.2 Determination of the optimum concentration of Nile Red

Serial concentrations of NR (0.05, 0.1, 0.2, 0.3, 0.4, and 0.6 $\mu\text{mol ml}^{-1}$) were prepared from a 1 mg ml^{-1} stock of NR dissolved in DMSO as shown in Table 2.10.

Table 2.10 Nile Red concentrations prepared from the 1 mg ml^{-1} Nile Red stock.

Nile Red ($\mu\text{mol ml}^{-1}$)	Primary stock 1 mg ml^{-1} (μl)	DMSO (μl)
0.05	16	984
0.1	32	968
0.2	64	936
0.3	100	900
0.4	128	872
0.6	192	808

The optimum algal concentration chosen from the previous experiment (Section 2.9.2.2.1) was prepared to the optimum OD at 595 nm. 10 μl of algal cells were added into 2 screw capped tubes, one of them was labelled as stained and the other was labelled as unstained as described in section 2.9.2.2.1. The rest of the experimental steps were done in the same way except adding 10 μl of each concentration of Nile Red to the stained tubes. The final concentrations of Nile Red (0.16, 0.32, 0.64, 1.0, 1.28, and 1.92 $\mu\text{g ml}^{-1}$) were added in place of the 100 $\mu\text{g ml}^{-1}$ (1 $\mu\text{g ml}^{-1}$ final concentration) of Nile Red used in section 2.9.2.2.1.

NR final Concentration ($\mu\text{g ml}^{-1}$)			0.16	0.32	0.64	1.0	1.28	1.92	Empty wells					
			1	2	3	4	5	6	7	8	9	10	11	12
stained Cells	R1	A	200	200	200	200	200	200	0	0	0	0	0	0
	R2	B	200	200	200	200	200	200	0	0	0	0	0	0
	R3	C	200	200	200	200	200	200	0	0	0	0	0	0
	R4	D	200	200	200	200	200	200	0	0	0	0	0	0
Unstained Cells	R1	E	200	200	200	200	200	200	0	0	0	0	0	0
	R2	F	200	200	200	200	200	200	0	0	0	0	0	0
	R3	G	200	200	200	200	200	200	0	0	0	0	0	0
	R4	H	200	200	200	200	200	200	0	0	0	0	0	0

Figure 2.5 96 well plate layout of the optimum Nile Red concentration with optimum concentration of algal cells. R1-R4 are technical replicates from the same concentration.

The readings from the plate reader were then exported to Excel, the four replicates of each concentration were averaged, and the calculation of the standard deviations were conducted. The values of the stained cells were then subtracted from the unstained for each concentration. The optimum concentration of Nile Red was chosen according to the highest value of the stained subtracted unstained cells. The procedure and settings of the plate reader were the same as shown in Table 2.8.

2.9.2.2.3 Determination of Neutral lipids of *D. armatus* and *Synechocystis* cells.

The neutral lipid determination of *D. armatus* and *Synechocystis* cells grown under normal and various stress conditions (High salinity, N starvation, various N sources) were carried out weekly for 4 weeks as described in section 2.9.2.2.1 after optimising the cell concentration and Nile Red concentration to the optimum concentration.

2.9.2.3 Triolein calibration curve

A calibration curve of standard neutral lipid was made using triolein based on Bertozzini *et al.*, (2011). A 10 mg ml⁻¹ triolein lipid standard stock was prepared by dissolving 50 mg of triolein (Sigma T7410) with 5 ml isopropanol. Then 1 ml of this stock was used in the experiment. Eight algal samples were prepared under the optimised cell and Nile Red concentration and followed the same steps of the procedure up to the addition of 50 µl of DMSO and microwaving the stained and unstained tubes. During this step 910 µl of dH₂O were added to the stained labelled tubes and 920 µl of dH₂O were added to the unstained labelled tubes. Then various volumes of triolein and isopropanol (total volume 20 µl) was added to each stained and unstained tube to provide different concentrations of triolein (0.2, 0.16, 0.12, 0.08, 0.06, 0.04, 0.02, and 0 mg ml⁻¹) as shown in Table 2.11.

Table 2.11 Concentrations of triolein mixture for Nile Red fluorescence calibration curve.

Conc. Of Triolein (mg/ml)	0.2	0.16	0.12	0.08	0.06	0.04	0.02	0
Triolein(µl)	20	16	12	8	6	4	2	0
Isopropanol(µl)	0	4	8	12	14	16	18	20

After that 10 µl of the optimum concentration of Nile Red obtained from section 2.7.2.2 was added to each stained labelled tube, microwaved for 60 s at high power. 1 ml from each stained and unstained labelled tube was then transferred to a multi-pipette

reservoir, then 200 µl aliquots of each stained and unstained tubes were transferred to the 96 well plate rows as shown in Figure 2.6

Conc. Of Triolein (mg/ml)			0.2	0.16	0.12	0.08	0.06	0.04	0.02	0	Empty wells			
			1	2	3	4	5	6	7	8	9	10	11	12
stained Cells	R1	A	200	200	200	200	200	200	200	200	0	0	0	0
	R2	B	200	200	200	200	200	200	200	200	0	0	0	0
	R3	C	200	200	200	200	200	200	200	200	0	0	0	0
	R4	D	200	200	200	200	200	200	200	200	0	0	0	0
Unstained Cells	R1	E	200	200	200	200	200	200	200	200	0	0	0	0
	R2	F	200	200	200	200	200	200	200	200	0	0	0	0
	R3	G	200	200	200	200	200	200	200	200	0	0	0	0
	R4	H	200	200	200	200	200	200	200	200	0	0	0	0

Figure 2.6 96 well plate layout of different concentrations of triolein mixture for the calibration curve. R1-R4 are technical replicates from the same concentration

The 96 well plate was then placed in the plate reader after removing the lid, the samples were run using same procedure described in Table 2.8. The results of the fluorescent intensity of both stained and unstained cells were then exported to an Excel sheet. The 4 replicates results of each concentration were averaged, and the standard deviation was calculated. The values of stained cells were subtracted from the unstained cells. The relationship between the concentrations of triolein mixture versus the Nile Red fluorescence intensity was illustrated by drawing a calibration curve. Then each fluorescence intensity value achieved by different treatments was converted to concentration of lipid based on the Excel sheet equations as follows

For *D.armatus* , $X=Y/53590$

For *Synechocystis*, $X= Y/192916$

Where X= concentration of Triolein (mg/ml) and Y =Nile Red Fluorescence Intensity

2.10 Relationship between OD and Dry Weight

The relationship between OD and the algal cell dry weight was measured, based on Storms *et al.*, (2014) with some modifications, by preparing a set of well grown *D. armatus* and *Synechocystis* cultures ($OD_{595}=1$) (final volume of each dilution is 30 ml) in 50 ml Falcon tubes using fresh BG11 medium as shown in Table 2.12 ml of each dilution was taken to measure the OD at 595 nm, then the sample was returned to the tube after measurement.

Table 2.12 Concentrations of *D. armatus* cells for preparation of Dry weight versus OD.

Tube number	Conc. (%)	Culture(ml)	Medium (ml)
12	0.0	0	30.0
11	8.3	2.5	27.5
10	16.6	5.0	25.0
9	33.3	10.0	20.0
8	41.6	12.5	17.5
7	50.0	15.0	15.0
6	58.3	17.5	12.5
5	66.6	20.0	10.0
4	75.0	22.5	7.5
3	83.3	25.0	5.0
2	91.6	27.5	2.5
1	100.0	30.0	0.00

All tubes were centrifuged at 3000 *g* for 5 min, the supernatants were discarded then the pellets were resuspended with 5 ml dH₂O and transferred to 15 ml Falcon tubes. The tubes were centrifuged, the supernatants were discarded and the pellets were resuspended with 1 ml dH₂O. Then the suspended cells were transferred to pre-weighed Eppendorf tubes. The tops of the Eppendorf tubes were removed, then holes were made in extra tops to seal the Eppendorf tubes containing the samples. Eppendorf

tubes were then frozen overnight at -80 °C and then freeze dried (lyophilised) for 24-48 hours until the samples were fully dried. The tops with holes were discarded and the Eppendorf tubes were resealed with their own tops and the tubes were weighed. The dry weight of each sample was calculated and a concentration curve was prepared using Excel. Then the OD value of the optimum cell concentration was converted to dry weight value (mg ml^{-1}) based on the Excel sheet equations as follows:

For *D. armatus* , $Y=0.5168x$

For *Synechocystis*, $y=0.5323x$

Where Y = Dry weight (mg/ml) and $x = \text{OD}_{595}$

Then, the percentage of neutral lipid was calculated by dividing the concentration of neutral lipid by the value of the cell dry weight and multiplying by 100.

2.11 Nuclear Magnetic Resonance (NMR) determination of neutral lipid

The lipid analyses of *D. armatus* cells using Proton Nuclear Magnetic Resonance ($^1\text{H-NMR}$) were carried out based on the method from Derome, (1987) with help from Prof Mike Williamson, MBB department –University of Sheffield. Duplicate 20 ml samples of well grown *D. armatus* cells ($\text{OD}_{595}=1$) were centrifuged for 10 min at 3000 g , the supernatants were discarded and the pellets were washed with 1 ml dH_2O . The cell suspensions were then bead beaten for 3 min at 3000 g , then each tube was centrifuged for 5 min at 3000 g using a microfuge. The supernatant of each tube was transferred to a new Eppendorf tube and a lid with a hole made from another Eppendorf tube was put on it, then samples were frozen at -80 °C overnight and freeze dried (lyophilised) for 24-48 hours until the samples were totally dried. The lids with holes were removed and the tubes were sealed with their own lids, and the weight of biomass was estimated by weighing the sample tubes. The biomass of the samples was solubilized by adding 400 μl of deuterated chloroform (CDCl_3) and 100 μl of deuterated methanol (CD_3OD), mixed and transferred to a 5 mm NMR tube, then 5 μl of chloroform (CHCl_3) was added as an internal standard. NMR spectra were obtained on a BrukerAvance 600 equipped with a cryoprobe. Data were recorded into 16k complex data points with simple pulse-acquire

pulse program and a 3 s recycle time. Fourier transformation was applied using a 1 Hz line broadening followed by manual baseline correction. All spectra were acquired using 8 scan (with 4 dummy background scans). Software Bruker Topspin V1.3 was used for processing and integration. The differentiation of all signals in the NMR spectra was based on the spectral features described by (Kumar *et al.*, 2014; Sarpal *et al.*, 2015).

2.12 Analysis and Quantification of Fatty Acid Composition

2.12.1 Transesterification of Algal Cells

Preparation of *D. armatus* fatty acid methyl esters (FAMEs) was conducted based on the procedure of *in-situ* direct transesterification plus gas chromatography (GC) adapted by (Van Wychen and Laurens, 2013) and (Laurens *et al.*, 2012). Total algal lipid (including phospholipid and galactoglycerolipid) were transesterified to FAME using an acid catalysed reaction.

An aliquot (40 ml from three replicate cultures) of late stationary *D. armatus* cells grown in nitrogen free BG11 medium (30 days growth) was centrifuged for 5 minutes at 2500 *g*, the supernatant was discarded and the pellet was resuspended with 1 ml of dH₂O. The cell suspension was transferred to new pre-weighed Eppendorf tube and sealed with a lid from another Eppendorf tube containing a hole, the tubes were frozen overnight, then freeze dried (lyophilised).

From each sample, 5-10 mg of freeze dried *D. armatus* were transferred to 2 ml crimp vials (9301-1388, Agilent). The following solutions were added respectively to each sample vial:

300 µl of 0.6 M HCl: methanol, 200 µl of chloroform: methanol (2:1 v/v) and 20 µl of tridecanoic acid methyl ester (C13: ME, 10 mg ml⁻¹) using gas-tight syringes (100 µl and 20 µl, Hamilton). The crimp vials were promptly sealed with PTFE/silicone/PTFE septa crimp caps (5181-1211, Agilent). The use of C13 methyl ester as a recovery standard was convenient for many reasons including monitoring the variability between FAME and the solvent evaporation. Moreover, utilising a free fatty acid (FA) as a recovery played an important role in correction for the efficiency of the transesterification

reaction. Despite this the inferred efficiency probably does not consider all the lipid because there were some non-FA lipid compounds transesterified. However, the improvements to this procedure led to the transesterification efficiency of several pure lipid compounds to be close to 100% (Laurens, personal communication, 2015).

Sealed vials were immediately transferred to a pre-heated hot plate at 85°C for 60 minutes to enable the transesterification reaction to happen. After incubation, the samples were removed from the hot plate and cooled at room temperature for at least 15 minutes. To extract FAME from the mixture, 1 ml of HPLC grade hexane was added to each vial using a gas tight syringe (1 ml polypropylene syringe, BD Plastipak) and hollow core needles (25 mm, BD Microlance) without removing the cap. This was achieved by piecing the cap with a second needle to equalise internal pressure (directed away from first needle). The vial was vortexed for 10 seconds then left to separate for 60 minutes at room temperature.

For GC analysis, samples were prepared by dilution depending on estimated FAME concentration. Samples with high lipid content (nitrogen starved treatment) were diluted by HPLC grade hexane by transferring 50 µl of the upper phase of the sample to a 2 ml GC vial with 450 µl of hexane. For low expected lipid samples (samples grown in normal medium) a 1:4 ratio was used. The same technique was used to avoid removing sample cap when transferring the upper phase, however, a 100 µl glass gas-tight syringe (Hamilton) was used in place of the plastic syringe, washing with hexane 3 times between samples. Once the dilution was prepared the vials were immediately capped. The remainder of two phase samples were recapped and stored at -20°C.

From each diluted sample, a 200 µl aliquot was transferred to a 300 µl GC vial (9301-1388, Agilent).

5 µl of pentadecane (C15, 1 mg ml⁻¹) was added to each vial. The new vials were capped immediately. Pentadecane was used as an internal standard to correct for instrument variability and solvent evaporation during FAME analysis.

2.12.1.1 Preparation of FAME Standards

A series of FAME standards were prepared from 10 mg/ml C4:0 - C24:0 FAME mix (18919-AMP, 37 Component Mix, Supelco) and HPLC grade hexane as follows: (500:500, 250:750, 100:900, 30:970, 10:990 μ l, respectively). In addition, a calibration verification standard (CVS) was created by mixing 90 μ l FAME mix and 910 μ l hexane. The standards were stored upright at -20°C until the samples were run using GC-MS.

2.12.1.2 GC-MS analysis of FAME

FAMES of the samples were analysed by gas chromatography mass spectrometry (GC-MS) using an AutoSystem XL Gas Chromatograph (CHM-100-790, Perkin Elmer) coupled with a TurboMass Mass Spectrometer (13657, Perkin Elmer). The GC was fitted with a Zebtron™ ZB-5ms, 30m x 0.25 mm ID x 0.25 μ m FT (7HG-G010-11, Phenomenex) GC capillary column. Samples were injected (5 μ l volume) via an auto-sampler onto the column and eluted at an injection temperature of 250°C with a 100:1 split ratio and a He constant carrier flow (1 ml min⁻¹). A temperature programme (FAME_FINAL) was optimised for peak separation of C18:1 fatty acid isomers. The optimised temperature programme was set to 120°C (hold for 1 minute) to 140°C (hold for 2 minutes) at 5°C min⁻¹, followed by ramp up to 170°C (hold for 2 minutes) at 2°C min⁻¹, and finally ramp up to 250°C at 1°C min⁻¹. The mass spectrometer was operated in electron ionisation (EI+) mode. Start mass was set to 50 and end mass to 600. Scan time was 90 minutes.

2.12.1.3 Quantification of FAME

Identification of sample peaks and relative quantification was performed using Turbomass software (Ver 5.2.4, Perkin Elmer) and the National Institute of Standard Technology (NIST) spectral database. Automatic and manual peak integration and base line separation were carried out in the quantification tool of the software. A response was calculated for each dilution point of each FAME component of interest based on the FAME standard dilution series. The response was calculated by the software using the following formula,

$$\text{Response} = \text{Area}_{\text{FAME}} \times \frac{\text{Conc}_{\text{S}}}{\text{Area}_{\text{S}}}$$

Where, $Area_{FAME}$ is the peak area (height and width) of a FAME component, $Area_{IS}$ is the peak area of the internal standard (pentadecane), and $Conc_{IS}$ is the known concentration of internal standard (set to relative quantity of 1 for each sample).

A linear regression was then performed with the response and relative FAME component concentration. The resultant slope equated to the response factor used to convert area to relative concentration. Due to the number of components within the samples the standard concentrations were set to relative concentrations of 500, 250, 100, 30 and 10. These relative concentrations represent the fractions of the original 10 mg ml^{-1} FAME standard (Section 2.12.1.1) multiplied by 1000 to increase resolution (software rounds to 2 decimal places). All linear regression had a R^2 of >0.99 . Subsequently the Turbomass software calculated the relative concentration (relative to FAME standard) of each FAME component within the sample extract using the following equation.

$$Conc_{rel} = Area_{FAME} \times RF$$

where, $Conc_{rel}$ is relative concentration, and RF is the response factor calculated by linear regression of FAME standard response.

FAME compounds within the sample which were not present in the FAME standard were calculated using recommended similar isomers (for example C16:2 concentration within the sample was calculated using C18:2n6 response factor) described in the NREL methodology ((Van Wychen and Laurens, 2013).

Relative concentrations were converted to normalised absolute values using a series of steps using Excel (Ver 14.0.7153.500, Microsoft). First, the relative concentration was converted to a fraction of the 10 mg ml^{-1} FAME standard by dividing by 1000. The same concentrations were relative to the standard concentration; therefore, a sample with a given concentration of exactly 500 was the same concentration as the 500 standard, which is half (0.5) the concentration of the original 10 mg ml^{-1} FAME standard (Section 2-12-1-1). The fraction is then multiplied by the absolute concentration ($\mu\text{g ml}^{-1}$) of that FAME component within the FAME standard. For example, C16:0 made up 5.98% of the

FAME mix, therefore was present at 598 $\mu\text{g ml}^{-1}$ within the 10 mg ml^{-1} FAME standard. Following equation was used for this step;

$$\text{Conc}_{\text{abs}} = \frac{\text{Conc}_{\text{rel}}}{1000} \times \text{Conc}_{\text{FS}}$$

where, Conc_{abs} is absolute concentration ($\mu\text{g ml}^{-1}$), Conc_{rel} is the relative concentration produced by the Turbomass software, and Conc_{FS} is the standard concentration of the relevant FAME component.

This absolute concentration is then normalised for the quantity of the recovery standard and the dilution factor used in preparation step (Section 2.12.1.1). This step is described in the following equation;

$$\text{Conc}_{\text{norm}} = \left(\left(\frac{\text{Conc}_{\text{abs}}}{\text{Conc}_{\text{abs-C13}}} \right) \times \text{Conc}_{\text{C13}} \right) \times \text{DF}$$

where, $\text{Conc}_{\text{norm}}$ is the normalised absolute concentration of FAME component ($\mu\text{g ml}^{-1}$), the $\text{Conc}_{\text{abs-C13}}$ is the calculated absolute concentration of C13:0 within the sample, Conc_{C13} is the known added concentration of C13:0 (after dilution), and DF is the dilution factor.

To convert to total FAME per unit of dry cell weight (mg), the sum of all FAME components was divided by the DCW (mg) used for each sample:

$$\mu\text{g mg DCW}^{-1} = \frac{\sum \text{Conc}_{\text{norm}}}{\text{DCW}}$$

Finally, the percentage of each component of the total FAME (fame profile) was calculated using the following equation:

$$\mu\text{g FAME mg DCW}^{-1} = \frac{\text{Conc}_{\text{norm}}}{\sum \text{Conc}_{\text{norm}}} \times 100$$

2.13 Flow Cytometry Analysis of Neutral Lipid Content

Flow cytometry technique was used for the analysis of neutral lipid in *D. armatus* cells irradiated with UV light for different time periods as described in section 2-14, in combination with Nile Red fluorescence based on the method described by Satpati and Pal, (2014)

2.13.1 Determination of DMSO Concentration

Different concentrations of DMSO ranging from (10-60%) were prepared with dH₂O and used to identify the best concentration of DMSO to be used in the experiment. An aliquot of 500 μ l from UV irradiated *D. armatus* cells for different time periods (OD=1.5 after 30 days culture) was transferred to a 2 ml Eppendorf tube, 7 of these tubes were labelled as stained and 7 were labelled as unstained, One of these tubes was not UV irradiated and treated as control Then, 5 μ l of 100 μ g ml⁻¹ (0.6 μ g ml⁻¹ final concentration) of Nile Red solution was added to stained tubes. From each concentration of DMSO, 295 μ l was transferred to the one of the stained tubes and 300 μ l was transferred to unstained tubes and the final concentrations of DMSO were (3,7,11,15,18,22%). All the tubes were vortexed and left in dark at room temperature for 10 min. After that, the stained and unstained tubes were washed (2-3) times with 1 ml of phosphate buffer (PBS), then the samples were transferred to a multi-pipette reservoir (Thermo Scientific). Using a multi-channel pipette, 200 μ l aliquots of each stained tube were transferred to the 96 well plate rows from A to D, offering 4 technical replicates of each concentration. The same step was done for the unstained tubes in rows E to H as shown in Figure 2-7.

DMSO Conc (%)			10	20	30	40	50	60	Empty wells					
			1	2	3	4	5	6	7	8	9	10	11	12
stained Cells	R1	A	200	200	200	200	200	200	0	0	0	0	0	0
	R2	B	200	200	200	200	200	200	0	0	0	0	0	0
	R3	C	200	200	200	200	200	200	0	0	0	0	0	0
	R4	D	200	200	200	200	200	200	0	0	0	0	0	0
Unstained Cells	R1	E	200	200	200	200	200	200	0	0	0	0	0	0
	R2	F	200	200	200	200	200	200	0	0	0	0	0	0
	R3	G	200	200	200	200	200	200	0	0	0	0	0	0
	R4	H	200	200	200	200	200	200	0	0	0	0	0	0

Figure 2.7 96 well plate layout of different concentrations of DMSO mixture for determination of the best concentration of DMSO that was used in the flow cytometry.

R1-R4 are technical replicates from the same concentration.

2.13.2 Optimising Nile Red Concentration

After determination of the ideal concentration of DMSO as described in section (2-13-1), the Nile Red concentration was optimised by preparing serial concentrations of Nile Red with DMSO ranging from (0.1 – 1.2 µg/ml final concentration). The same steps were carried out except adding 5 µl of each concentration of Nile Red to one of the stained tubes. After the cell washing with PBS, the stained and unstained tubes were transferred to run through the flow cytometry.

2.13.3 Flow Cytometry Analysis

The analysis of *D. armatus* cells staining with Nile Red were carried out using a high-speed flow cytometer BD LSRII (BD Bioscience, Figure 2.8) based on (Velmurugan *et al.*, 2013). To obtain the fluorescence readings, the Nile Red stained cells at different concentrations were excited with a 475-nm laser, and the emission was 568/42 nm while the unstained cells were utilised as an auto-fluorescence control. The features of the *D. armatus* cells including cell size and granularity using flow cytometry were obtained by Forward scatter (FSC) and side scatter (SSC) signals. Flow cytometry data were analysed depending on many parameters including the stained cells grandparents' percentage, and median of the stained cells using Flow Jo software.



Figure 2.8 High speed flow cytometry BD LSRII Flow cytometry

2.14 Random Mutation of *D.armatus* Cells

Induced random mutations using Ultra Violet (UV) light were used to attempt to increase the lipid content of *D. armatus cells* based on method described by (Bougaran *et al.*, 2012). Well grown *D. armatus* cells (OD_{595} approximately 1) were irradiated for different time periods (3, 6, 9, 12, 16, 32, 48, 60 min) using a UV – C lamp at 254 nm

(Upland, CA 91786 USA). The UV exposure was achieved by adding 12 ml of the *D. armatus* culture into a 90-mm sterile Petri dish (Thermo Scientific), the plate was transferred under the UV lamp and after taking off the lid of the Petri dish the distance between the lamp and the dish was about 13.5 cm.

Three replicates were prepared for each irradiation time. The cells were transferred into pre-autoclaved 100 ml BG11 medium flasks. To minimise the probability of photoreactivation that would lead to photorepair of UV-Induced damage, the flasks were kept in dark for 24 h. The OD₅₉₅ and cell count for each flask were measured directly after exposure and over the next 8 days. The samples were then incubated for 30 days. Then, the neutral lipid content of the mutated cells was analysed as described in 2-13-3 using cells at OD 1.5 =10⁶, and Nile Red concentration at 128 µg/ml.

2.14.1 UV Mutant Cells Sorting

After the data of UV mutant cells were analysed, the optimum condition cells were sorted using (BD FACS Aria™ IIU, Figure 2.9) based on (Terashima *et al.*, 2015). The optimum condition of samples were re-exposed to UV at the time that achieved the highest mean of stained cells as described in section 2-13-3. Then the samples were re-prepared as described in section 2-14-1 but with one concentration of Nile Red (the concentration that gave the highest mean of stained cells). After that, 1 ml of the unstained sample (control) was run through a high-speed flow cytometry to make a gate. The spreading of stained cells was exploited as a control to fix the high lipid gate for expected mutant cells. The upper 3% of the stained cells was fixed as a high lipid gate. Then, all cells that chop down the gate were accumulated into sterile vials containing 1 ml autoclaved BG11 medium.

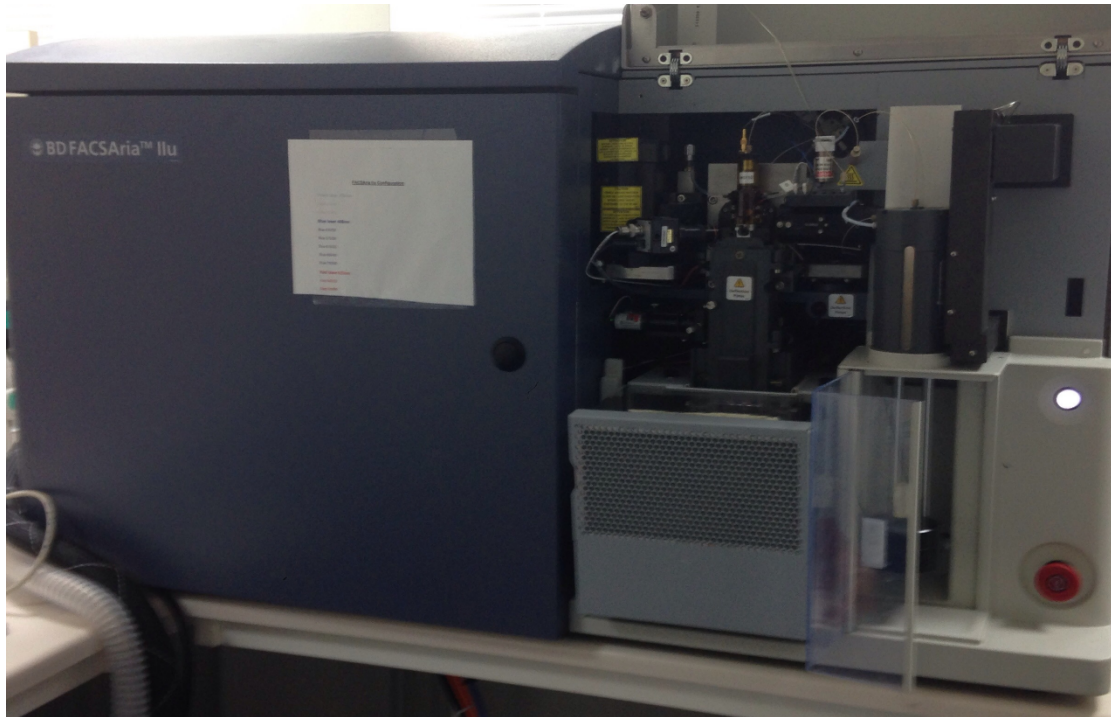


Figure 2.9 BD FACS Aria for sorting of mutant cells

2.14.2 Selection of Mutated Cells

The sorted cells were transferred to 96 well plate according to (Lim *et al.*, 2015) for the selection of single mutated cells. Single cell cloning serial dilution technique was used to achieve single sorted cells. All the wells of the plate filled with 100 μl of BG11 medium. 1000 sorted cells were transferred from the sorted tube to the first well of the plate (A1) to the final volume of 200 μl . then 100 μl was transferred from well A1 to B1 after mixing well, the steps were continued to the well H1, then 100 μl of the mixture was discarded from H1 well. 100 μl of the diluted cells were transferred to the A2 wells (A2 to H2) and then transferred consequently to all wells of the plate. Finally, 100 μl of the diluted cells were transferred to (A1-H1) wells of the plate from A12-H12) wells. The same single cell technique was conducted with the wild type cells to be exploited as a control. Then the plates were incubated at $25 \pm 1^{\circ}\text{C}$ with continuous light ($50 - 70 \mu\text{mol m}^{-2} \text{s}^{-1}$). All the cells in each well was tested on the next day using an inverted microscope (Olympus CK40 culture microscope) to differentiate the wells that contain single cells and label the well. After the single cells were grown well, the growth was transferred to a 12-well plate containing 2 ml BG11 medium. After the cells grown well they were

transferred into a 250-ml flask containing 100 ml BG11 medium. The cells were grown for a month, and subsequently the neutral lipid content of 13 single UV mutated cells and the wild type cells (used as control) were analysed using Flow cytometry after staining with 1 µg/ml and followed the same steps of flow cytometry analysis of neutral lipid described in section 2.13.2 and 2.13.3.

2.14.3 Nile Red determination of the wild type and UV exposed *D.armatus*. neutral lipid

The neutral lipid of both wild type and UV exposed *D. armatus* cells grown on both normal BG11 and N free BG11 for 14 days were determined using Nile red dye as described in section 2-9-2-2-1 using an optimum concentration of cells ($OD_{595}=50\%=200 \mu\text{g ml}^{-1}$ Dry weight) of cells and Nile Red concentration ($1 \mu\text{g ml}^{-1}$), the neutral lipid concentration and percentage of lipid were determined as described in section 2.10.

2.15 statistical analysis

Comparison of mean values of highest stress condition against the normal conditions were conducted using Excel T test, in all cases, comparisons that showed a *p* value <0.05 were deemed significant.

**Chapter Three Isolation
and Identification of Pond
Water Isolate and
Synechocystis sp. PCC6803**

3.1 Introduction

More than 100,000 of various microalgae species occur worldwide, However, just around 30,000 species have identified (Mata *et al.*, 2010). In recent years, many algal research institutes and culture collections have attempted to classify and store different algal species, for instance, about 4000 strains and 1000 species of fresh water algae have been identified and maintained in the Collection of Freshwater Algae at the University of Coimbra, Portugal (Mata *et al.*, 2010). Fresh water microalgae have been one of the optimum sources for production of variable bioproducts that could be utilized in industrial fields such as lipids, which are being considered as a promising source for biodiesel feedstock (Chisti, 2007; Sharma *et al.*, 2014), antioxidants and emulsifiers used in nutrition sector (Chisti, 2007; Ahmed *et al.*, 2014).

Among the vast number of isolates, only a few species of microalgae have been exploited as feedstock sources for biodiesel production (known as oleaginous microalgae) including *Chlorella* sp., *Botryococcus*, *Scenedesmus* sp. and *Nannochloropsis* (Nascimento *et al.*, 2013; Rodolfi *et al.*, 2009; Selvarajan *et al.*, 2015; Gour *et al.*, 2016). Many factors have influenced the selection of microalgal strains for biodiesel production and the framework for selection of ideal microalgae has been illustrated by Griffiths and Harrison, (2009). Fast growth rate under regional weather of the selected area is considered a vital factor that affects the choice of a candidate microalga. Numerous studies have recognized the key factors that lead to a robust growth rate of microalgae and consequently enhance the lipid content like temperature, pH, light period and nutrition (Lv *et al.*, 2010; Adams *et al.*, 2013; Sforza *et al.*, 2012). However, the growth dynamics of each microalga is mainly dependent on the geographical location that it was isolated from. Therefore, optimisation of growth conditions is essential for each isolated strain. Moreover, the screening of an ideal microalgal strain for biodiesel production should not only rely on the percentage of lipid, but also on the lipid profile i.e. degree of unsaturation, chain length etc. (Ren *et al.*, 2013).

The accurate identification of microalgal strains is an important part of the selection process for oleaginous microalgae useful for biodiesel production. In phylogenetic terms, it is possible that closely related strains to existing oleaginous algae have the

ability to produce high lipid (Duong *et al.*, 2012). The conventional protocols of identifying microalgae have passed through different parameters including the traditional total reliance on characterization of cell morphology and colony shape (Boyer *et al.*, 2001). Another taxonomic technique of algal identification is based on the life cycle and shapes of flagellated cells (Christensen, 1964). Mattox and Stewart, (1984) have explored different methods of algal classification based on the characteristics of the basal body in flagellated cells and cytokinesis during mitotic division. All these microscopic based techniques probably provide an overview of the algal group in the sample. However, it seems to be an imprecise way for strain identification from a mixed culture because of a) well qualified expertise in algal morphology is required; b) shortage of morphological differences between closely related microalgal genus or species may lead to mistakes in classification and c) it is time consuming (Hu *et al.*, 2008; Abou-shanab *et al.*, 2011).

Recently, molecular DNA based protocols have become universally utilized for the taxonomic description of microalgae isolated from natural diversity. This modern technique for classification seems to be a golden criterion that offers unequivocal sequences related to a large number of algae isolated from different environments and saved in the various gene bank sequence databases (Gour *et al.*, 2016). However, these modern techniques triggered a drop in the percentage of officially termed new algal species from 90% in 2000 to 20 % in 2010 (Clerck *et al.*, 2013). Molecular taxonomy of microalgae has been based mainly on a pair of primers that correlated to the most diverse group of microorganisms, recovering a short marker (around 700bp) of sufficient difference for precise differentiation (CBOL Plant Working Group, 2009). Many markers have commonly been exploited for identification of some algal strains, for instance *rbcl* (rubisco large subunit), ITS (internal transcribed spacer), and *tufA* (plastid elongation factor). However, 18S rDNA is a frequent molecular marker used in the phylogeny of green algae (Baldauf *et al.*, 1990; An *et al.*, 1999; Hall *et al.*, 2010; , Buchheim *et al.*, 2011; Vieira *et al.*, 2016) which represents a highly conserved gene. Other genes may be necessary to differentiate between closely related green algae.

The objective of the work described in this chapter was to isolate a local microalgal strain(s) from water samples collected from Weston Park, Sheffield, United Kingdom,

identify the strain using 18S rDNA, and ITS region primers. Moreover, confirm the identity of *Synechocystis* sp. PCC6803 obtained from Prof. Hunter's lab using 16S rDNA (analogous gene in prokaryotic cells).

3.2 Results

3.2.1 Growth of strains

Two standard strains of *Synechocystis* sp. PCC6803 (Vermass & Nixon, see Figure 2.2.) were grown in BG11 media as described in section 2-3. The growth rates of both *Synechocystis* strains were investigated daily to choose the fastest growing strain based on the growth curve of each strain for a week. The results showed that the Vermass *Synechocystis* strain grew faster than Nixon strain in BG11 medium (Figure 3.1). Moreover, Nixon strain cells were found as double cells under microspore examination which was probably an undesirable feature for ongoing experiments. Therefore, the Vermass *Synechocystis* strain was chosen for all future work.

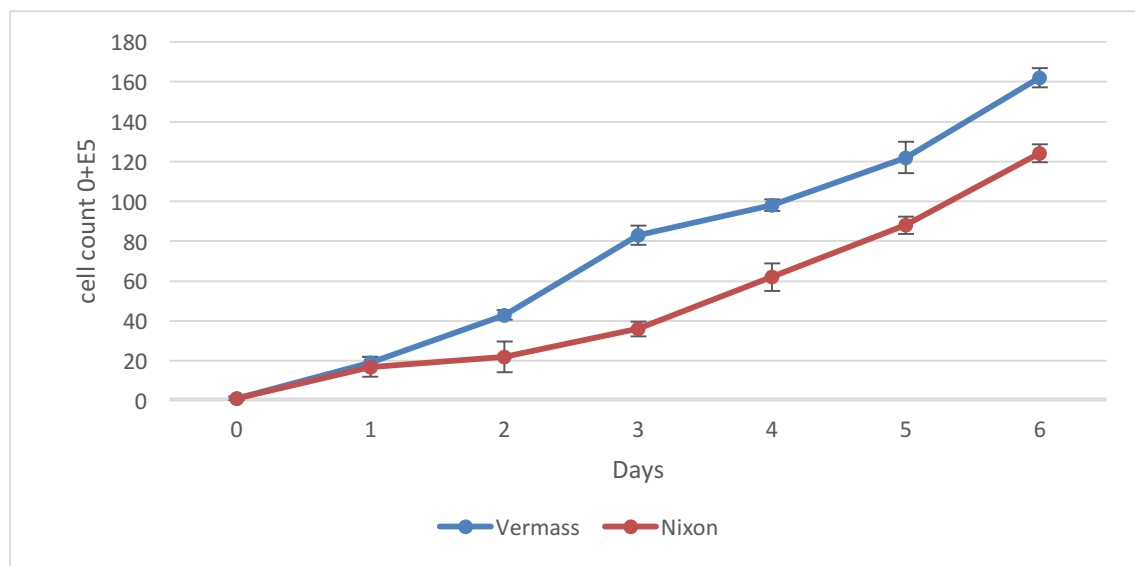


Figure 3.1 Growth curve comparison of two *Synechocystis* PCC6803 strains (Vermass and Nixon)

For pond water samples, the results of microscopic examination of the samples collected from different places in Weston Park were contaminated with bacteria. Therefore, different purification techniques were conducted including Percoll gradients and centrifuge washing techniques (section 2.6) until obtained an axenic strain. During this process, one green microalga became dominant in the axenic cultures and it appeared under the microscope to be morphologically similar to *Scenedesmus* i.e. 2 to 4 rod-shaped cells joined by their long axes forming coenobia.

3.2.2 Molecular Identification of *Synechocystis* sp. and pond water isolate

3.2.2.1 Genomic DNA extraction of Pond water isolate and *Synechocystis* sp.

For precise identification of *Synechocystis* and the pond water isolate, molecular identification was performed as described in section 2.7. The genomic DNA of *Synechocystis* sp. strain was extracted using two protocols (CTAB and ZR Microbe Soil Kit). The results in Figure 3.2 showed that there is no band of genomic DNA using CTAB protocol. In contrast, Figure 3.3 showed clear bands of genomic DNA extracted from *Synechocystis* sp. using ZR microbe Soil Kit

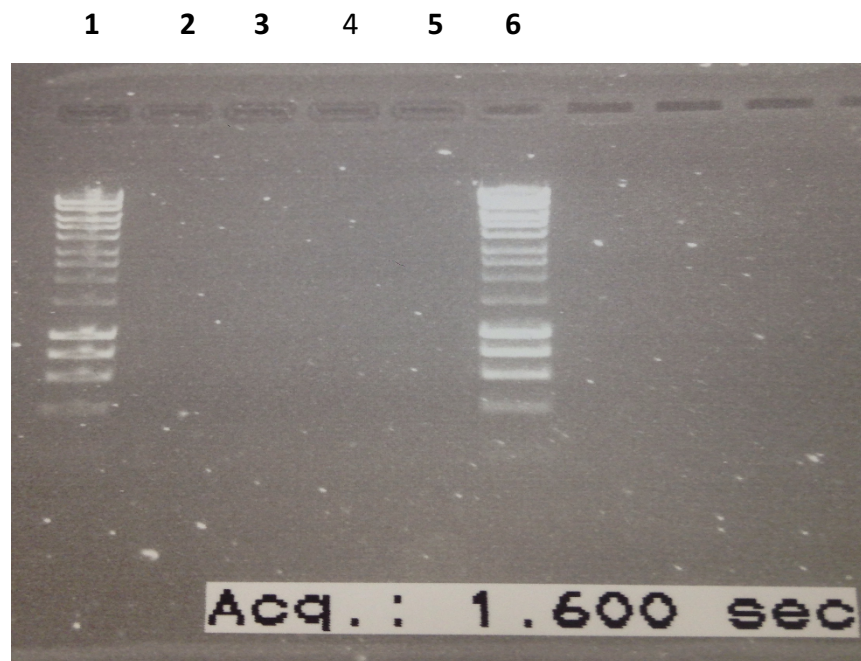


Figure 3.2 Extraction of DNA from *Synechocystis* sp. PCC6803 using CTAB protocol and run in a 1% Agarose gel . Lane 1: 1Kb DNA ladder; Lanes 2, 3, 4, 5: *Synechocystis* PCC 6803 genomic DNA extracted from 5 ml ,10 ml, 15 ml,and 20 ml culture (OD₅₉₅=1); Lane 6: 1Kb DNA ladder

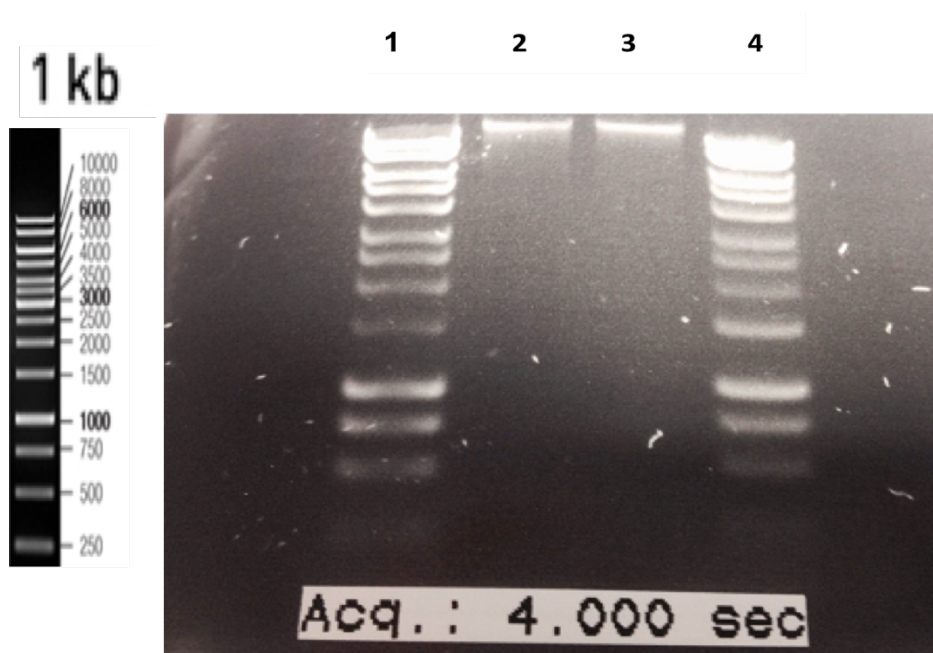


Figure 3.3 Extraction of DNA from *Synechocystis* PCC6803 using ZR Microbe Soil kit protocol and run in a 1% Agarose gel. Lane 1: 1Kb DNA ladder; Lane 2: *Synechocystis* PCC 6803 genomic DNA extracted from 20 ml culture ($OD_{595}=1$); Lane 3: *Synechocystis* PCC 6803 genomic DNA extracted from 40 ml culture ($OD_{595}=1$); Lane 4 : 1 Kb DNA ladder.

For pond water isolate, genomic DNA extraction was carried out using ZR Microbe Soil Kit protocols. The results showed clear bands of genomic DNA figure (Figure 3.4).

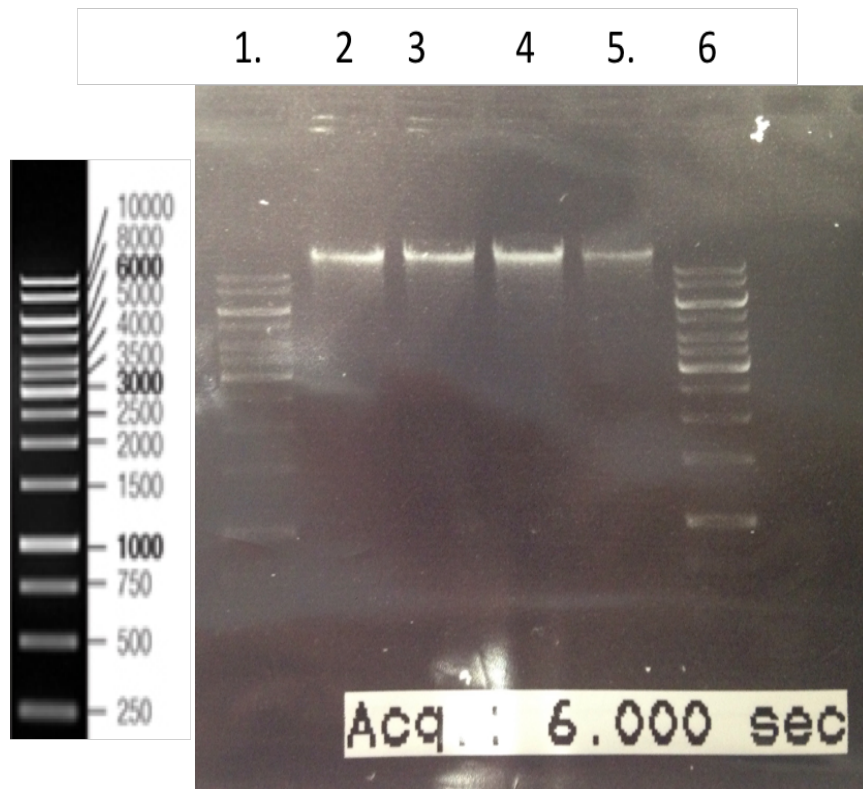


Figure 3.4 Extraction of DNA from pond water isolate using ZR Microbe Soil kit protocol run in a 1% Agarose gel. Lane 1: 1Kb DNA ladder; Lanes 2, 3, 4, 5: pond water isolate genomic DNA extracted from 5, 10, 15 and 20 ml of well grown culture (OD=1), Lane 6: 1Kb DNA ladder.

3.2.2.2 PCR amplification

Synechocystis sp. PCC6803 genomic DNA was amplified using 16S rRNA primers as described in section 2-7-3. The results showed successful amplification of the 16S rDNA genes (Figure 3.5) with two clear bands (approximately 1500 bp)

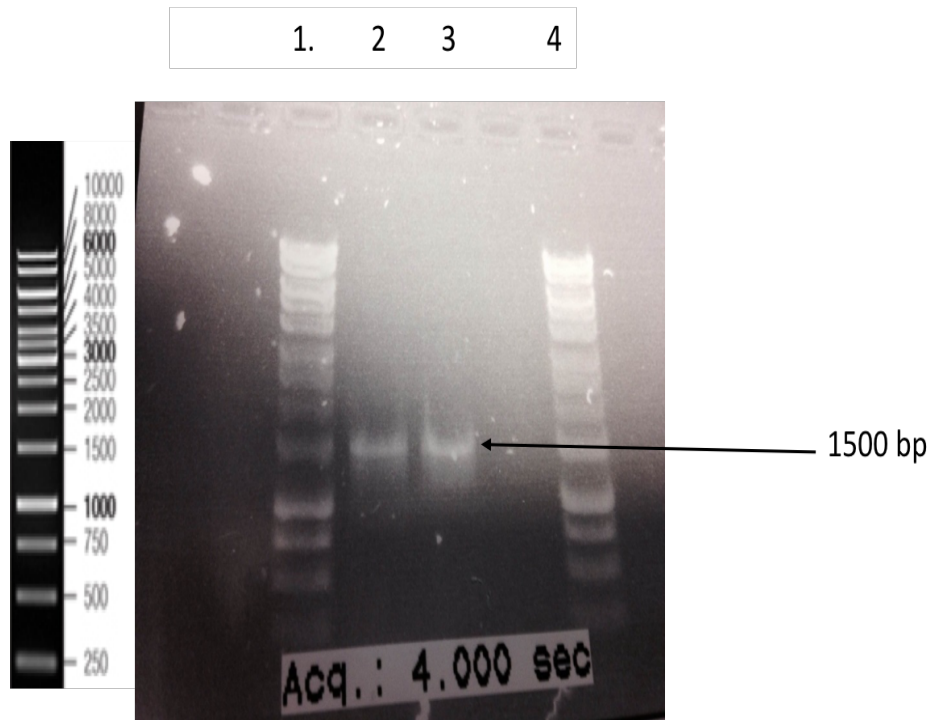


Figure 3.5 PCR amplification of *Synechocystis* PCC 6803 genomic DNA using 16S rRNA primers. Lane 1: 1Kb ladder, Lanes 2, 3: 16S rRNA PCR amplification of *Synechocystis* PCC 6803 genomic DNA, Lane:4: 1Kb ladder.

For pond water isolate, the 18S rRNA genes were amplified using two different 18S rRNA primers (Lim & Sheehan) as described in section 2.7.3. Figure 3.6 showed the successful amplification of 18S rRNA using Lim primers by the appearance of clear bands (approximately 500 bp). While, there was no band when Sheehan primers were used.

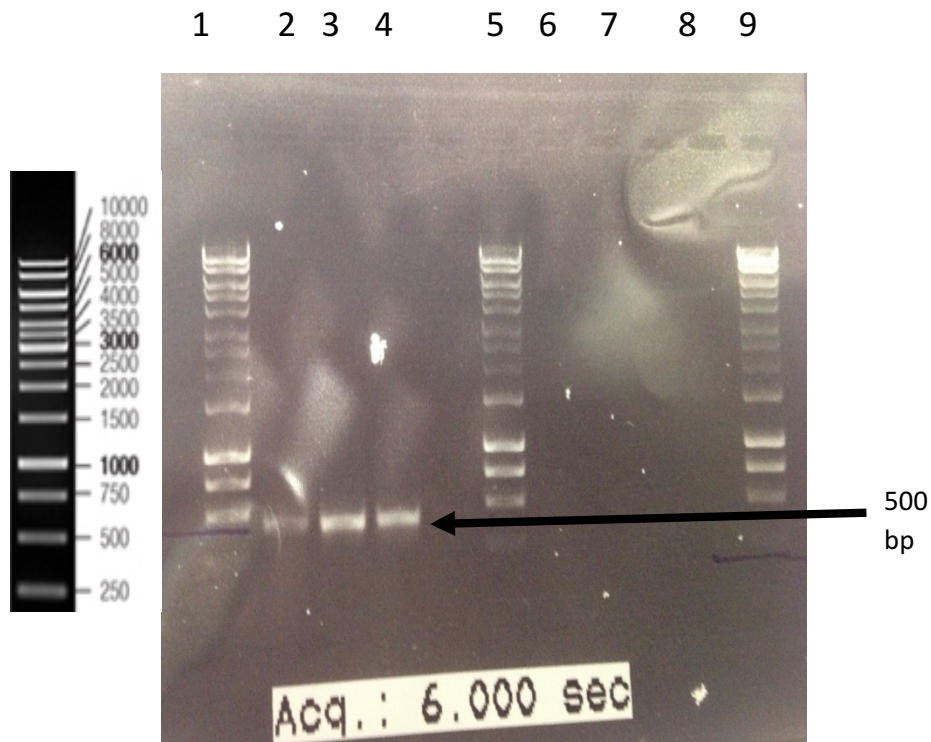


Figure 3.6 PCR amplification of pond water isolate using 18S rRNA Lim & Sheehan primers. Lane 1: 1 Kb DNA ladder, lanes 2, 3, 4: 700 bp amplified DNA using 18S rRNA Lim primers, Lane 5: 1Kb ladder, Lanes 6, 7, 8: no DNA amplified using 18S rRNA Sheehan primers Lane 9: 1Kb ladder.

The PCR amplified DNA of both *Synechocystis* and the pond water isolate were then cleaned up using a PCR purification kit as described in section 2-7-4. Then the cleaned-up DNA was measured using a Nanodrop spectrophotometer as described in section 2-7-5.

3.2.2.3 Sequencing and Identification of the strains using Blast

Both PCR amplified DNA of *Synechocystis* and the pond water isolate were sent for sequencing (Eurofins/MWG). After the sequences were returned, 958 bases of Forward 16S rRNA and 959 bases of reverse 16S rRNA were successfully sequenced (Appendix A). The Blast of these sequences using NCBI website confirmed that both forward and reverse 16S primer sequences were matched with *Synechocystis* PCC 6803 (99% Identity). For the pond water isolate, only 512 bases of forward 18S rRNA Lim primers and 509 bases of Reverse 18S rRNA Lim primers were sequenced (Appendix B). After Blast the sequence in the NCBI website the results showed that both forward and reverse 18S rRNA Lim primer sequences matched many different highly matched (99% identity) sequences. Table 2.1 showed the top 5 matches between (99-97%) sequence identity.

Table 3.1 Significant alignment with initial 18S Forward sequence of Pond water strain

Species Matched	Query match (total score)	Accession number
<i>Tetradesmus acuminatus</i>	99%	LC192133
NIES-92	1793	
<i>Tetradesmus obliquus</i> E1	99%	KX427160
	1793	
<i>Tetradesmus obliquus</i>	99%	KU900221
CCAP 276/3A	1793	
<i>Scenedesmus</i> sp. Y7	97%	JF950557
	1760	
<i>Scenedesmus</i> sp. Y5	97%	JF950556
	1754	

However, with this length of sequence further molecular identification was required to confirm the species identification as *Tetrademus* or *Scenedesmus* sp. Therefore, the pond water isolate genomic DNA was amplified using ITS1, ITS2 and 5.8S primers and Figures 3.7 and 3.8 showed successful amplification of the pond isolate ITS genes.

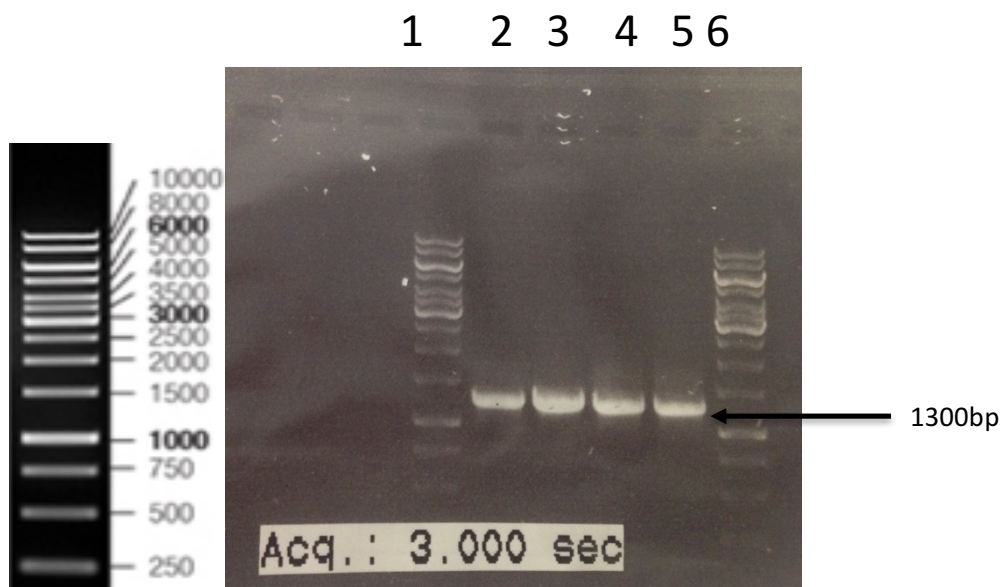


Figure 3.7 PCR amplification of the pond water isolate strains using ITS1 primers.

Lane 1: 1 Kb DNA ladder, lanes 2, 3, 4, 5: 1300 bp amplified DNA, Lane 6: 1Kb ladder.

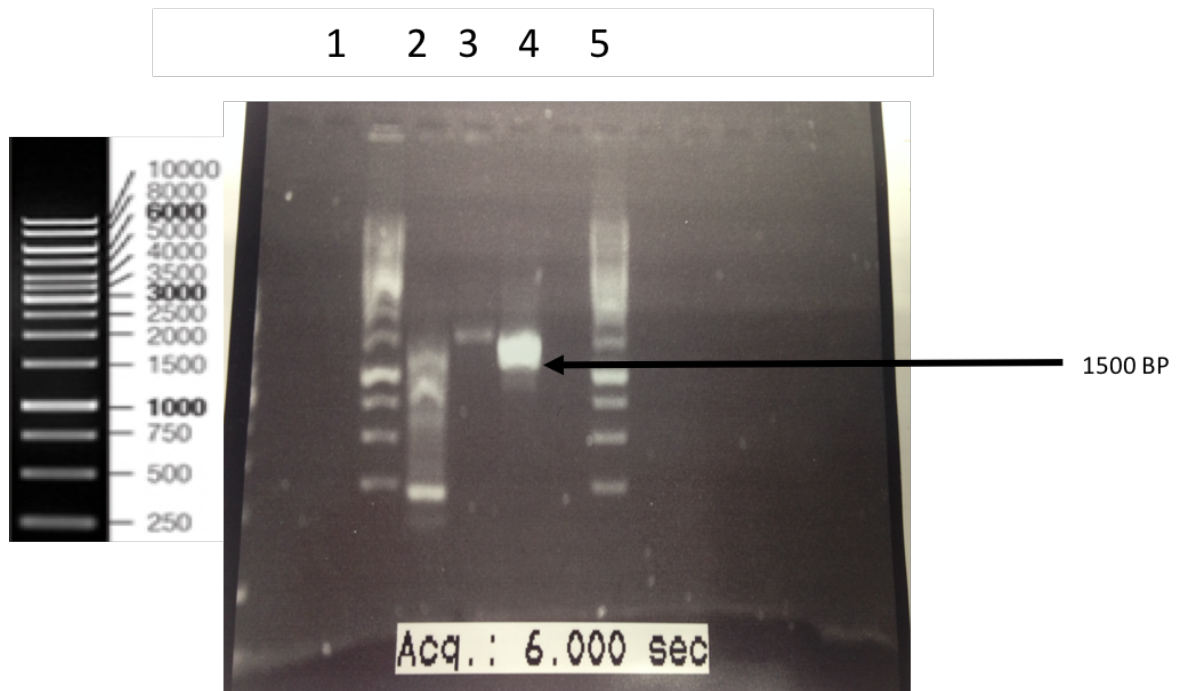


Figure 3.8 PCR amplification of the pond water isolate using ITS2 and 5.8S rDNA primers. Lane 1: 1 Kb DNA ladder, lanes 2, 3: PCR amplification of ITS2 primers, Lane 4: PCR amplification of 5.8S rDNA primers and Lane 6: 1Kb ladder.

After cleaned up using PCR purification kit, PCR products were sent for sequencing and the results showed that 996 bases of forward and 919 bases of reverse ITS1 primers, (Appendix C), 950 bases of forward and 1058 bases of reverse ITS2, (Appendix D) 868 bases of forward and 990 bases of reverse 5.8S rDNA (Appendix E) were successfully sequenced. The Blast of these sequences by NCBI website proved that forward and reverse primers were highly matched with *Desmodemus armatus* with (99% identity)

3.2.4 Growth curve of *Desmodesmus armatus* and *Synechocystis* PCC 6803

Growth curve determinations for both *Desmodesmus armatus* and *Synechocystis* sp. strains were carried out as described in section 2.4.2. Figure 3.8 shows the growth curve of *D. armatus* cells over 26 days cultivation. The results showed clearly that *D. armatus* reached stationary phase in about 24 days.

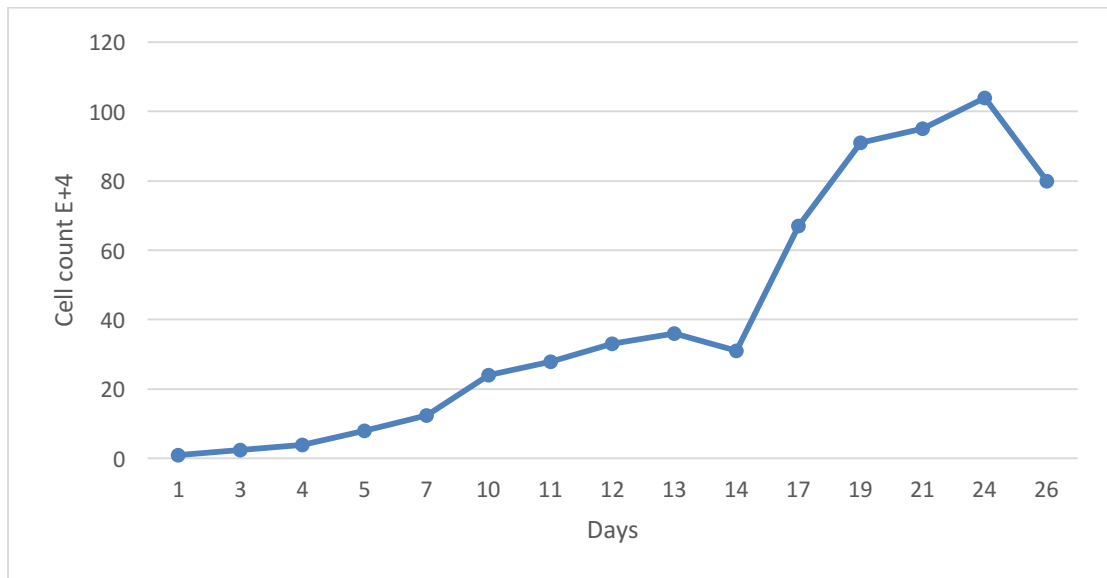


Figure 3.10 Growth curve of *Desmodesmus armatus* cells grown over 26 days cultivation. Each point is the average of three technical repeats from one growth flask.

Figure 3.9 shows the growth curve of *Synechocystis* sp. strain over 23 days incubation. It is clear that stationary phase was reached after 17 days cultivation.

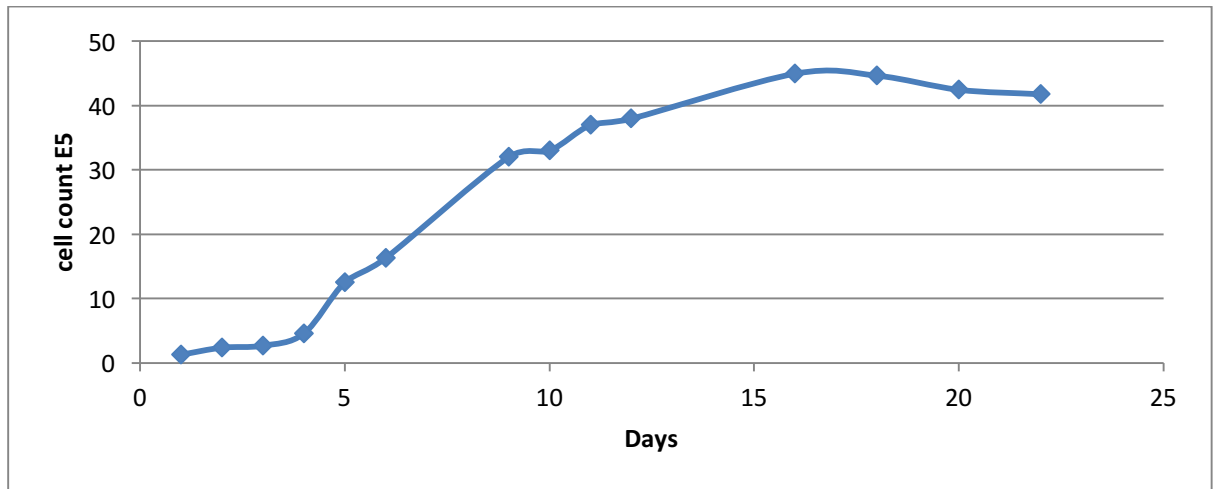


Figure 3.11 Growth curve of *Synechocystis* PCC 6803 after 23 days cultivation. Each point is the average of three technical repeats from one growth flask

3.2.5 Relationship between cell count versus OD₅₉₅.

The relationship between cell count and OD for *D. armatus* and *Synechocystis* sp. PCC 6803 was investigated as described in section 2-8. Figures 3.10 and 3.11 show the results, which indicate that there is a good linear relationship between OD and cell number up to about an OD₅₉₅ of 1 for both species.

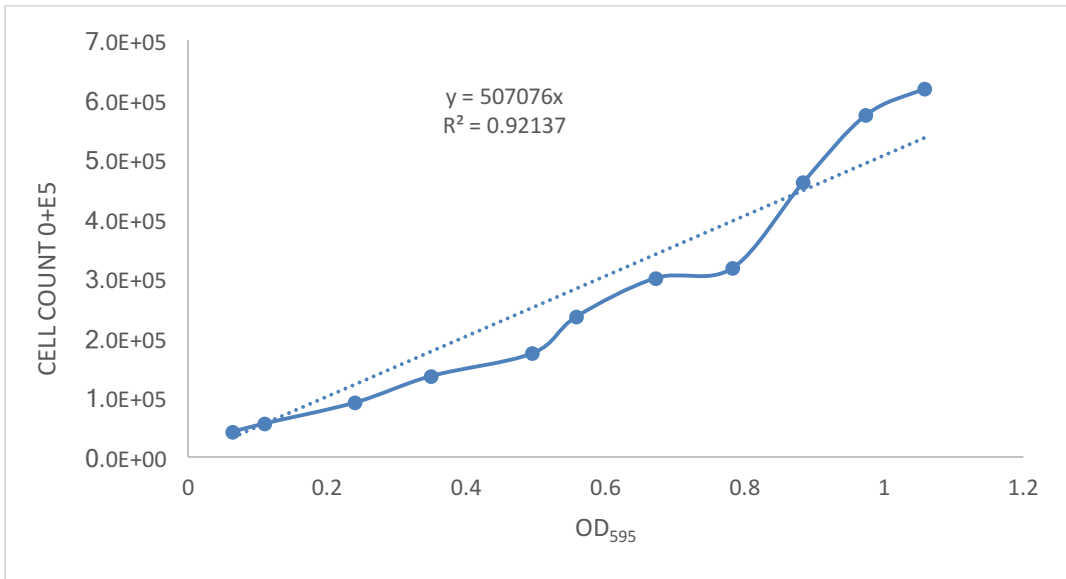


Figure 3.12 Relationship between *D. armatus* OD₅₉₅ and cell count

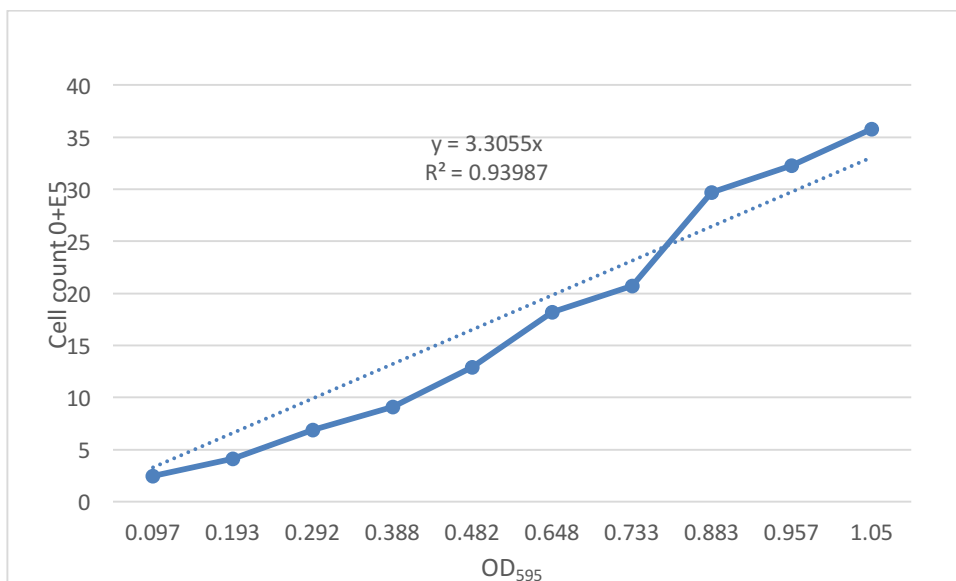


Figure 3.13 Relation between *Synechocystis* sp. OD₅₉₅ and cell count.

3.3 Discussion

3.3.1 Identification and characterisation of Pond Water Isolate *and Synechocystis* sp.

Before identification of the candidate strains, it was important to confirm that the cultures were axenic. *Synechocystis* PCC6803 strain was examined under light microscope to confirm the purity of the single colonies and 16S rRNA sequences were used as molecular markers to confirm that the *Synechocystis* PCC6803 strain that was obtained from another laboratory in Department of Molecular Biology and Biotechnology had been correctly identified. The comparison of 16S rRNA partial sequence using the NCBI website confirmed our strain as *Synechocystis* PCC6803 by showing (99%) identity with other *Synechocystis* PCC6803 sequences. Many studies have used 16S rRNA primers as a key for the taxonomy of all cyanobacteria including *Synechocystis* sp. PCC6803 (Allewalt *et al.*, 2006; Hameed and Hasnain, 2012). 16 S rRNA sequencing is considered as a backbone for bacterial taxonomy (Clarridge, 2004).

For the pond water samples, serial purification steps including light microscopic examination were conducted to obtain an axenic culture. The light microscopic examination of the axenic culture of pond water sample showed that the strain looked like a *Scenedesmus/Desmodesmus* species based on the high number of cells forming coenobia, cell dimensions and the occurrence of spines. However, due to the very close similarity of characteristic morphological and metabolic features between species of *Desmodesmus* and *Scenedesmus* (Kessler *et al.*, 1997). Radha *et al.*, (2013) pointed out that an ideal protocol for precise identification between close related *Scenedesmedaceae* and other closely related microalgae is the combination of molecular and morphological identification. For molecular characterisation purposes, whole DNA sequencing is not necessary and can be replaced by sequencing small specific conserved genes which are widely investigated in microalgae. Nuclear ribosomal RNA (rRNA); mitochondria genes, plastid genes (*rbcl*); and ITS genes are the commonly conserved genes that play an important role for microalgal identification (Mutanda *et al.*, 2011). As noted above for *Synechocystis* PCC6803, rRNA genes have been exploited widely as an ideal template for the taxonomy of the unknown organism because they are universal and contain both highly conserved and flexible domains (Fox

et al., 1977; Woese, 1987). In eukaryotic cells, rRNA is divided into the coding part composed of 18S, 5.8S, and 28S rDNA and the non-coding part which is composed of external transcribed spacer (ETS), internal transcribed spacer 1 (ITS1), and internal transcribed spacer 2 (ITS2).

Molecular identification of PCR amplified Weston Park pond strain sequence using 18S rRNA primers indicated that the strain belonged to *Tetradasmus/Scenedesmus* sp. with 97 – 99% identity. Partial 18S rRNA sequence is a common target region for identification of unknown algae including *Scenedesmus* sp. isolated either from fresh or marine water (Eland *et al.*, 2012; Lim *et al.*, 2012; Sathya and Srisudha, 2013; Chen *et al.*, 2014; Gour *et al.*, 2016).

For further confirmation, detection of the ITS region sequences proved that the pond water strain is with 99% identity closely related to many *Desmodesmus* sp. after Blast analysis of the sequence in NCBI website. Furthermore, the sequences that showed high matching (99%) aligned using the Muscle alignment method. A phylogenetic tree constructed using maximum likelihood emphasized that the pond water strain is closely related to different *Desmodesmus* clades and particularly to the *Desmodesmus armatus* clade.

Many studies have pointed out that the internal spacer1 (ITS1) and internal spacer2 (ITS2) sequences of rRNA are considered to be an ideal and flexible tool to be exploited to address the taxonomy of close relationships between very close related microalgae, including *Scenedesmus/Desmodesmus* species, because these two molecular markers are more variable (Hadi *et al.*, 2016). ITS1 and ITS2 regions of DNA are part of the noncoding regions that can be trusted for the identification of microalgae because they are repeated in high copy number within the algal genome (Kocot and Santos, 2009). Various studies used ITS region as a trustworthy molecular marker for phylogenetic taxonomy of closely related *Scenedesmus species* within other *Scenedesmedaceae* family strains (Hegewald and Wolf, 2003; Gour *et al.*, 2016; Hadi *et al.*, 2016).

Scenedesmus as a genus was first distinguished in 1829 and it contained all autosporic coccal green algae with flat or curved coenobia. Approximately 1300 taxa of *Scenedesmus* were distinguished until 1926 when Chodat divided these taxa into

subgenera to achieve a more convenient way for understanding the close relationships between *Scenedesmus* species (Chodat, 1926). *Desmodesmus* as a genus was first classified as a subgenus of *Scenedesmus*, however the taxonomic relationship between *Scenedesmus* and *Desmodesmus* has passed through different stages based on the parameter of classification. Hegewald, (1978) differentiated *Desmodesmus* sp. and *Scenedesmus* sp. into separate subgenera based on the ultrastructure of the cell wall, in which species with four sporopollenimic wall layers and with peculiar sub-microscopic features on the outer sporopollenimic layer belonged to subgenus *Desmodesmus* Chodat. In contrast, species with three sporopollenimic wall layers that lack structure or with ribs shaped in the hemicellulosic wall layer were classified as *Scenedesmus* and *Acutodesmus* Hegewald.

18S rRNA was another taxonomic factor that was used for differentiation between *Desmodesmus* and *Scenedesmus* species. The 18S rRNA sequence investigation provides additional data that divided *Scenedesmus* species into two main subgenera which were *Desmodesmus* as individual subgenus and both *Scenedesmus* and *Acutodesmus* as subgenera (Kessler *et al.*, 1997; Lewis, 1997). However, another study demonstrated that 18S rRNA is not variable enough to be used as a taxonomic parameter because of the insufficient variation to distinguish between close related *Desmodesmus* and *Scenedesmus* species (Hegewald and Hanagata, 2000). Therefore, *Desmodesmus* was separated as a distinct genus based on the primary cell wall structure and the significant variation in the length of the ITS2 sequence. Moreover, the ultra-structure study of the cell wall of *Desmodesmus* and *Scenedesmus* species also clearly distinguished that the non-spiny form belonged to *Scenedesmus* and the spiny form was classified as *Desmodesmus* (An *et al.*, 1999; Van Hannen *et al.*, 2002).

Desmodesmus is now recognised as a common coccoid green microalga which can be isolated from different freshwater ponds rivers and brackish water around the world (Vanormelingen *et al.*, 2007). The number of studies involving *Desmodesmus* species is significantly lower than *Scenedesmus* species. The reason was illustrated by Lürling, (2003) in which it was noted that the researchers still did not understand the new taxonomic differentiation between *Desmodesmus* and *Scenedesmus*. He collected all

the literature related to *Scenedesmus* species. from 1989 to 2003. During this period, more than 500 non-spiny and about 450 spiny isolates were collected. Many spiny *Desmodesmus* isolates were classified as *Scenedesmus* like *S. quadricauda*, *S. armatus* and *S. abundans*. Table 2-2 shows the revised top 5 frequent isolates of *Scenedesmus* and *Desmodesmus* species (Lürling, 2003).

Table 2.2 The revised differentiation between five most frequent *Desmodesmus* and *Scenedesmus* isolates collected from the literature survey between (1989-2003)
adapted from (Lürling, 2003)

<i>Scenedesmus</i> (non-spiny)		<i>Desmodesmus</i> (spiny)	
species	# hits	species	# hits
<i>S. obliquus</i>	287	<i>D. quadricauda</i>	228
<i>S. acutus</i>	149	<i>D. subspicatus</i>	76
<i>S. acuminatus</i>	28	<i>D. armatus</i>	35
<i>S. bijugatus</i>	18	<i>D. communis</i>	13
<i>S. dimorphus</i>	13	<i>D. abundans</i>	12

Desmodesmus armatus has been exploited to produce a variety of products due to their high content of protein that can reach 23% of dry weight after 40 days cultivation (Cheban *et al.*, 2015). Moreover, *Desmodesmus* sp. cells are composed of other essential products such as vitamins, carbohydrates, essential amino acids, and both macro and micro-elements, which are widely utilised as a food source for mollusks, fish and crustaceans (Becker, 2007).

Desmodesmus species can be grown in a variety of aquatic environments and they can adapt to different stress conditions. Therefore, they could alter their regular multicellular form into single cell form when exposed to chemical signals extracted from zooplankton grazers (Lürling, 2003). Moreover, Koike *et al.*, (2013) recorded for the first time that a *Desmodesmus* species was considered as a parasite that caused an algal infection in fishes in Japan.

Chapter Four

Determination and Quantification of Neutral Lipid

4.1 Introduction

Throughout the world, the method that could be utilized for measurement of algal lipid content was one of the main critical arguments between researchers because there is no standardised protocol that could be relied upon for precise and accurate lipid measurements in all microalgal strains considered for biofuel production (Li *et al.*, 2014).

There are different techniques that have been used for the determination and quantification of algal lipids such as gravimetric method which is the conventional method for algal lipid assessment. This protocol mainly uses cell disruption and solvent extraction of algal biomass lipids. The total algal lipids are quantified by drying and weighing the lipid extract (Kumari *et al.*, 2011). However, numerous studies have reported that this method is undesirable technique for quantification of microalgal lipid in terms of loss of some of the lipid content after additional steps required to differentiate various types of lipid fractions such as transesterification and chromatographic separation. Moreover, other drawbacks of gravimetric method are that it is a time consuming and labour-intensive manipulation (Bertozzini *et al.*, 2011). Furthermore, another disadvantage of gravimetric method is that not only total lipid will be assessed but also other non-fatty acids containing lipids, like pigments or sterols, are also involved in the determination method. These non-fatty acid will increase the total lipid content (>50%). Therefore, for the specific goal of determination of the neutral lipid content of microalgae for biodiesel production it is not recommended to use gravimetric method because of the overestimation of total lipid content (Breuer *et al.*, 2013).

In situ screening of algal lipid content using spectrophotometry have been recommended in recent years to be one of the favourite protocols for determination of algal lipids. Fluorescence spectroscopy has been considered to be the easiest, most rapid and cheapest analysis tool to assess the lipid content based on a fluorescent dye (mainly Nile Red). The excitation and emission filters of the spectroscopy are used to read the fluorescence of the dye which is related indirectly to the lipid content (Cirulis *et al.*, 2012).

Nile Red (NR, 9-diethylamino-5H-Benzo[α]phenoxazine-5-one) is a lipid soluble fluorescent probe that has been widely utilised to assess the lipid content in different organisms including zooplankton (Alonzo and Mayzaud, 1999), mammalian cells (Genicot *et al.*, 2005), bacteria (Izard and Limberger, 2003) and yeast (Sitepu *et al.*, 2012).

The vital feature of employing Nile Red as a fluorescent dye was to accomplish a quick screening of oleaginous microalgae to allow the selection of promising strains for economically feasible production of biofuel (Chisti, 2008).

Nile Red has the ability to pass through the cell barriers including the cell wall, cell membrane and dissolve in the intracellular neutral lipid showing a golden yellow fluorescence for neutral lipids, red for chlorophyll auto fluorescence and polar lipids. In combination with organic solvents like dimethyl sulfoxide (DMSO) which have been used with different microalgal species in terms of facilitating the staining of microalgae with Nile Red (Pancha *et al.*, 2014; Wu *et al.*, 2014).

The effectiveness of Nile Red to pass through the algal cell wall and consequently determine the neutral lipid relies on the accurate wavelength of excitation and emission of the microscopy filter. These wavelengths depend mainly on the hydrophobicity of the carrier solvent utilized. In general, the excitation wavelength for determination of neutral lipid by Nile Red must be less than 570 nm because Nile Red will present as a general lipid dye at more than 570 nm. While at wavelength higher than 590 nm, the selection feature of lipid droplet by Nile Red will be lost (Greenspan *et al.*, 1985). Overall, the selection of excitation and emission wavelength is varying between different algal species and sometimes with the same species, for example (Ren *et al.*, 2015) demonstrated that 530/568 nm were ideal excitation and emission wavelengths for *Scenedesmus* species. On the other hand, other studies stated that an optimum excitation/emission is 490/580 nm (Chen *et al.*, 2011) and 530/604 nm (Siegler *et al.*, 2012). These variations in the emission and excitation wavelength are based mainly on the individual microalgal isolates and neutral lipid composition of fatty acids ((Chen *et al.*, 2009).

The utilisation of Nile Red for evaluation of neutral lipid has increased dramatically in the last two decades as shown in Figure 4.1.

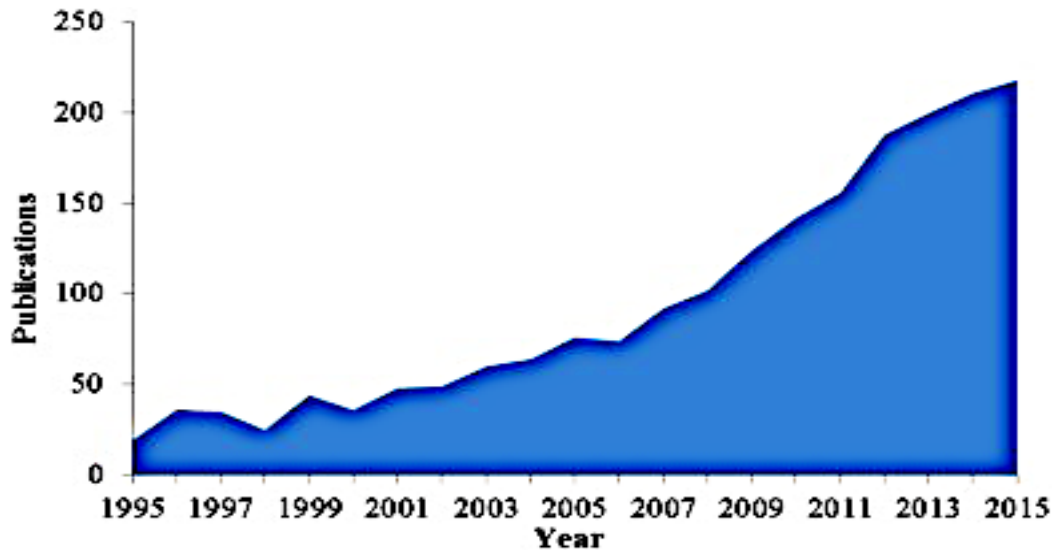


Figure 4.1 Number of publications related to the utilisation of NR to evaluate the neutral lipids in different cells from 1995-till May 2016. Adapted from (Aleman-Nava, et al., 2016).

Various strategies have been utilized to alter external growth conditions to over stimulate accumulation of neutral lipid in microalgae, such as increasing salinity of the algal medium, nutrient starvation or depletion especially the sources of nitrogen and phosphorus in the algal medium, pH and light intensity (Zhu *et al.*, 2016).

The content of microalgal lipid plays a vital role in the selection of a strain as a source for biodiesel production. Therefore, different analytical techniques such as Gas Chromatography (GC) and Mass Spectrophotometry (MS) alone or combined, and Nuclear Magnetic resonance (NMR) are being used widely as tools for the compositional evaluation of the lipid profile such as types of saturated or unsaturated fatty acids, directing the production and characteristics of feed stock, and their conversion to biodiesel (Bharti and Roy, 2012; Sarpal *et al.*, 2016).

The objectives of this chapter are to optimise the conditions that are required to accurately utilise Nile Red for determination of the neutral lipids in both *Desmodesmus armatus* and *Synechocystis* PCC 6803 under normal growth conditions (i.e. growing them in BG11 medium). Furthermore, investigate the influence of stress conditions involving salinity (0.2, 0.4 M NaCl); nitrogen starvation (25%, 10% NaNO₃ BG11); nitrogen depletion (N Free BG11); and different nitrogen sources (NH₄Cl, Urea) on the neutral lipid accumulation in both strains. Moreover, free fatty acids are analysed after transesterification using (GC-MS) technique for the strain that showed the highest neutral lipid content.

4.2 Results

4.2.1 Fluorescence microscopy for visualisation of lipid droplets

The accumulation of neutral lipids in *D. armatus cells* was visually confirmed by examining the fluorescence of Nile Red in cells grown under normal and stress conditions (nitrogen depletion) using fluorescence microscopy. This demonstrated the ability of Nile Red to penetrate the algal cells and bind to the intracellular lipid as described in section 2.9.1. The images in Figure 4.2 clearly show the yellow fluorescence related to the binding of Nile Red with the neutral lipid inside the cells (right hand image).

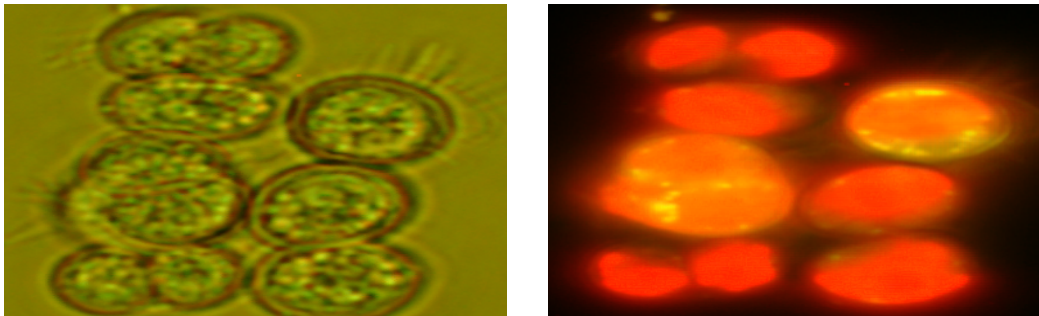


Figure 4.2 Number of publications related to the utilisation of NR to evaluate the neutral lipids in different cells from 1995-till May 2016. Adapted from (Aleman-Nava, et al., 2016).

The results have provided indirect indication of the marked increase in the amount for neutral lipid in the cells grown under various stress conditions. Moreover, these results have offered a justification to continue further experiments to utilise Nile Red dye method for quantification of neutral lipid in *D. armatus cells*.

4.2.2 Determination of Neutral Lipid Using Nile Red

As the fluorescent intensity of Nile Red is variable, the precise evaluation of neutral lipid in algal cells required an optimization of two factors: algal cell concentration and Nile Red concentration.

4.2.2.1 Optimization of *Desmodesmus armatus* and *Synechocystis* PCC6803 Cell concentration

The concentrations of algal and cyanobacterial cells optimised as described in section 2.9.2.2.1. Figures 4.3 and 4.4 showed the fluorescence intensity of *D. armatus* and *Synechocystis* cells respectively at different concentrations ranging from 12.5%-100% at different incubation times. The optimum concentration of *D. armatus* and *Synechocystis* cells were based on the balance between the values of cell normalization, concentrations of the algal strain and the staining time. The optimum concentration of *D. armatus* cells was 50% of cells in 14 minutes. While for *Synechocystis* 75% concentration of cells in 14 minutes appeared to be the best concentration of cells

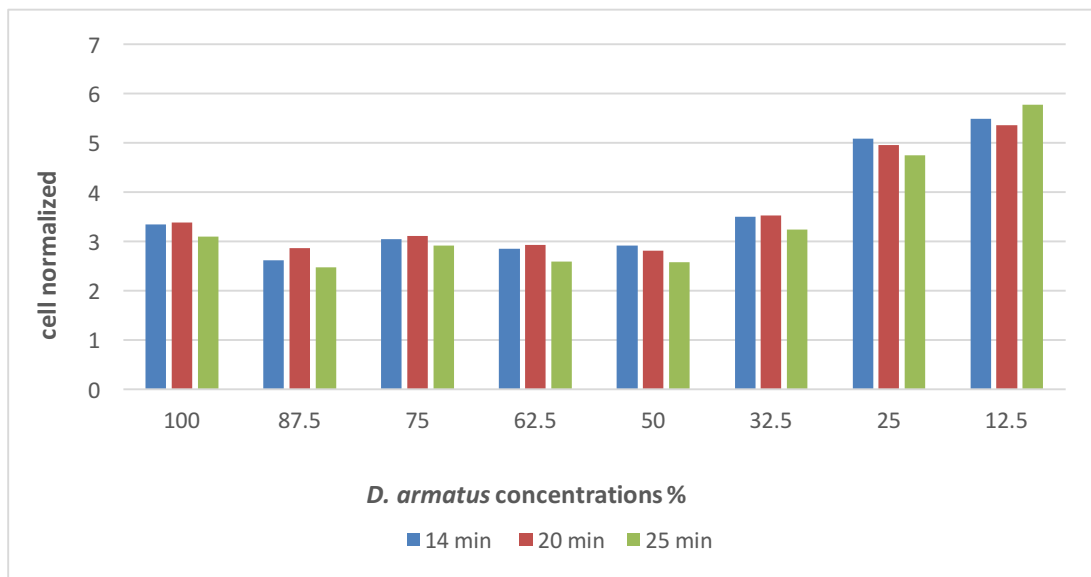


Figure 4.3 Optimization of NR staining time and cell concentration on fluorescence intensity of the green alga *D. armatus*. The optimum conditions were 50% of cells in 20 min. Each column represents the normalised value of each concentration

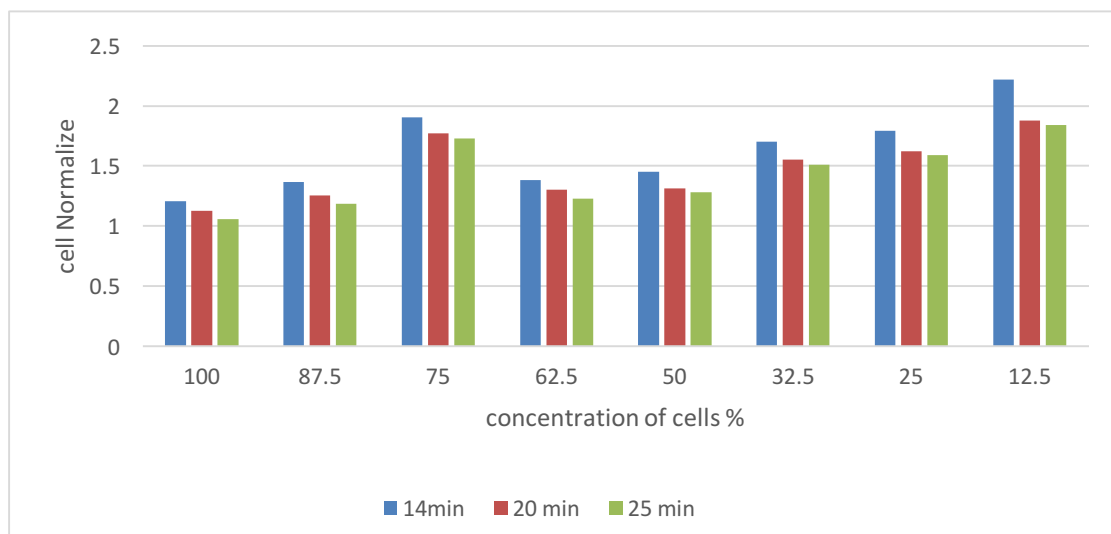


Figure 4.4 Optimization of NR staining time and cell concentration on fluorescence intensity of the *Synechocystis* PCC 6803. The optimum conditions were 75% after 14 mins staining. Each column represents the normalised value for the cells. Error bars represent technical repeats (n=3).

4.2.2.2 Optimization of Nile Red concentration

The optimization of Nile Red concentration was conducted as described in section 2.9.2.2.2. Figure 4.5 shows the fluorescent intensity of *D. armatus* cells stained with different Nile Red concentrations. It is obvious that $1 \mu\text{g ml}^{-1}$ had the highest fluorescent intensity after 20 min incubation followed by 1.3 and $0.64 \mu\text{g ml}^{-1}$ respectively.

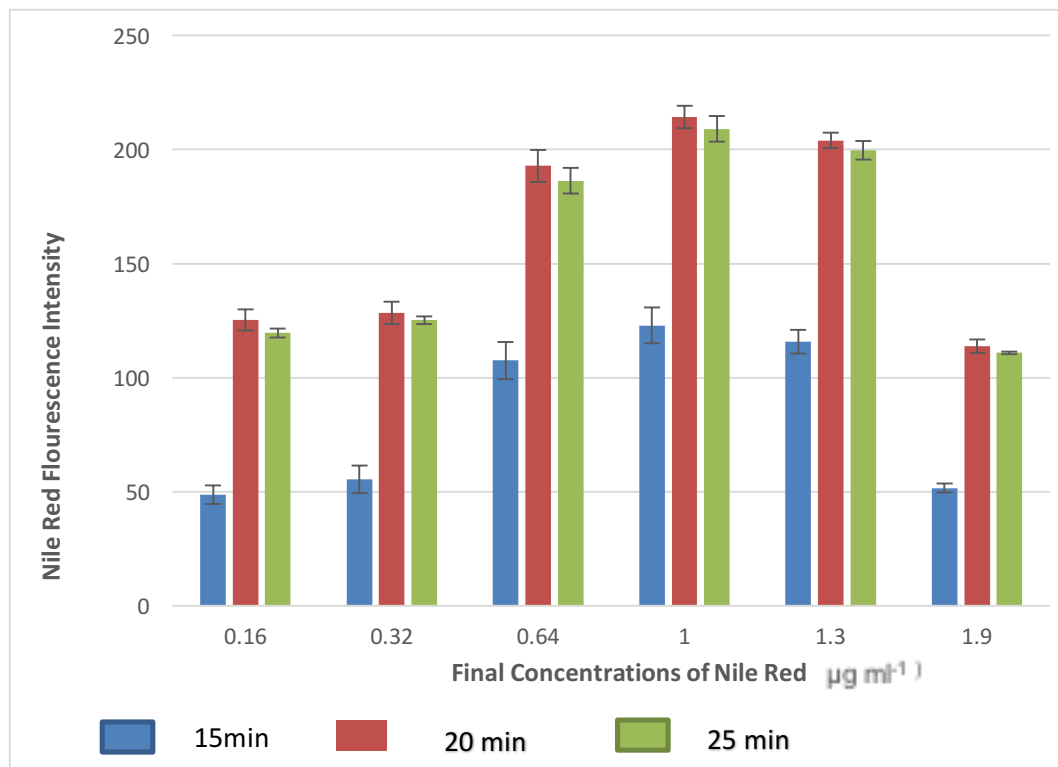


Figure 4.5 Optimization of NR staining concentration for the green alga *D. armatus* cells. The optimum cell concentration of 50% was used, and the amount of staining was measured after 15, 20, and 25 min. Each column represents the difference between the average of four stained and four unstained readings. Error bars represent technical repeats (n=3).

For *Synechocystis* PCC6803, Figure 4.6 shows clearly that the highest fluorescent intensity of different Nile Red concentrations was $1.9 \mu\text{g ml}^{-1}$ after 15 min. However, $1.3 \mu\text{g ml}^{-1}$ was selected as an optimum concentration of Nile Red

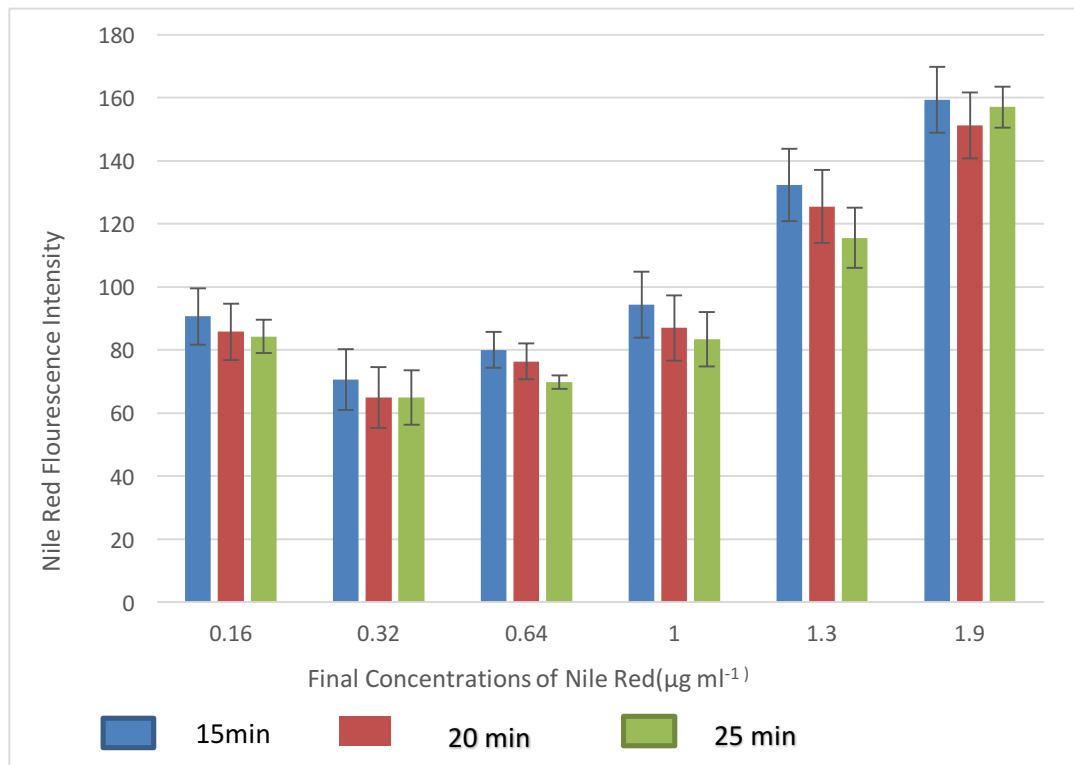


Figure 4.6 Optimization of NR staining concentration for the *Cyanobacterium Synechocystis* PCC6803 cells. The optimum cell concentration of 75% was used, and the time of staining was 15, 20, and 25 min. Each column represents the difference between the average of four stained and four unstained readings. Error bars represent technical repeats (n=3).

4.2.3 Effect of Salinity on the growth of *D. armatus* and *Synechocystis* cells

To investigate the effect of high salinity as a stress condition on the neutral lipid accumulation. Both *Synechocystis* and *D. armatus* cells were grown in 0.2 M NaCl BG11 and 0.4 M NaCl BG11 separately as described in section 2.2.1.1. The neutral lipid measurements of both strains were evaluated once a week for 33 days using an optimum concentration of *D. armatus* cells $OD_{595} = 50\%$ concentration of cells, and $1 \mu\text{g ml}^{-1}$ concentration of Nile Red. Figure 4.7 shows that the highest Nile Red fluorescent intensity of *D. armatus* cells has observed at 0.2 M NaCl followed by 0.4 M NaCl and normal *D. armatus* cells respectively after 33 days incubation.

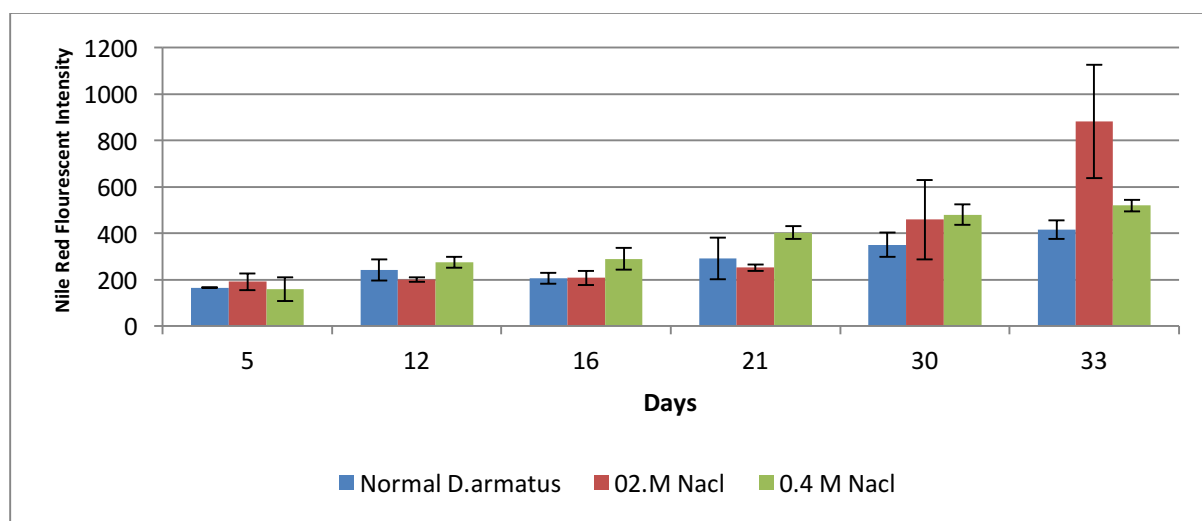


Figure 4.7 Nile Red Fluorescence Intensity measurements of *D. armatus* cells grown in BG11 media with: zero concentration of NaCl, 0.2 M and 0.4 M NaCl respectively. Each measurement represents the difference between the average of four stained and four unstained readings. Error bars represent technical repeats (n=3).

For *Synechocystis*, the effect of 0.2 M NaCl and 0.4 M NaCl was measured using optimum concentration of cells $OD_{595} = 0.75$ and Nile Red concentration ($1.3 \mu\text{g ml}^{-1}$). Figure 4.8 shows clearly that the 0.4 M NaCl and 0.2 M NaCl increased the neutral lipid content in terms of fluorescent intensity value during the first 8 days incubation. However, both salt stress conditions dramatically decreased the neutral lipid content after nearly a month of incubation when compared with the neutral lipid content of the normal condition (BG11) which showed the highest fluorescent intensity. Therefore, increasing the salinity for long-term incubation was deemed not to be a convenient stress condition to boost the neutral lipid accumulation in *Synechocystis* cells.

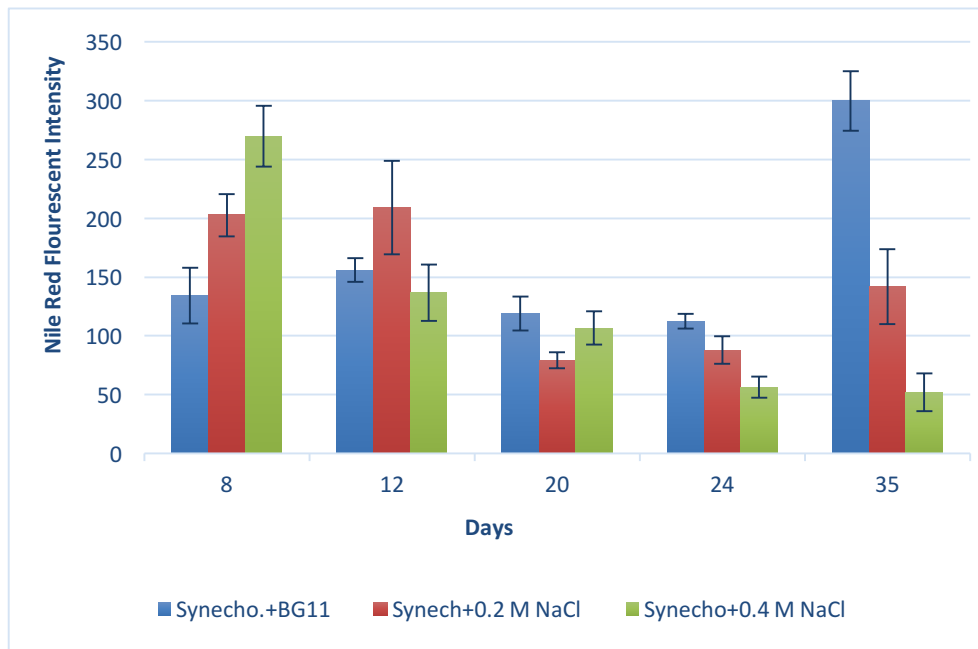


Figure 4.8 Nile Red fluorescent intensity measurement of *Synechocystis* cells grown in BG11 media with: zero concentration of NaCl, 0.2 M NaCl, and 0.4 M NaCl respectively. Each measurement represents the difference between the average of four stained and four unstained readings. Error bars represent technical repeats (n=3)

4.2.4 Effect of nitrogen depletion

The effect of nitrogen depletion on the neutral lipid accumulation in both *D. armatus* and *Synechocystis* were examined as described in section 2.2.1.2. Both strains were grown in 25%, 10%, and absence of NaNO₃ that was the source of Nitrogen in BG11. For *D. armatus* cells, Figure 4.9 shows that the highest Nile Red intensity has emerged in N free BG11 followed by 10% and 25% respectively.

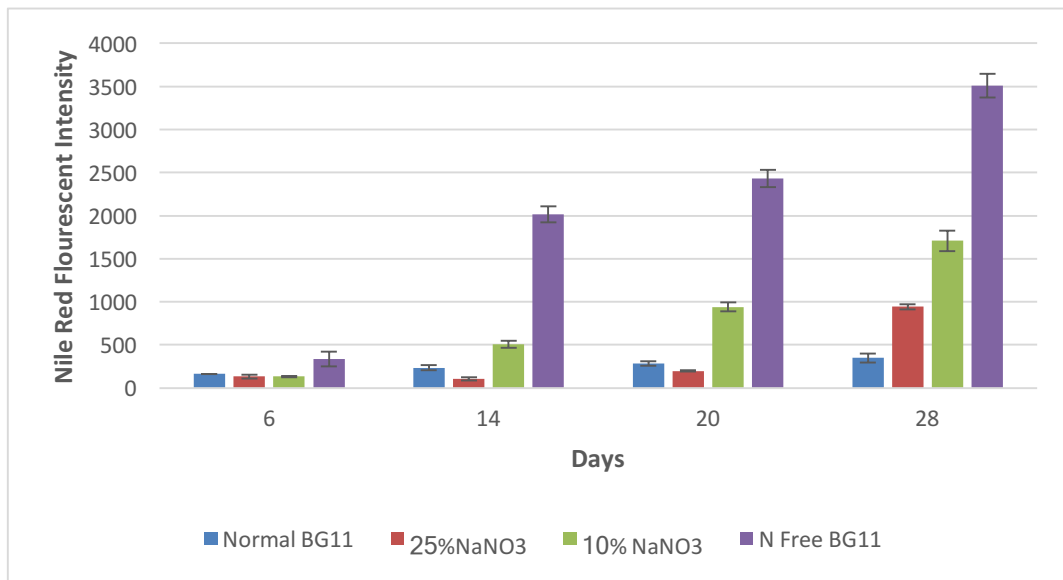


Figure 4.9 The fluorescent Intensity of *D. armatus* cells grown under normal BG11, 25% NaNO₃, 10% NaNO₃ and N Free BG11. NaNO₃ was used as a source of nitrogen in the medium. Each measurement represents the difference between the average of four stained readings and four unstained readings. Error bars represent technical repeats (n=3).

Figure 4.10 shows the Nile Red fluorescent intensity of *Synechocystis* strain grown under 10% NaNO₃ BG11, and absence of NaNO₃ (N Free BG11). It is obvious that the highest fluorescence intensity was shown by *Synechocystis* cells grown in N free medium.

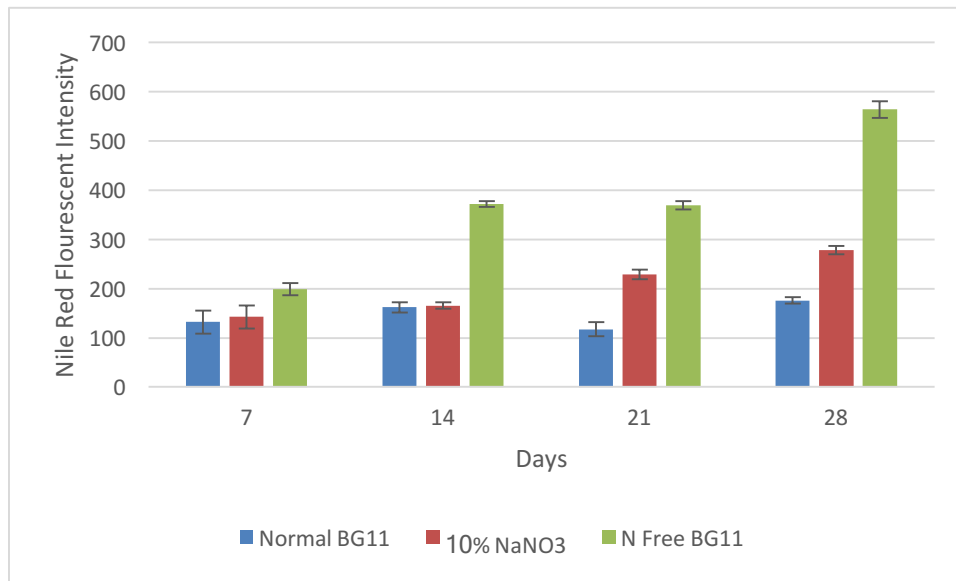


Figure 4.10 The fluorescent Intensity of *Synechocystis* cells grown under Normal BG11, 10% NaNO₃, and N Free BG11. NaNO₃ was used as a source of Nitrogen in the medium. Each measurement represents the difference between the average of four stained and four unstained readings. Error bars represent technical repeats (n=3).

4.2.5 Effect of Different Nitrogen Sources

The effects of different sources of N on the neutral lipid accumulation in *D. armatus*, and *Synechocystis* cells were investigated as described in section 2-2-1-3. NH_4Cl and urea replaced NaNO_3 as a source of nitrogen in the medium in which the concentration of N was equal in all sources. Figure 4.9 shows the fluorescent intensity of *D. armatus* cells grown under different nitrogen sources which were: 10% NaNO_3 , NH_4Cl , and urea respectively. The results showed clearly that NaNO_3 at low concentration induced the highest fluorescent intensity in contrast with the other sources of nitrogen.

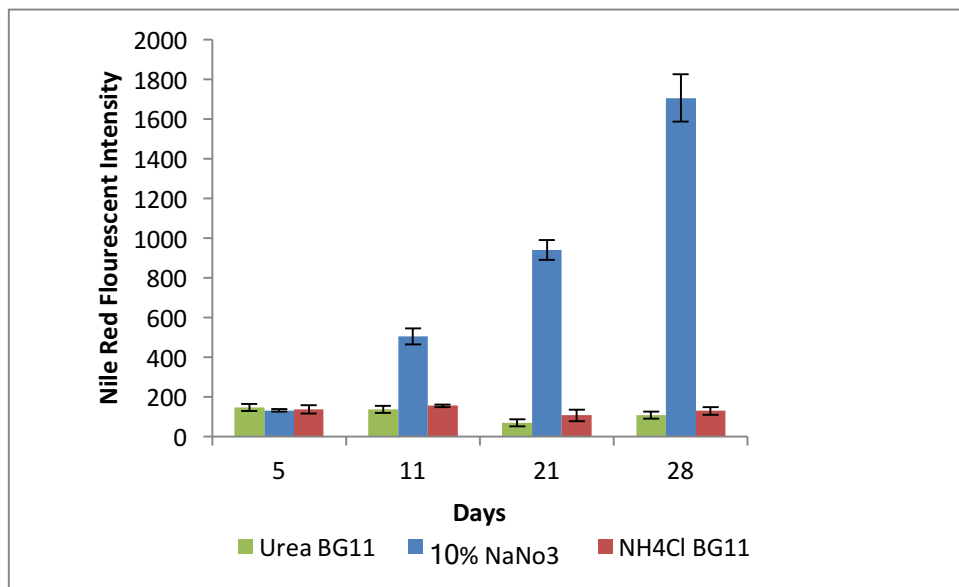


Figure 4.11 The fluorescent intensity of *D. armatus* cells grown under different N sources that are: 10% NaNO_3 , NH_4Cl , and urea. Each measurement represents the difference between the average of four stained and four unstained readings. Error bars represent technical repeats (n=3).

For *Synechocystis*, the effect of different N sources showed that NH_4Cl was the best source of N after 18 days incubation based on the highest Nile Red fluorescence intensity followed by 10% NaNO_3 , and urea respectively as shown in Figure 4.12

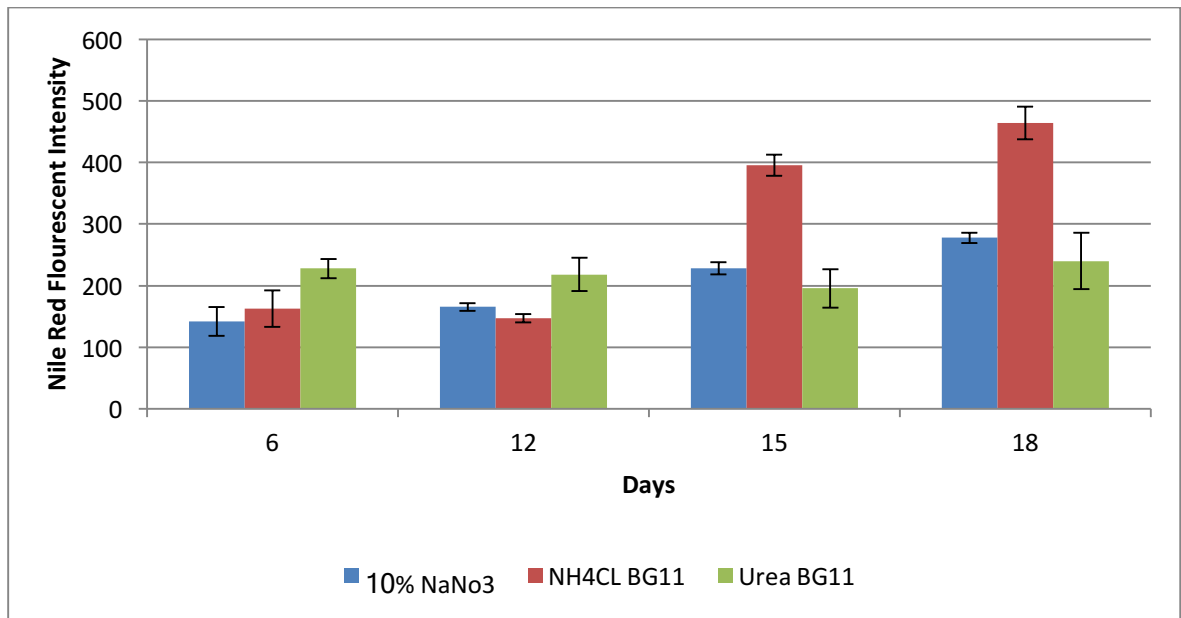


Figure 4.12 The fluorescence intensity of *Synechocystis* cells grown under different N sources that are: 10% NaNO_3 , NH_4Cl , and urea. Each measurement represents the difference between the average of four stained and four unstained readings. Error bars represent technical repeats (n=3).

4.2.6 Triolein calibration curve

The previous experiments were based on Nile red fluorescence intensity of a standard amount of algal/cyanobacterial biomass. To allow quantification of neutral lipid in the cells, a calibration curve of a standard neutral lipid (Triolein) was made as described in section 2.9.2.3 to convert the values of Nile Red fluorescent intensity achieved by exposure of both *D. armatus* and *Synechocystis* cells to normal and stress conditions. Figures 4.13 and 4.14 show the linear calibration curves for *D. armatus* and *Synechocystis* cells respectively. The Nile Red fluorescent intensity values were then converted to concentrations of neutral lipid (mg ml^{-1}).

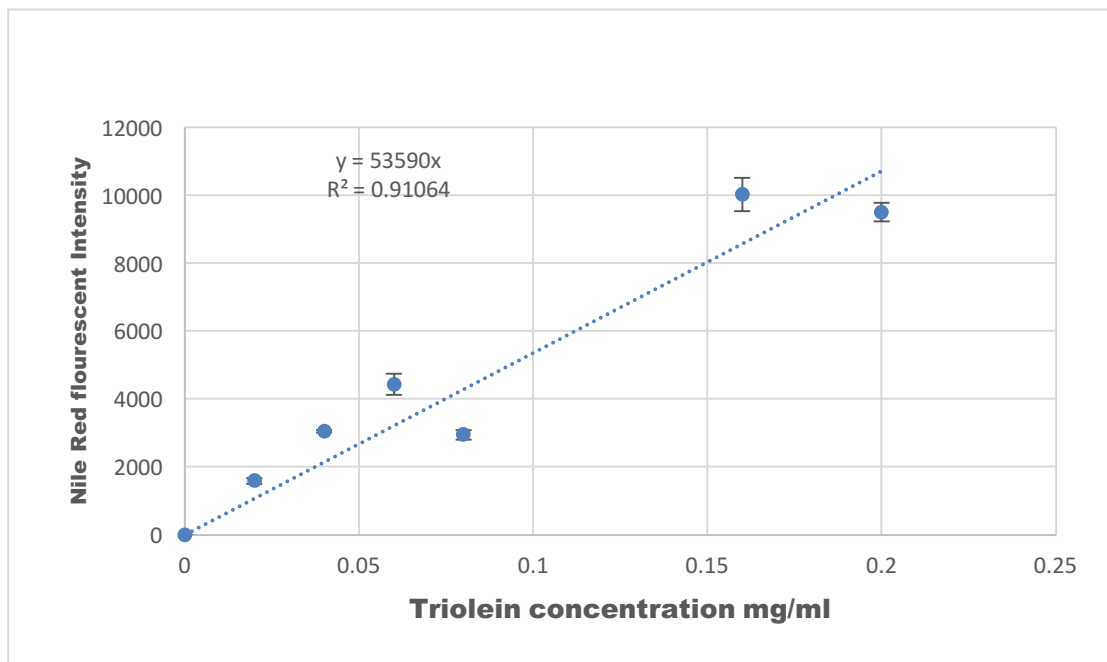


Figure 4.13 Linear correlation between fluorescence intensity and triolein concentration of *D armatus* cells for the conversion of fluorescence intensity readings to triolein equivalents. Each measurement represents the difference between the average of four stained and four unstained readings. Error bars represent technical repeats (n=3).

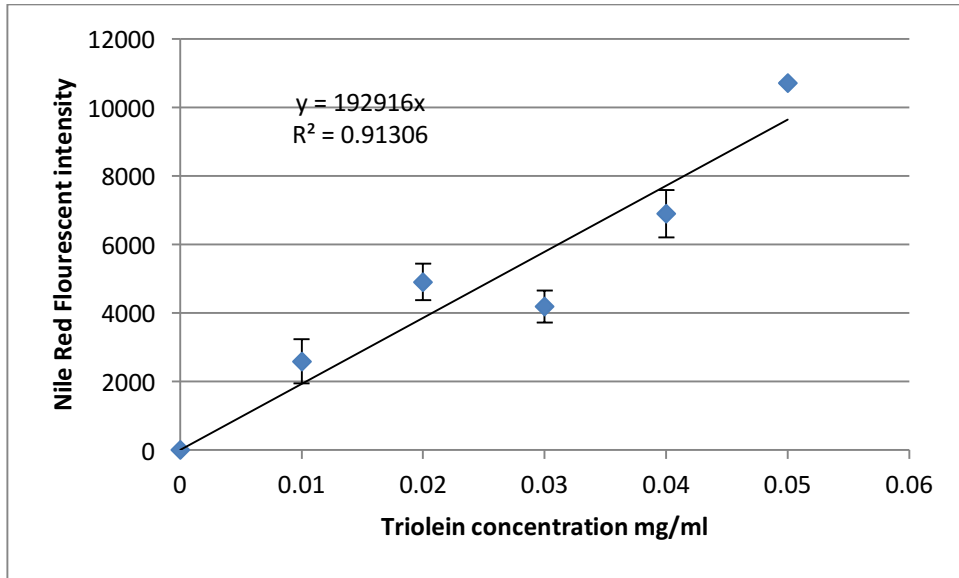


Figure 4.14 Linear correlation between fluorescence intensity and triolein concentration of *Synechocystis* cells to allow the conversion of fluorescence readings to triolein equivalents. Each measurement represents the difference between the average of four stained and four unstained readings. Error bars represent technical repeats (n=3).

4.2.7 Relation between OD and Cell Dry weight.

The relation between OD and cell dry weight was determined for both *D. armatus* and *Synechocystis* strains as described in section 2.10 (Figures 4.15 and 4.16). The aim of this experiment was to convert the OD value of the optimised concentration of cells to dry weight (mg ml^{-1}). Then each value of neutral lipid concentration will be divided on the value of the dry weight and multiplied by 100 to give the percentage (%) of neutral lipid.

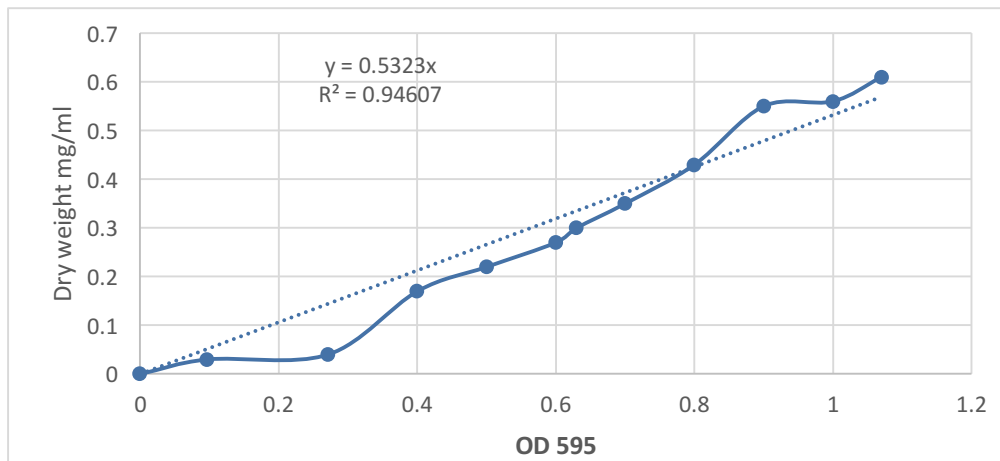


Figure 4.15 Linear relation between OD and dry weight of *D. armatus* cells

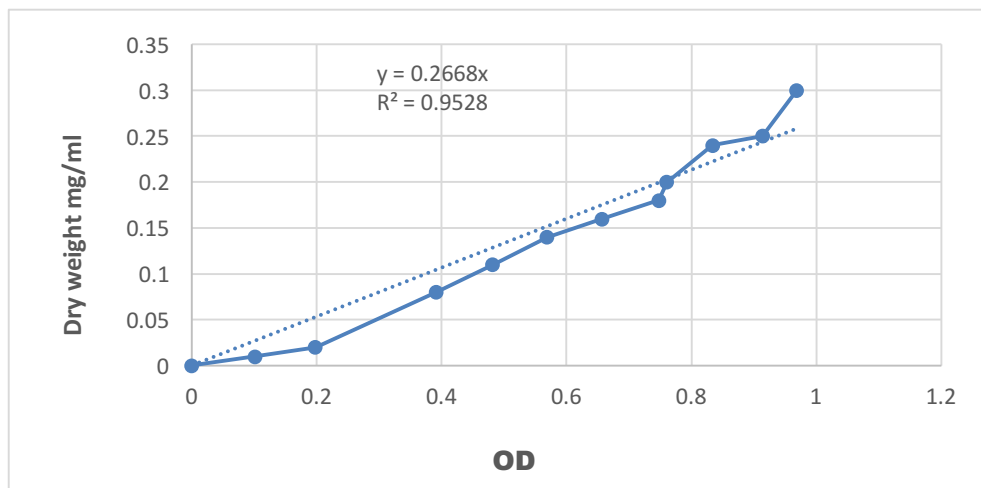


Figure 4.16 Linear relation between OD and cell dry weight of *Synechocystis* cells

4.2.8 The lipid content of *D. armatus* and *Synechocystis* cells

The concentration of neutral lipid content and lipid percentage (%) were calculated based on the triolein calibration curve and the relationship between OD and dry weight of the cells that offered the optimum concentration of biomass that is (OD₅₉₅=50%=200 µg ml⁻¹ Dry weight) for *D. armatus* and (OD₅₉₅=75%=400 µg ml⁻¹ Dry weight) for *Synechocystis* cells as described in section 4.2.7. Table 4.1 shows the lipid content and percentage of lipid accumulated by *D. armatus* cells under normal, 0.2 M NaCl and 0.4 M NaCl after 30 days. The highest lipid content and percentage of lipid was achieved by 0.2 M NaCl grown cells (15.5 µg/ml, 8%) after 30 days.

Table 4.1 Lipid content of *D. armatus* grown under normal and different salinity concentrations.

Sample	Day	Actual Biomass content(µg/ml)	Optimised Biomass content(µg/ml)	Neutral lipid content (µg/ml)	Percentage lipid content of DCW%
<i>D.armatus</i> +BG11	5	300	200	2.9	1.45
	12	700	200	4.2	2.1
	16	950	200	5.1	2.6
	21	1100	200	6.2	3
	30	1400	200	7.3	3.65
<i>D. armatus</i> +0.2M BG11 NaCl	5	155	200	3.3	1.65
	12	385	200	3.5	1.75
	16	363	200	3.6	1.8
	21	350	200	4.4	2.2
	30	340	200	15.5	8.0
<i>D.armatus</i> +0.4 M BG11 NaCl	5	155	200	2.7	1.35
	12	190	200	4.8	2.4
	16	275	200	5.0	2.5
	21	350	200	7.0	3.5
	30	110	200	9.2	4.6

Table 4.2 shows the neutral lipid content in *Synechocystis* grown under normal condition (normal BG11 medium), 0.2M NaCl, and 0.4M NaCl. The highest readings were obtained with normal BG11 medium after 30 days (shown in bold).

Table 4.2 Lipid content of *Synechocystis* PCC6803 grown under normal and different salinity concentrations.

Sample	Day	Actual Biomass content($\mu\text{g/ml}$)	Optimised Biomass content($\mu\text{g/ml}$)	Neutral lipid content ($\mu\text{g/ml}$)	Percentage lipid content of DCW%
<i>Synechocystis</i> +BG11	5	634	400	0.7	0.1
	12	874	400	0.8	0.2
	16	1187	400	0.6	0.15
	21	1325	400	0.5	0.15
	30	1404	400	1.5	0.4
<i>Synechocystis</i> +0.2M BG11 NaCl	5	636	400	1.0	0.3
	12	689	400	1.0	0.3
	16	1060	400	0.4	0.1
	21	1219	400	0.4	0.2
	30	1537	400	0.7	0.4
<i>Synechocystis</i> +0.4 M BG11 NaCl	5	132	400	1.3	0.3
	12	620	400	0.7	0.2
	16	780	400	0.6	0.1
	21	1113	400	0.2	0.07
	30	1325	400	0.2	0.07

The effect of nitrogen starvation on neutral lipid accumulation in *D.armatus* was investigated by growing this strain under normal BG11, 25% NaNO₃, 10% NaNO₃. and N Free BG11 media. Table 4.3 shows that N Free BG11 medium induced the highest neutral lipid content after 28 days incubation.

Table 4.3 Lipid content of *D. armatus* grown under different concentration of NaNO₃.

Sample	Day	ActualBiomass content(µg/ml)	Optimised Biomass content(µg/ml)	Neutral lipid content (µg/ml)	Percentage lipid content of DCW%
<i>D.armatus</i> +Normal BG11	5	300	200	2.3	1.15
	11	680	200	1.8	0.9
	21	1100	200	6.2	3.1
	28	1400	200	7.3	3.65
<i>D.armatus</i> +25% NaNO ₃ BG11	5	300	200	2.3	1.15
	11	775.	200	1.8	0.9
	21	900	200	3.4	1.7
	28	980	200	1.6	0.8
<i>D.armatus</i> +10% NaNO ₃	5	330	200	2.3	1.15
	11	670	200	8.9	4.5
	21	750	200	16.5	8.25
	5	840	200	29.9	15
<i>D.armatus</i> + N Free BG11	5	227	200	5.8	2.9
	11	299	200	35.4	17.7
	21	320	200	42.7	21
	28	344	200	61	30.5

Table 4.4 shows clearly that *Synechocystis* strain accumulated highest amount of neutral lipid when grown under N Free BG11 medium after 28 days when compared with cells grown in normal BG11 and 10% NaNO₃ BG11.

Table 4.4 Lipid content of *Synechocystis* grown under different concentration of NaNO₃.

Sample	Day	Actual Biomass content(µg/ml)	Optimised Biomass content(µg/ml)	Neutral lipid content (µg/ml)	Percentage lipid content of DCW%
<i>Synechocystis</i> +BG11	7	634	400	0.7	0.2
	14	874	400	0.8	0.2
	21	779	400	1.1	0.3
	28	1404	400	1.3	0.3
<i>Synechocystis</i> +10% NaNO ₃	7	470	400	0.7	0.2
	14	764	400	0.9	0.25
	21	779	400	1.2	0.3
	28	795	400	1.4	0.35
<i>Synechocystis</i> +Free N BG11	7	243	400	1.0	0.25
	14	205	400	1.6	0.4
	21	171	400	1.9	0.5
	28	164	400	2.9	0.75

The effect of using different N sources on the lipid accumulation in *D. armatus* was examined. Table 4.5 shows that NaNO₃ at low concentration (10%) was the best source of nitrogen for *D. armatus* lipid production because it accumulated the highest amount of neutral lipid content (29.9 µg/ml) after 28 days incubation when compared with other different sources of N (urea and NH₄Cl)

Table 4.5 Lipid content of *D. armatus* grown with different Nitrogen sources.

Sample	Day	Actual Biomass content(µg/ml)	Optimised Biomass content(µg/ml)	Neutral lipid content (µg/ml)	Percentage lipid content of DCW%
<i>D.armatus</i> +10% NaNO ₃ BG11	5	300	200	2.3	1.15
	11	775	200	8.9	4.5
	21	900	200	16.5	8.25
	28	980	200	29.9	15
<i>D.armatus</i> +Urea BG11	5	130	200	2.4	1.2
	11	266	200	2.7	1.35
	21	551	200	1.9	0.7
	5	642	200	2.3	1.25
<i>D.armatus</i> + NH ₄ Cl BG11	5	77	200	2.5	1.25
	11	135	200	2.4	1.2
	21	215	200	1.2	0.6
	28	229	200	1.8	0.9

Table 4.6 shows interesting results of the effect of N sources on the neutral lipid accumulation in *Synechocystis* strain. NH₄Cl was found to be the best source of N in *Synechocystis* based on the highest lipid content and percentage of lipid achieved after 18 days incubation in comparison with other N sources used (10% NaNO₃, and urea)

Table 4.6 Lipid content of *Synechocystis* PCC6803 grown under different Nitrogen sources.

Sample	Day	Actual Biomass content($\mu\text{g/ml}$)	Optimised Biomass content($\mu\text{g/ml}$)	Neutral lipid content ($\mu\text{g/ml}$)	Percentage lipid content of DCW%
<i>Synechocystis</i> +10% NaNO ₃	6	470	400	0.7	0.2
	12	764	400	0.8	0.2
	15	779	400	1.1	0.3
	18	795	400	1.4	0.35
<i>Synechocystis</i> +NH ₄ Cl BG11	6	522	400	0.8	0.2
	12	676	400	0.7	0.2
	15	641	400	2.0	0.5
	18	661	400	2.4	0.6
<i>Synechocystis</i> +Urea BG11	6	118	400	1.2	0.3
	12	113	400	1.1	0.35
	15	101	400	1.0	0.25
	18	124	400	1.2	0.3

4.2.9 Fatty Acid profile of N free BG11 stressed *D. armatus* cells

The fatty acid profile of *D. armatus* cells was determined using GC-MS (section 2.12) on esterified samples from cells grown under N Free BG11 medium. The highest content of neutral lipid was observed under this stress condition. The results in Figure 4-17 showed that linoleic acid and palmitic acid dominated the percentage of fatty acid methyl esters in N depleted *D. armatus* cells. Small amounts of oleic acid (C18:1) and polyunsaturated fatty acids were also detected.

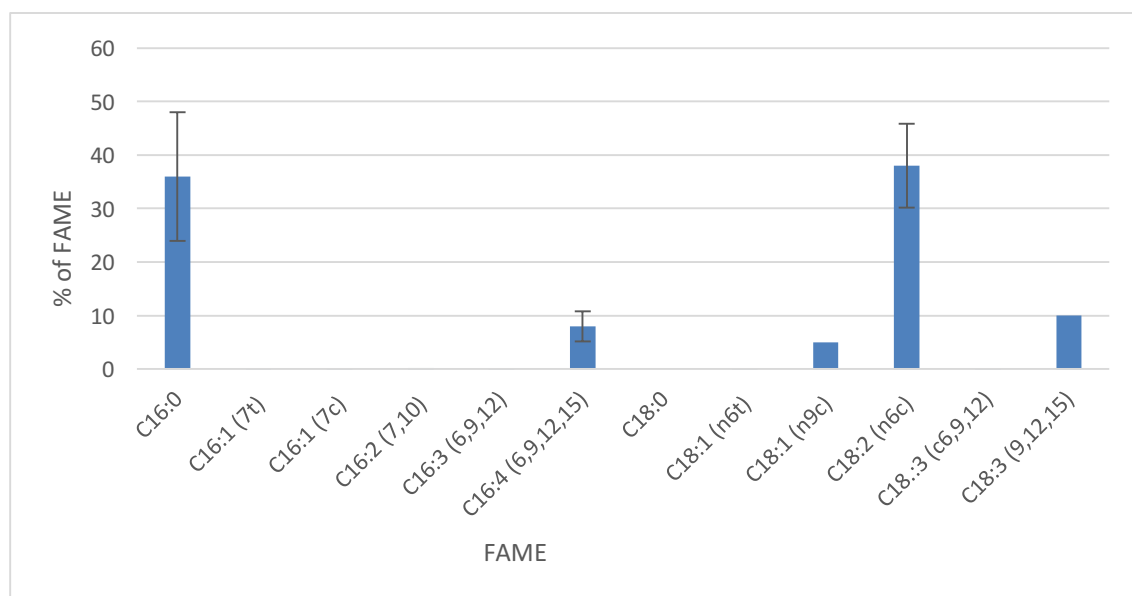


Figure 4.17 Fatty acid methyl ester profile of *D. armatus* cells grown under N Free BG11. Each column represents the average of three readings. Error bars represent biological repeats (n=3).

4.2.10 Determination of lipid content using NMR

The NMR spectral features of *D. armatus* lipid content extracted from cells grown in normal (BG11) and stress conditions (0.2 M NaCl, N Free BG11) were determined. The extraction was carried out by bead beating of the cells and then using chloroform and methanol as solvents. The ^1H NMR spectra are shown in Figure 4.18. Table 4.7 shows the results of chemical shift and functional groups analysis of the neutral lipids (TAG and FFA) and polar lipids and their fatty acid content. It is clear that the fatty acid content of cells grown in N free medium is much higher than for cells grown in normal BG11 medium.

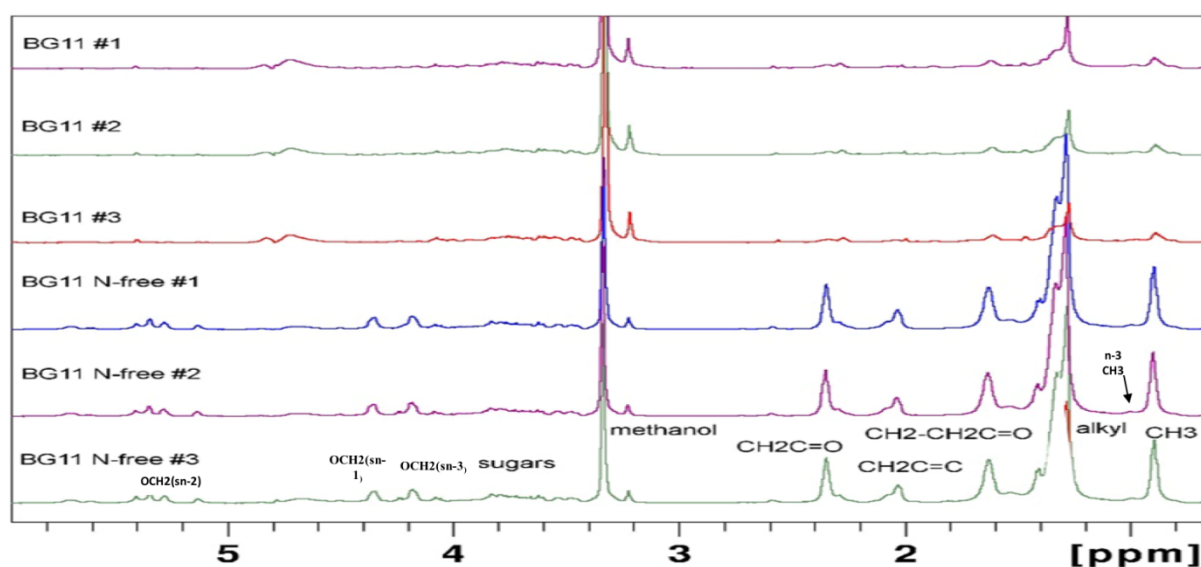


Figure 4.18 NMR spectra of *D. armatus* grown under normal BG11 and N Free BG11.

Table 4.7 ^1H NMR chemical shift (ppm) of functional group and values of *D. armatus* grown under normal medium (BG11) stress N Free BG11.

Chemical shift (ppm)	Functional group	<i>D.armatus+</i> BG11	<i>D.armatus+</i> Free BG11
0.8	-CH ₃ of all FA except PUFA	30	108
1	-CH ₃ of PUFA	9	11
1.4	-(CH ₂) _n of all FA	149	680
1.62	CH ₂ CH ₂ C=O of all FA	27	107
2.05	CH ₂ CH=CH of all FA	15	53
2.32	CH ₂ C=O of FFA	21	58
2.8	(CH-CH) _n CH ₂ of PUFA	3	49
4.2	OCH ₂ (<i>sn</i> -3) of TAG	6	31
4.36	OCH ₂ (<i>sn</i> -1) of TAG	3.5	25
5.36	OCH(<i>sn</i> -2) of TAG	2	19

4.3 Discussion

The method of quantification of neutral lipid from different algal cells using Nile Red fluorescence varies depending on the algal species. Therefore, different parameters required to be optimized for *D. armatus* including: Nile Red concentration, type of solvent, stain time, and concentration of algal cells (Rumin *et al.*, 2015).

4.3.1 Influence of microwaves and solvents on investigation of neutral lipid

To boost the probability of Nile Red penetration to *D. armatus* and *Synechocystis* cells a protocol was carried out in two steps (Chen *et al.*, 2009): using organic solvent because Nile Red is quenched in water (Greenspan *et al.*, 1985), and microwaving the cells. In the current work, two protocols were used to quantify the neutral lipids. One of these protocols depended mainly on using acetone as a stain carrier and used Nile Red directly. Poor results were found probably because acetone was not a good solvent carrier. One negative impact of using Nile Red in determination of neutral lipid was due to the dye failure to pass through the algal cells because of the rigidity of the algal cell wall and cytoplasmic membrane which might affect the penetration of dye and consequently it will not reach the target (intracellular lipid) (Chen *et al.* 2011) Many studies found that DMSO was a good organic solvent to be exploited as a stain carrier with Nile Red in terms of increasing the fluorescent intensity as much as 10-fold (Chen *et al.*, 2009; Frick *et al.*, 2014) than other solvents used including acetone, ethanol, ethylene glycol, and diaminotetraacetic acid (Cooksey *et al.*, 1987; Castell and Mann, 1994; Doan and Obbard, 2011; Siegler *et al.*, 2012; Wong *et al.*, 2014).

Two microwave steps in combination with an organic solvent have revealed that the neutral lipid content of the algal cells, in terms of fluorescent intensity, was increased. Previous experiments found that the fluorescent intensity of the algal cells was lower when using organic solvent alone even at high concentration because of the fluorescence quenching of Nile Red under high concentration of DMSO (Chen *et al.*, 2009). The influence of two steps of microwaving on the marked increase in the fluorescence intensity of *D. armatus* and *Synechocystis* cells was probably related to the attribution of the

molecular collisions speed enhancing and consequently simplifying the entrance and interaction of Nile Red with intracellular algal neutral lipids.

4.3.2 Influence of algal cell concentration and time of staining

The influence on Nile Red staining of different concentrations of *D. armatus* and *Synechocystis* cells was determined due to the fact that the Nile Red (NR) staining varies with the cell concentration. The results are shown in Figures 4.3 and 4.4 respectively and 50% of cell concentration ($=24 \times 10^4$ cells) with 14 minutes staining time was selected as the optimum conditions for *D. armatus* cells. While 75% cell concentration ($=15 \times 10^6$ cells) with 20 minutes staining time was chosen as the best conditions for *Synechocystis* cells. The selection of optimum concentration of *D. armatus* and *Synechocystis* cells were based on the balance between the cell-normalised value, the ratio of NR/concentration of algal cells, and the time of staining. The normalization technique was used because it is an accurate method to compare the fluorescent intensity readings of the same sample or different samples; they were prepared at the same cell density or the same amount of biomass (Chen *et al.*, 2009).

The ratio of NR/cells plays an important role for precise measurement of neutral lipid in cells. Pick and Rachutin-zalogin, (2012) reported that a high ratio of NR/cells was not favourable because it causes stacking of Nile Red dye, and consequently raises the possibility of quenchers in the samples. The excitation/emission wavelengths (485/580 nm) were chosen based on the results of Chen *et al.*, (2011), who found the optimal excitation/emission wavelengths for *Scenedesmus* sp. were 490/580 nm.

Moreover, the time of staining for the algal cells with Nile Red is considered to be a crucial factor for achieving the highest fluorescence intensity and it largely depends on the cell wall structure of the selected strain and therefore it is species dependent (Balduyck *et al.*, 2015). Our results showed that the maximum fluorescence intensity was achieved after 14 minutes for

D.armatus because the fluorescence intensity was slightly decreased with 20 minutes incubation. On the other hand, 20 minutes was selected to be an optimal staining time for *Synechocystis* because the fluorescence intensity was higher after 20 minutes in comparison with 14 minutes. In general, Pick and Pick and Rachutin-zalogin, (2012) stated that the values of fluorescence intensity decreased between (50%-90%) after 20 min staining with Nile Red due to the quenching with long staining time because of the stacking of Nile Red molecules, partial solubility of different concentration of Nile Red or quenchers of the sample.

4.3.3 Influence of Nile Red concentration

The influence of Nile Red concentrations on the quantification of fluorescent intensity were investigated in both *D. armatus* and *Synechocystis* sp. as shown in section 4-2-2-2. The optimum Nile red concentration was selected based on the balance between high and low Nile Red concentrations because of the drawbacks of relying on the lowest or highest concentration. The optimum concentration of Nile Red for *D. armatus* was ($1 \mu\text{g ml}^{-1}$), and for *Synechocystis* ($1.3 \mu\text{g ml}^{-1}$). The importance of dye concentration was related to the fact that the fluorescence intensity varies based on the concentration with an increase in the dye concentration above the optimal one, then the fluorescence decreased with the further increase in the dye concentration probably because of excess intense collisional quenching of the dye molecules at high concentration (Lakowicz, 2006). Several papers have reported that the fluorescence intensity depends on the concentration of Nile Red. (Chen *et al.*, 2009; Huang *et al.*, 2009; Xu *et al.*, 2013). Greenspan *et al.*, (1985) referred to the fact that at low concentration the interaction between the Nile Red dye and hydrophobic core is increased. Furthermore, the quenching of the dye was decreased when compared with excess of Nile Red. However, Pick and Rachutin-zalogin, (2012) observed that low concentration of Nile Red affect on the interaction between the dye and lipid droplets and consequently decrease the possibility of the dye to access through hydrophilic quenchers. On the other hand, the selection of a high Nile Red

concentration would probably lead to it reacting not only with the neutral lipids but also with the phospholipidic coat and hydrophobic surface of proteins (Sackett and Wolff, 1987). Overall, the optimum concentration of Nile Red for microalgae staining ranged between (0.1-100 $\mu\text{g ml}^{-1}$) depending on different species (Chen *et al.*, 2009; Huang *et al.*, 2009; Govender *et al.*, 2012).

4.3.4 Influence of Salinity on the neutral lipid accumulation

Figure 4.7 and Table 4.1 showed the influence of salinity on the neutral lipid accumulation in *D. armatus* over different lengths of growth in the presence of high salinity. For *D. armatus cells*, an increase in the NaCl concentration in BG11 medium to 0.2 M triggered a significant increase ($p < 0.05$) in the neutral lipid content (15.5 $\mu\text{g ml}^{-1}$) in contrast with growth in normal medium (7.3 $\mu\text{g ml}^{-1}$) or in 0.4 M NaCl (9.2 $\mu\text{g ml}^{-1}$) after 33 days incubation. These results agreed with both (Kaewkannetra, Enmak and Chiu, 2012; Salama *et al.*, 2013) who reported that an increase in the concentration of NaCl induced an increase of lipid production in *Scenedesmus sp.* However, increasing the concentration of NaCl higher than 0.3 M is not preferable in terms of inhibiting the photosynthesis efficiency of the selected microalgae and consequently decreasing the productivity of biomass and lipid.

Figure 4.8 showed the effect of the salt stress (0.2 and 0.4 M NaCl) on *Synechocystis* PCC 6803 after 33 days. The results showed that salt stress increased significantly (p value = 0.29) the neutral lipid content in the first days of incubation. However, after a month of growth the neutral lipid content decreased in contrast with normal BG11 medium. These results agreed with (Songruk *et al.*, 2015) who found that the low concentration of NaCl (0.1 and 0.15 M NaCl) enhanced the total lipid content of *Synechocystis PCC6803* after 9 days. While, high concentration of NaCl (0.4 M NaCl) did not boost the lipid content in comparison with normal BG11. (Allakhverdiev *et al.*, 1999) stated that low concentration of salt stress induced the intracellular lipid content due to the trigger of NaCl itself which probably stimulate membrane-bound enzymes and modifies the membrane fluidity.

4.3.5 Influence of nitrogen depletion

The effects of Nitrogen depletion on the neutral lipid content were investigated in both *D. armatus* and *Synechocystis* cells. Figure 4.9 and Table 4.3 showed clearly that N free BG11 significantly enhanced (t-test =0.01) the neutral lipid content ($61 \mu\text{g ml}^{-1}$) in comparison with other nitrogen starvation concentration 25% NaNO_3 ($1.6 \mu\text{g ml}^{-1}$) and 10% NaNO_3 ($29.9 \mu\text{g ml}^{-1}$) after 28 days growth. These results agreed with (Rattanapoltee and Kaewkannetra, 2013; Xia *et al.*, 2016) who demonstrated that the neutral lipid content of *Scenedesmus* cells enhanced when the concentration of NaNO_3 is decreased. Furthermore, *Scenedesmus* sp. grown on approximately 5% NaNO_3 BG11 at 25° C was found to accumulate the highest lipid content at different temperatures in comparison with the same strain grown under normal BG11 (Xia *et al.*, 2016). Numerous studies emphasized the fact that Nitrogen depletion or starvation increased significantly the level of lipid content in different microalgae (Dean *et al.*, 2010; Zhang *et al.*, 2013). The ideal theory to explain the effect of nitrogen starvation on enhancing the lipid content of microalgae is that when microalgae grow in medium with deficient concentration of nitrogen the protein synthesis required for growth will be affected and consequently excess carbon derived from the photosynthesis process is accumulated in the storage molecule that is triglyceride (Scott *et al.*, 2010).

For *Synechocystis*, Figure 4.10 and Table 4.4 illustrated the influence of nitrogen depletion on the neutral lipid content. N Free BG11 medium was found to be an ideal stress condition because of the significant increase (t-test =0.03) in the neutral lipid content ($2.9 \mu\text{g ml}^{-1}$) when compared with the neutral lipid content of normal BG11 ($1.3 \mu\text{g ml}^{-1}$) and 10% NaNO_3 ($1.4 \mu\text{g ml}^{-1}$) respectively. These results disagreed with (Monshupanee and Incharoensakdi, 2013) who demonstrated that nitrogen starvation did not dramatically increase the lipid content (in form of Diacyl glycerol DAG) of *Synechocystis* PCC6803 in comparison with significant increase of glycogen and polyhydroxybutyrate (PHB). Moreover, our results disagreed with Sheng *et al.*, (2011), who reported that an attempt to increase the lipid content of *Synechocystis* were restricted when he tried different solvents to evaluate the ideal method for lipid extraction from *Synechocystis* cells. The explanation of these changes in the results probably related to the use of Nile Red in combination with microwaves to evaluate the

neutral lipid content in *Synechocystis* cells where the other studies used conventional method of total lipid determination.

4.3.6 Influence of different nitrogen sources

Ammonium chloride and urea were used to investigate the effect of different nitrogen sources on the neutral lipid accumulation in both *D. armatus* and *Synechocystis* strains. Figure 4.11 and Table 4.5 showed clearly the significant increase in the neutral lipid content of *Desmodesmus* cells ($29.9 \mu\text{g ml}^{-1}$) grown under 10% NaNO_3 after 28 days growth in comparison with ($1.9 \mu\text{g ml}^{-1}$) for urea and ($1.8 \mu\text{g ml}^{-1}$) for NH_4Cl respectively.

Our results agreed with (Ren *et al.*, 2013) (who stated that NaNO_3 was considered an ideal source of nitrogen in terms of enhancing both the biomass concentration and lipid content of *Scenedesmus* cells. Arumugam *et al.*, (2013) confirmed our results by showing that NaNO_3 was the best source of nitrogen for *Scenedesmus* because of an increase in the biomass yield in comparison with other sources of nitrogen. Moreover, Xin *et al.*, (2010) reported that *Scenedesmus* grown at a low concentration of NaNO_3 accumulated high percentage of lipid content.

The effect of different nitrogen sources and concentration on the amount of lipid accumulated by different microalgae has been investigated. One study demonstrated that NH_4Cl plays a crucial role in boosting total lipid content of *Scenedesmus*; 1.5 fold more than NaNO_3 and 2 fold more than urea after 10 days cultivation (Yilancioğlu *et al.*, 2016). Furthermore, (Makarevi *et al.*, (2011) reported that urea represents the optimum source of nitrogen in terms of biomass productivity under low concentration of NaNO_3 . Some species of *Chlorella* preferred ammonium as their nitrogen source (Rodolfi *et al.*, 2009). While, other species of *Chlorella* preferred to utilize urea as a source of nitrogen (Amin *et al.*, 2013). Overall, it is clear that various sources of nitrogen can be successfully exploited to induce increased lipid content in different microalgae.

For *Synechocystis*, our results agreed with (Hauf *et al.*, 2016) who found that the total fatty acids level was increased when *Synechocystis* PCC 6803 was grown under nitrogen starvation in combination with replacing NaNO_3 by NH_4Cl as a source of nitrogen. Moreover, (Richter *et al.*, (1999) demonstrated that *Synechocystis* and other cyanobacteria have the ability to accumulate ammonium nitrogen inside the cells in

polypeptide form called cyanophycin, under nitrogen starvation this polymer tends to be degraded by a hydrolytic enzyme cyanophycinase. According to the results of neutral lipid determination from *Synechocystis* in which the neutral lipid accumulation under different stress conditions were low, we decided to stop further experiment with this strain because although there were other techniques including metabolic engineering of *Synechocystis* cells, the yields were still low (Ruffing, 2014). Furthermore, Ruffing, (2014) reported that *Synechococcus* sp. PCC 7002 is more favourable than *Synechocystis* PCC 6803 as a cyanobacterial host to direct conversion of CO₂ into Free Fatty Acids (FFA) in terms of the potential drawbacks of *Synechocystis* FFA product on the host cell physiology.

4.3.7 Fatty acid profile of nitrogen starved *D. armatus* cells

Figure 4.17 shows the results of fatty acid profile of *D. armatus* total lipid after 30 days incubation under nitrogen depletion (N Free BG11 medium).

The results showed 11 fatty acids methyl esters of different carbon length. However, the most abundant fatty acid methyl esters belonged to palmitic acid C16:0 (39%), Linoleic acid C: 18:2 (38%), alpha linoleic C: 18:3 (10%), hexadecane-tetraenoic acid C16:4 (8%), and Oleic acid C18:1 (5%) respectively. Our results agreed with many studies ((Tan and Lin, 2011; Islam *et al.*, 2013; Gour *et al.*, 2016) who reported that the main fatty acid in *Scenedesmus* cells under stationary growth phase (with different percentages) were palmitic acid, linoleic acid, alpha linoleic, hexadecane-tetraenoic acid and oleic acid. Moreover, the percentage of unsaturated fatty acids in our *D. armatus* strain is favourable as a biodiesel resource world wide (SFA 39%, MUFA 5%, PUFA 56%) and it was a bit lower in comparison with other *Scenedesmus* sp. and soybean oil (Ramos *et al.*, 2009; Gour *et al.*, 2016). The occurrence of oleic methyl ester in biodiesel develops the properties of biodiesel (Knothe, 2008; Prabakaran and Ravindran, 2012). Therefore, our strain of *D. armatus* appears to be a desirable feedstock for biodiesel production in terms of the strain types of fatty acid methyl esters and the percentage of SFA, MUFA, and PUFA which showed close relation to the lipid profile features of crops.

4.3.8 ¹H-NMR determination of lipid content

The main interesting features for NMR characterization of the microalgal neutral lipid content is the ability to assess the composition of biological mixture with smallest amount of the extract that significantly minimizes the complication of chromatographic separation or chemical derivatization (Bearden, 2012). Moreover, NMR spectroscopy can identify the lipids and other biological metabolites within the entire cells because of their ability to investigate the interior of intact cells (Beal *et al.*, 2010; Merkle and Syvitski, 2012). The ¹H-NMR spectrum of *D. armatus* extract showed the specific signals of glycerides, fatty acids and other components as described in Table 4.7. These chemical shift signals were distinguished based on the comparison with spectral features of soybean, and fish oil according to (Kumar *et al.*, 2014; Sarpal *et al.*, 2015). The algal extract shows signals at 4.2, 4.36, and 5.36 ppm which are related to the proton signals of different triglyceride moieties. Signals at 0.8 ppm are related to the terminal methyl groups of saturated C14, C18 or *n-6 /n-9* of unsaturated fatty acids C18:1, C18:2, while the signals at 1 ppm belonged to terminal methyl group of *n-3* types of 3 or more than 3 double bonds, which indicates that the TAG comprised both saturated and unsaturated fatty acids chains. The spectra also indicate a signal at 1.4 ppm that referred to long alkyl chain (CH₂)_n. The spectra also showed different signals at 2.32 ppm belonged to FFA and at 2.8 ppm related to C18:3. As shown in Table 4.7, the results of ¹H-NMR showed an increase in the content of all lipids in stressed *D. armatus* cells in comparison with the same microalga grown under normal conditions. When the results of NMR and GC-MS results are compared it is clear that *D. armatus* grown under N free BG11 medium accumulated a high percentage of TAG in the form of saturated and unsaturated fatty acids which makes it a promising candidate for biodiesel production.

**Chapter Five Attempts to
Enhance the Neutral Lipid
Content of *Desmodium
armatum***

5.1 Introduction

In the last decade or so, microalgae have been suggested as a convenient alternative, renewable, environmentally-friendly source of energy that could be an ideal option to solve the common worldwide problems related to fossil fuel exhaustion and greenhouse gas emissions (Chisti, 2007). However, the production cost of biodiesel from microalgae is till now one of the main barriers that require hard efforts to overcome to be economically feasible. Therefore, to address this crucial problem, improvements in algal biomass production and the rate of lipid biosynthesis are required because they represent the main factors that have a large effect on reducing the cost of biodiesel production. However, it is recognised that increasing lipid synthesis almost invariably decreases biomass levels (Sharma *et al.*, 2012).

An improvement in the algal strain lipid yield can be achieved by two main approaches: metabolic (biochemical) engineering as described in Chapter 4 of this thesis using environmental stresses such as nitrogen limitation and genetic engineering using overexpression of enzymes or blocking of competing metabolic pathways (Manuelle *et al.*, 2009). For the latter approach, random mutagenesis (Doan and Obbard, 2012) or insertional mutagenesis tools (Terashima *et al.*, 2015) can be used. Transformation systems for algae were initially developed in diatoms such as *Phaeodactylum tricornutum* (Zaslavskaja *et al.*, 2000) and then expanded to include green algae e.g. *Chlamydomonas reinhardtii* and the eustigmatophyte alga *Nannochloropsis* (Kilian *et al.*, 2011). Initially, the percentage of successful results was not high, essentially because the function of key genes and enzymes that regulate the lipid metabolism, synthesis, and accumulation in many algae species were not recognised (Khozin-goldberg and Cohen, 2011). However, our understanding of algal lipid metabolism is improving, but this is nonetheless a barrier to advanced genetic engineering of algae.

Inducing random mutations shows a significant benefit in comparison with genetic engineering tools basically because it does not require an investigation of the biochemical and genetic details of the selected microorganism. Mutagenesis using different physical or chemical mutagens can be used to induce a higher rate of mutation than the natural rate of the wild type microorganism (Kodym A., 2003). Among these mutagens, ultra violet light (UV) is one of the most common physical mutagens which

induces mutations that are frequently triggered by the formation of pyrimidine dimers on the same strand of DNA. Mutations caused by UV are generally detected at the methyl-CpG sites (Ikehata and Ono, 2011). The damage to the DNA of microalgae caused by UV influences several physiological processes like growth, photosynthesis, biochemical composition and nutrient uptake (Shelly *et al.*, 2005; Hader, 2006; Hughes, 2006; Wong *et al.*, 2007). Because of the ease of UV mutagenesis, it is considered to be a convenient and rapid genetic modification tool that can be used on various microalgal isolates to perturb their lipid production (Vigeolas *et al.*, 2012). Additionally, Chiew-yen *et al.*, (2004) reported that UV light had a negative influence on the growth rate of a *Chlorella* species, a significant improvement in the lipid content was also detected after exposure to UV light.

Once mutagenesis has taken place, the algal mutant cells must be selected for improved lipid productivity. Many approaches depend on time consuming techniques where the cells are plated after mutagenesis, then the phenotypic features are used to differentiate the mutant cells e.g. a phenotypic screen using iodine vapours was used to identify mutant cells unable to accumulate starch (Zabawinski *et al.*, 2001). Another phenotypic factor is the appearance of small antenna size in mutant cells of the diatom *Cyclotella* after plating (Huesemann *et al.*, 2009). These phenotypic approaches could be easily detected in the lab, but are not suitable for large scale screening programmes.

Developments in flow cytometry techniques have produced a favourable tool to sort out the problems related to selection of mutant cells. Thousands of cells can be investigated per second, and consequently this technique began a new period of quick cell mutant generation (Betz *et al.*, 1984; Davey and Kell, 1996). Flow cytometry is currently considered as a powerful tool that can analyse cells at high flow rate (up to 100,000 cells per second) and to differentiate between low signals that make it a good way to investigate several features and physiological parameters within a short time. For instance, cell size and granularity (internal complexity of the cell) can be measured in different microorganisms like bacteria, fungi, yeast and mammalian cells (Hyka *et al.*, 2013; Velmurugan *et al.*, 2013)). In terms of microalgae, flow cytometry is exploited as a desired method to separate a mutant cell from a complex population based on a distinct characteristic of microalgal photosynthetic pigments (chlorophyll, carotenoids,

and sometimes phycobilins) that show robust fluorescence intensity in combination with lipid binding dyes such as Nile Red and BODIPY (Cirulis *et al.*, 2012). The mutant cells then can be sorted from a mixture of cells by fluorescence activated cell sorting (FACS) technique. FACS permits a single mutated cell to be automatically sorted depending on the fluorescence of the stained cell. FACS is a safe and non-lethal technique that provides a flexible way for cell sorting.

The objectives of this chapter are:

1. The determination of the neutral lipid content of *D. armatus cells* using flow cytometry technique in combination with Nile Red.
2. To induce random mutation in *D. armatus* cells using UV-C light as a mutagen.
3. To utilize fluorescent activated cell sorting (FACS) technique for screening of *D. armatus* mutated cells and sorting of the mutated cells.
4. To compare the neutral lipid content between wild type and UV mutated *D. armatus* by isolation of RNA, compare the gene expression between the two strain using cDNA microarray technique.

5.2 Results

5.2.1 Determination of the influence of DMSO

The optimum concentration of DMSO was determined as described in section 2.13.1. Figure 5.1 shows that 15% (final concentration) DMSO was the best concentration to be used as a stain carrier for determination of lipid content using flow cytometry in combination with Nile Red.

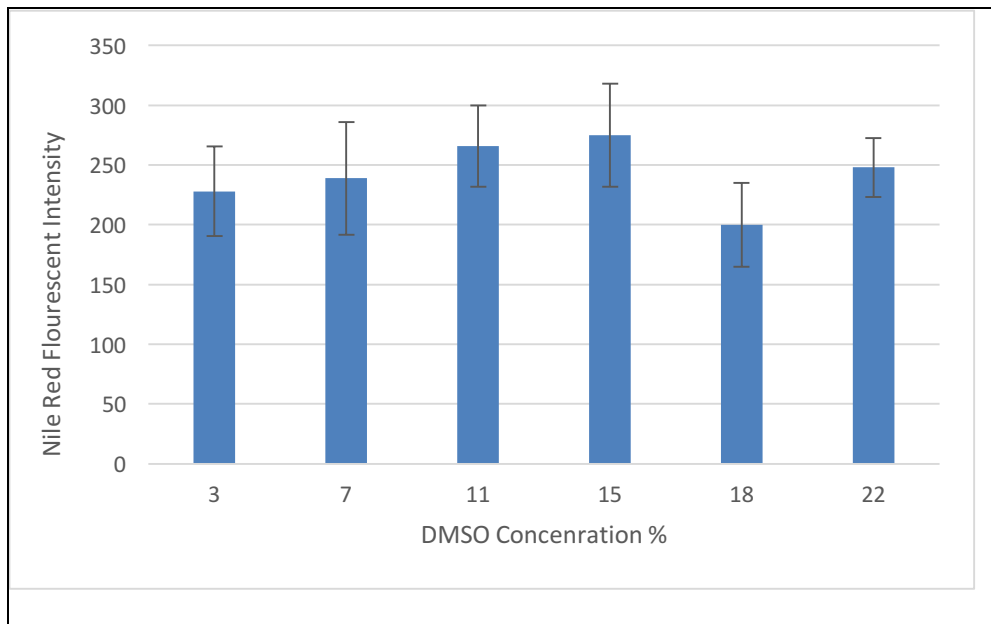


Figure 5.1 Optimisation of DMSO concentration for use as a stain carrier.

5.2.2 Optimising the concentration of Nile Red

The proper use of Nile Red staining solution is crucial to achieve the highest fluorescence and consequently produce the ideal staining of target clones. Serial concentrations of Nile Red dissolved in DMSO were prepared to optimise an appropriate concentration to be used in the flow cytometry technique as described in section 2.13.2. Table 5.1 showed the analysis of Flow cytometry results using flow Jo software in which it is obvious that the concentration 0.8 µg/ml was the ideal concentration of Nile Red in terms of percentage of stained cells.

Table 5.1 Flow cytometry analysis of *D. armatus* sp. cells stained with different concentration of Nile Red. Each value is the average of 3 technical repeats.

Specimen number	Final Nile Red concentration µg/ml	Cell population	Stained cells population	% of stained cells
1	unstained	10289	22	2.71
2	0.1	10269	6963	78.1
3	0.2	10205	8555	88.8
4	0.4	10199	8973	92.3
5	0.6	10248	8941	91.6
6	0.8	10159	9662	97
7	1.2	10174	9315	94.7

Figure 5.2 revealed the FSC vs SSC area plot of scattered unstained (A) and stained *D. armatus* with different concentrations of Nile Red(B-G). The unstained cells were utilised to draw the gate that distinguish between the stained and unstained cells. The stained cells showed uniform scatter.

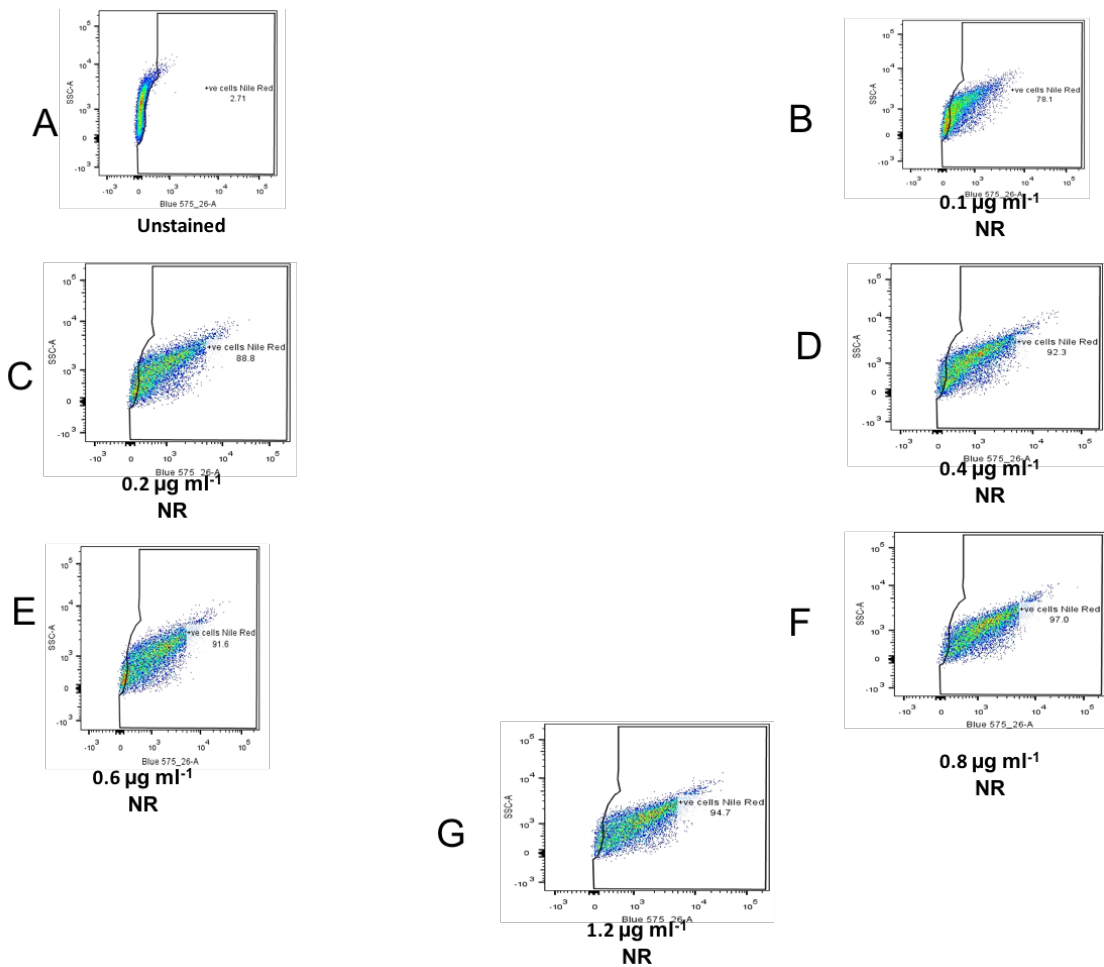


Figure 5.2 Flow cytometry analysis of *D. armatus* cells unstained and stained with different concentrations of Nile Red.

- A)** Forward scatter (FSC) (blue 575) vs Side scatter (SSC) two dimensional (2D) plots of unstained *D. armatus* cells.
- B)** Forward scatter (blue 575) vs Side scatter (SSC) two dimensional (2D) plots of *D. armatus* cells stained with Nile Red at final concentration (0.1 $\mu\text{g/ml}$)
- C)** FSC (blue 575) vs SSC two dimensional (2D) plots of *D. armatus* cells stained with Nile Red at final concentration (0.2 $\mu\text{g/ml}$)
- D)** FSC (blue 575) vs SSC two dimensional (2D) plots of *D. armatus* cells stained with Nile Red at final concentration at final concentration (0.4 $\mu\text{g/ml}$)
- E)** FSC (blue 575) vs SSC two dimensional (2D) plots of *D. armatus* cells stained with Nile Red at final concentration (0.6 $\mu\text{g/ml}$)
- F)** FSC (blue 575) vs SSC two dimensional (2D) plots of *D. armatus* cells stained with Nile Red at final concentration (0.8 $\mu\text{g/ml}$)
- G)** FSC (blue 575) vs SSC two dimensional (2D) plots of *D. armatus* cells stained with Nile Red at final concentration (1.2 $\mu\text{g/ml}$)

5.2.3 Random mutation of *D. armatus* cells using UV mutagens

UV mutagens were used to induce random mutation in *D. armatus* cells to enhance the neutral lipid content in the mutated cells. *Desmodesmus armatus* cells were exposed to UV light at different times as described in section 2.14. Figure 5.3 showed clearly that the wild type (zero min – no exposure to UV) showed a clear enhancement in the biomass in terms of cell counts for 8 days, while the UV-exposed strains showed a significant decrease in growth rate and final biomass, especially for the longer UV exposure times (30, 48, and 60 min).

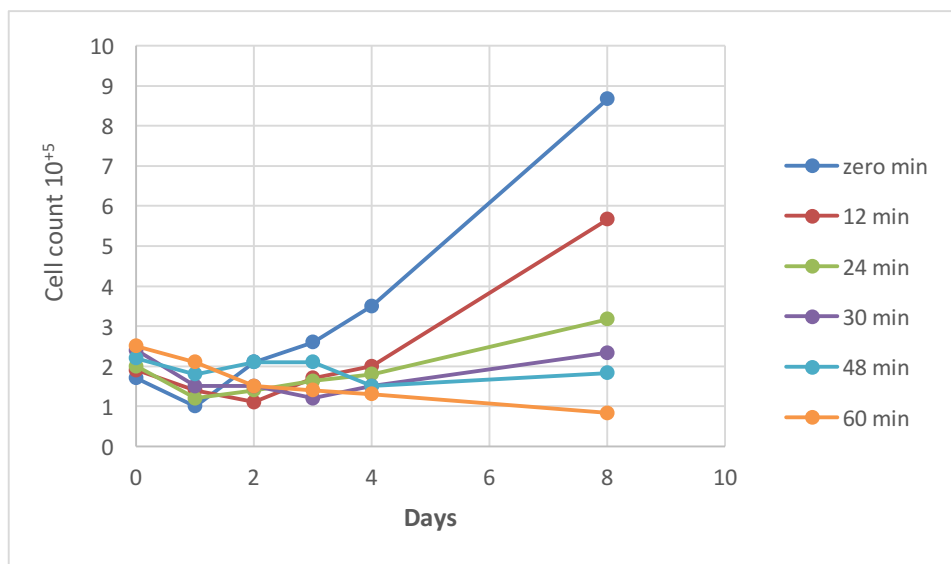


Figure 5.3 The growth of *D. armatus* cells exposed to UV mutagenesis for different lengths of time.

5.2.4 Flow cytometry of UV irradiated *D. armatus* cells

The neutral lipid contents of the *D. armatus* cells irradiated with UV for different time periods were measured as described in section 2.14. The flow cytometry analysis of the UV irradiated cells was carried out as described in section 2.13.3. Table 5.2 showed that 30 minutes is the optimum time in which the neutral lipid content was the highest in terms of the median of the UV exposure time and the biggest value of neutral lipid percentage. Also, unstained cells (control) were used to show the level of autofluorescence of the chlorophyll and other photosynthetic pigments.

Table 5.2 Flow cytometry analysis of UV irradiated *D. armatus* cells for different time periods. Each value is the average of three replicates.

Sample	% of stained cells	Cells median	% of neutral lipid
Unstained (Control)	2.3	116	0
zero min	99.8	3726	0.3
9 min	99.2	4654	0.8
12 min	99.7	6055	1.6
24min	99.8	7303	2.2
30 min	99.7	7514	3.0
36 min	99.5	5436	1.7
48 min	99.6	4389	1.0
60 min	99.5	4463	0.8

5.2.5 Fluorescence activated cell sorting (FACS) of the UV irradiated *D. armatus* cells

The UV irradiated *D. armatus* cells that showed highest neutral lipid yield after analysis using flow cytometry (30 min UV exposure) were sorted as described in section 2.14.1. Figure 5.4 A showed the fluorescent scatter of the stained cells (Red) , while B revealed the gate which represents the edges that were used by the sorting unit to substantially isolate 2.9% (21000 cells ml⁻¹) of the highest lipid content that were sorted and collected in the sterile tube (blue).

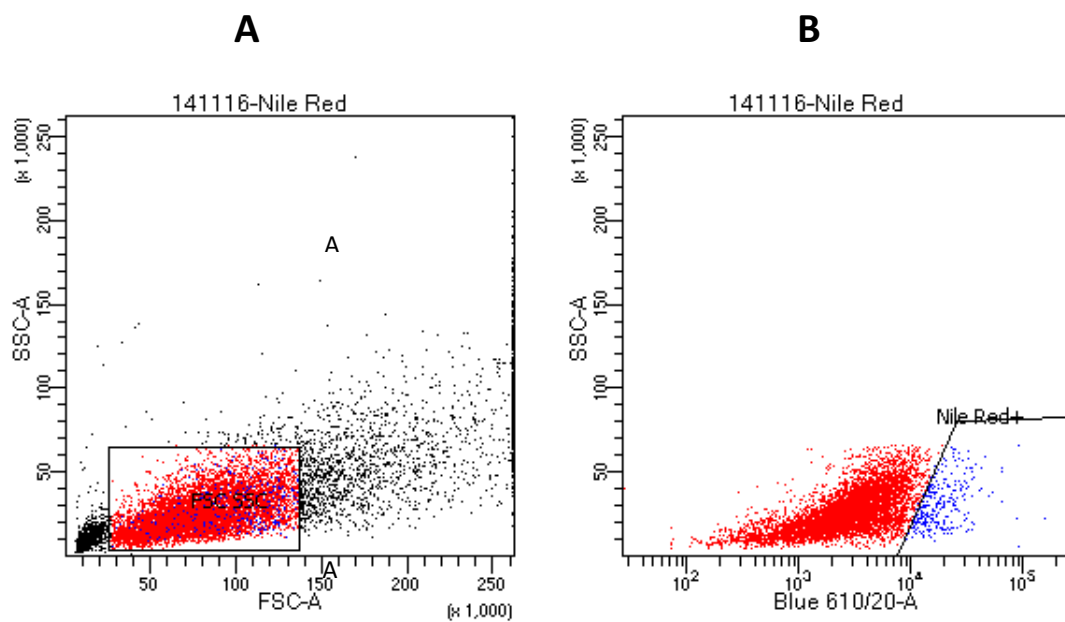


Figure 5.4 FACS analysis of 30 min UV mutated *D. armatus*.

- A) Dot spot of UV mutated *D. armatus* cells population
- B) Dot spot of sorted of UV mutated *D. armatus* cells (2.9%)

5.2.6 Screening of the mutated cells

After the cells were sorted, a single cell technique was carried out to screen the mutated cells in terms of TAG accumulation that differentiate between single cells as described in section 2.14.2. The neutral lipid contents of 12 mutant cells and one wild type cell were analysed. Table 5.3 summarised the results in which among the 12 UV irradiated single cells it was noted that the cell H12 accumulated TAG 5 fold higher than the wild type cell H5 in terms of median values.

Table 5.3 Flow cytometry analysis of neutral lipid content in both a single wild type cell (H5) and 12 single UV mutated sorted cells (A4 to H12). The letters and numbers are related to the well of the 96 well plate.

Well number of the cells	% +Nile Red	Cells Median Fluorescence Intensity
H5 (Wild type) unstained	1.4	209
H5 (wild type) stained	99	2714
A4	98.4	3622
A10	99.2	6510
B7	98.8	4697
C2	99	3960
C8	99.3	4970
E5	99.1	3957
E9	99.3	4653
F3	99.1	4618
F12	99.1	5869
G5	98.8	4482
H11	98.4	5247
H12	99.6	10160

5.2.7 Determination of the neutral lipid in Wild type and sorted UV exposed *D. armatus*

The lipid concentration and lipid percentage of both wild type and sorted UV exposed cells were determined after 15 days incubation was described in sections in 2.14.3 and 4.2.7. The result (Table 5.4) shows approximately doubled increase in the neutral lipid content and lipid percentage in the sorted UV mutated *D.armatus* cells (H12) grown under N free BG11 in comparison with wild type *D.armatus* cells grown on the same medium.

Table 5.4 lipid content of both wild type (H5) and sorted UV mutated (H12) grown under normal and N free BG11 for 18 days

Sample	Actual Biomass concentration($\mu\text{g/ml}$)	Optimised Biomass concentration ($\mu\text{g/ml}$)	Neutral lipid content ($\mu\text{g/ml}$)	Percentage lipid content of DCW%
H5 +BG11	870	200	8.5	4.25
H5+N free BG11	370	200	37	18.5
H12 +BG11	820	200	13	6.5
H12+Nfree BG11	420	200	70	35

5.3 Discussion

5.3.1 Flow cytometry for analysis of neutral lipid in *D. armatus* cells.

Among various conventional techniques used for measuring the algal lipid contents, flow cytometry has become the most common and favourable technique for determining the algal lipid yields even with single cell resolution. The distinct features of flow cytometry are use of the instrument is low cost and the instruments are commonly found in universities and hospitals, the measuring protocol for the lipid yield is easy and well-known and simultaneously can be exploited to measure other parameters like the cell size; granularity, autofluorescence of pigments (chlorophyll, carotenoids), and the enzyme activity of the single cell. Moreover, the fast characterisation and sorting of cells by flow cytometry allows the investigation and identification of desired yield of cells and the achievement of an axenic culture (Montero, *et al.*, 2011; Hyka *et al.*, 2013; Chioccioli *et al.*, 2014).

Many studies stated that flow cytometry is a promising tool for measuring the algal lipid content on a single-cell basis in combination with a lipophilic probe such as Nile Red and BODIPY (Guzmán *et al.*, 2011; Satpati *et al.*, 2016). Cirulis *et al.*, (2012) stated that NR is more desirable than BODIPY to stain microalgae because the NR fluorescence signal is less effected by the overall concentrations of dye. Both DMSO as an organic solvent for the dye and Nile Red concentration were optimised to enhance the effectiveness and efficiency of NR to stain the neutral (intracellular) lipids. Fifteen % concentration was recorded to be the best concentration of DMSO. These results disagreed with Satpati and Pal, (2014) in which they reported that 40% was an optimum concentration of DMSO for achieving high fluorescent intensity of Nile Red. Our results found that the optimum concentration of NR was 0.8 µg/ml which agreed with the values of Cabanelas *et al.*, (2016). Moreover, our results were close to Chen *et al.*, (2009) who reported that 0.5 µg/ml was the optimum concentration of NR. In contrast, our results again disagreed with Satpati and Pal, (2014) who recorded that 5 µg/ml was the optimum concentration of NR used to stain different strains of microalgae.

Overall, the selection of the optimum concentration of NR varies between different microalgal species, because each microalgal strain has a different response to NR fluorescence in terms of their cell wall composition which effects the penetration of NR through the cells and the organic solvent used as a stain carrier (Rumin *et al.*, 2015). The optimum concentration of Nile Red was selected based on the highest fluorescent intensity of *D. armatus* cells which was 97% after flow cytometry analysis.

5.3.2 Random mutation of *D. armatus* cells

Various tools have been utilised to enhance the lipid content of the microalgae. Among these methods, mutagenesis has been reported to be an ideal protocol to breed an algal strain with a remarkable increase in the lipid content (Manandhar-Shrestha and Hildebrand, 2013). Random mutagenesis is the easiest approach for dramatic increases in the metabolite productivity of microorganisms including lipid accumulation. However, the main drawback is that its accuracy level is low therefore, the screening of the highest putative mutant is crucial (Carlton and Brown, 1981). Ultra Violet light has been used successfully to induce random mutation in microalgal cells that led to significant increases in the lipid accumulation in microalgal cells (Bougaran *et al.*, 2012; Vigeolas *et al.*, 2012; Anthony *et al.*, 2015). Our results revealed a significant decrease in the growth of the cells particularly those exposed to UV-C for long time (30, 48, 60 min) that agreed with Friesner *et al.*, (2004) and Anthony *et al.*, (2015) who also reported that UV decreased the biomass of the irradiated microalgae. Both UV-C and UV-B exposure cause an abundance of DNA photoproducts which probably enhances the opportunity for mutation during cell replication (Jiang and Taylor, 1993) Moreover, Sato *et al.*, (1995) documented that the growth rate of UV mutated *Chlamydomonas reinhardtii* was lower than the wild type strains because of the drop in the photosynthetic O₂ evolution that was associated with CO₂ fixation.

5.3.3 Flow cytometry analysis of the UV mutated *D. armatus*

The results of our study revealed the utilisation of flow cytometry in combination with Nile Red to investigate the optimum UV exposure duration that led to the production of a high value mutated cell with high lipid content. UV exposure time of 30 min was found to be the optimum time for inducing random mutation in *D. armatus* cells in terms of high median values with reference to the lipid content. Our results closely agreed with Liu *et al.*, (2015) who stated that 24 min exposure to UV was the best duration to produce mutant cells.

Several reports documented that flow cytometry was successfully utilised for evaluation and screening of the lipid droplets in mutated and parent algal cells. Doan and Obbard, (2012) exploited random induced mutagenesis to evaluate the increase in neutral lipid composition in *Nannochloropsis* sp. cells using flow cytometry with NR. Bougaran *et al.*, (2012) reported a remarkable rise in lipid yield after flow cytometry analysis of *Isochrysis galbana*. Another study confirmed the active uses of flow cytometry for screening of mutant cells with rich lipid content in *Chlorella* sp. effectively exploited flow cytometry to differentiate mutant cells with perturbed lipid yield from a collection of 1800 transformants and consequently determined the phenotype in 31 mutants (Manandhar-Shrestha and Hildebrand, 2013)

5.3.4 Florescence Activated cell sorting (FACS)

FACS technique was used effectively to separate the UV mutated *D. armatus* cells that showed hyperlipidic content in comparison with the wild type cells. Using single cell technique, individually sorted NR stained cells were grown in 96 well plates. Among 13 single generated sorted cells, a cell with hyperaccumulation of lipids (5 fold higher than the wild type cells) was successfully separated using FACS. Although there are several conventional techniques that can be utilised for the selection of cells with distinct features that can be conducted manually like infinite dilution or micro operation, FACS method is preferable because it is quicker, enabling the separation of a higher number of sorted cells and consequently a rapid revival of the selecting cells.

Various reports documented the efficient role of FACS techniques for isolation of cells with desired traits as revealed through flow cytometry. (Montero *et al.*, 2011) reported firstly the combination of flow cytometry and FACS to detect, separate and select the cells with rich lipid yield from cultures of *Tetraselmis suecica*. Moreover, in recent years FACS tool has been used widely to isolate mutant cells with hyper lipid content from *Nannochloropsis* (Doan and Obbard, 2012), *Chlamydomonas reinhardtii* (Velmurugan *et al.*, 2013; Xie *et al.*, 2014; Terashima *et al.*, 2015) and *Chlorella* (Manandhar-Shrestha and Hildebrand, 2013). Our results revealed a high percentage of cells stained with NR were recovered after FACS. The toxicity of dye, the organic solvent (DMSO, acetone) and the FACS procedure are the initial factors that play a crucial role on the cell viability after FACS process. Our results agreed with (Terashima *et al.*, 2015; Cabanelas *et al.*, 2016) who also reported that a high percentage of stained sorted cells were recovered after FACS operation. While our results disagreed with Velmurugan *et al.*, (2013) who documented that the sorted NR stained *C. reinhardtii* cells failed to recover from the sorting process. The recovery rate differences are probably because we washed the cells with PBS 2-3 times after staining to remove any excess of the NR dye and the organic solvent from the sample as described in Terashima *et al.*, (2015).

5.3.5 Nile Red determination of wild type and UV mutated cells

The phenotypic detection of rich content lipid generated from random mutated microalgae that were grown under nutrient starvation has paved the way for further investigation to realise the molecular and genetics mechanisms that induce the cell to hyperaccumulation of lipid. Our results revealed an interesting increment (35%) in the lipid content of UV mutated sorted cells (H12) in comparison with the wild type cells (H5) (18.5%). Our result agreed with Xie *et al.*, (2014) who showed a massive enhancement in the lipid content of FACS sorted *Chlamydomonas reinhardtii* after N starvation. Moreover, Satpati and Pal, (2015) reported an increase in the neutral lipid content of the FACS sorted *Chlorella ellipsoidea* and *Chlorococcum infusionum* after

nitrogen depletion. Lim *et al.*, (2015) isolated two FACS sorted cells with huge increase in the lipid content (114%, and 123%) after cultivation in N depleted growth condition.

Chapter Six Discussion, Conclusions, and Future Work

6.1 Discussion

Over the last few decades, microalgae have been examined as an optimum source of renewable, carbon neutral, environmentally friendly source of energy that can be utilised efficiently to overcome the drawbacks of Green House Gases triggered mainly from the continuous burning of conventional fossil fuel sources of energy (Rastogi *et al.*, 2015)

The first step in our research project, as outlined in Chapter 3, was focused on isolation of local fresh water microalgal strains from Weston Park in Sheffield (UK). Various techniques were used to achieve an axenic strain including streaking on agar plate, Percoll solution treatment, and serial centrifugation. Our work emphasized that the identification of the unknown microalgal strain based on conventional microscopic tools was found to be insufficient to distinguish between *Desmodesmus* and *Scenedesmus* species because of their closely related morphological features. Therefore, molecular identification approaches are now required for accurate taxonomy of the microalgal cells. Ribosomal DNA (in particular 18S rDNA) is the common DNA marker used to eliminate the gaps in the precise taxonomy of microalgal species. However, our results highlighted that using 18S rDNA alone as a molecular marker did not lead to a species identification of the isolated alga. Our results outlined that the Internal Transcribed Spacer (ITS) region (including ITS1, 5.8 S rDNA and ITS2 sequences) emerged as valuable DNA barcodes that can solve the close evolutionary relationship between *Desmodesmus* and *Scenedesmus*. Final identification of our local isolate that as *Desmodesmus armatus* was based on the sequences of 18S rDNA, 5.8S rDNA, ITS1 and ITS2. Moreover, the phylogenetic tree construction confirmed the precise taxonomy of our local strain (Hadi *et al.*, 2016). The identification of the model cyanobacterium, *Synechocystis* PCC 6803, was confirmed through the molecular barcode 16S rDNA that is the essential molecular tool for identification of prokaryotic microorganisms.

The fourth chapter of the thesis focused on the investigation of the neutral lipid content of both *D. armatus* and *Synechocystis* sp. based on a fluourometric approach in combination with the lipophilic Nile Red dye. DMSO is the organic solvent that was used to facilitate the transition of NR through the algal cells for the accurate *in situ* detection of lipid droplets. Fluourometric assessment of lipid has many advantages over the

conventional gravimetric determination e.g. it is an *in situ* measurement that matches the fluorescence of the dye with the TAG content of the microalgal cells while, the gravimetric method evaluation required extraction of total lipid from the algal biomass using various organic solvents that might trigger loss of some lipid content during extraction. Also, gravimetric measurements are for all lipids present, whereas NR specifically measures TAG. Moreover, the fluorescence measurement can be utilised effectively to measure the lipid yield over time of culture that provides a proper background of the cell culture homogeneity while the gravimetric and chromatographic method is time consuming and not suitable for many repeat measurements (Rumin *et al.*, 2015).

The first step in measurement of the neutral lipid content of *D. armatus* and *Synechocystis* strains started with the optimisation of the cell concentration, dye concentration and incubation time in the presence of the dye to avoid any probability of NR fluorescence quenching because NR fluorescence varies based on the species and the conditions of the assessment (Halim and Webley, 2015). Various cultivation conditions were performed to induce the TAG accumulation in both *strains*. Our results revealed that nitrogen starvation was the optimal stress condition in which both strains accumulated the highest yield of neutral lipid. However, the maximum neutral lipid production under N starvation in *Synechocystis* cells was much less than *D. armatus* because *Synechocystis* sp. cells tend to produce high amounts of glycogen as the main storage product while neutral lipid was produced at a low level (Monshupanee and Incharoensakdi, 2013). A recent study stated that N starvation is an ideal approach to massively enhance the lipid content in *Desmodesmus* sp. however, the biomass productivity is highly decreased with this stress condition and this is a serious drawback for commercial production (Rios *et al.*, 2015).

Nitrogen is a vital component of chlorophyll synthesis and crucial proteins of the two photosystems. Thus, any shortage in the nitrogen source leads to inhibition of both structural and physiological components of the cells including the degradation of chlorophyll and thylakoid membranes. Under N starvation, photosynthesis cannot be stopped completely because it is mainly dependent on the abundance of light. Microalgae species tend to protect the integrity of photosynthesis and cell structural

components by storing the excess carbon produced by photosynthesis as neutral lipids via the induction of the TAG pathway to remodel and accumulate high levels of neutral lipid in the cytosol (Martin *et al.*, 2014).

The lipid profiles of *D. armatus* grown under normal and N starvation conditions were analysed using the GC-MS techniques after extraction of the neutral lipid using hexane as a non-polar solvent. This revealed interesting data as N starved *D. armatus* cells accumulated both PUFA i.e. linoleic acid C18:2 (n6c) and saturated fatty acids i.e. palmitic acid C16:0. These two fatty acids dominated the free fatty acids (FFA) percentage of the lipid profile after transesterification of the TAG. The FFA content plays a crucial role in selecting microalgae isolated from various aquatic environments for commercial utilisation as an optimum source for biodiesel production. In our experiment Tridecanoic acid methyl ester (C13:0) was exploited as an internal standard and the FAME quantification was carried out based on peak area of each FAME in comparison with that of the internal standard. Moreover, a mixture of fatty acid standards (C4-C24) is used as an additional standard to estimate the lipid concentrations depending on the peak areas ratio. Gas chromatography is a chromatographic approach that is commonly used to separate a mixture of lipids (fatty acids) based on size and uses various standards to distinguish the separated lipids. Mass spectrometry is generally used in combination with GC to further identify the lipid content based on the relation between their mass when ionised and split in the mass spectrometer (Paik *et al.*, 2009).

Further identification of the lipid content in *D. armatus* cells grown under normal condition (BG11 medium) and N starvation conditions was conducted using ¹H Nuclear Magnetic Resonance (NMR) and the results confirmed the variation in the lipid yield between the two strains based on the abundance of TAG and the FFA content in the stressed *D. armatus* cells. NMR technique is basically used to offer a good knowledge of the targeted sample structure based on combination between the magnetic field of the equipment and nuclei of atoms in the sample and measured the resonant rate emitted from the sample. This relation can be exploited to initiate a spectrum of chemical shifts in which the values of the spectral peaks of the targeted molecule can

be compared with standards or with another known sample to measure the level of that molecule in the candidate sample (Sarpal *et al.*, 2015).

Chapter 5 of the thesis highlighted the attempt to increase the neutral lipid content of the local strain *D. armatus* cells through the random mutation of the cells using UV-C as a mutagen. After optimising the optimum UV exposure time, the lipid content of the *D. armatus* cells was investigated using flow cytometry techniques in combination with NR dye. The outcome was a UV mutated cell line with a large enhancement in the neutral lipid yield (5 fold higher than the wild type yield of neutral lipid) based on the median values in fluorescence activated cell sorting (FACS). Random mutation using various physical and chemical mutagens is considered to be an optimum tool to overcome the problem of the high cost of biodiesel produced from microalgae and to help make it economically feasible. Moreover, UV mutagens contribute to alter the type of fatty acids produced in wild type and UV mutated cells in which the yield of PUFA is increased in the UV mutated cells (Lim *et al.*, 2015). The FACS approach was used in this study to assess, sort, and select the UV mutated cells with high neutral lipid level and compare their lipid production with the wild type cells at the single cell level in combination with NR dye. The concentration of the NR dye was optimised to avoid any toxicity of the dye on the cell growth after sorting. The strategy of selecting the desired mutated cells using FACS technique is based merely on the morphological features of the cells (forward and or side scatter) of the flow cytometry channel and the autofluorescence of the cells (Montero *et al.*, 2011).

6.2 Conclusions

The following major conclusions can be drawn from the current study:

- Molecular identification using various DNA markers (18S rDNA, 5S rDNA, ITS1, and ITS2 sequences) is an optimum approach for the accurate classification and construction of the phylogenetic tree of unknown microalgae.
- The fluorometric technique of using NR dye is an efficient tool for the quantification of neutral lipid in microalgae.
- Nitrogen starvation is the key stress condition to greatly enhance the neutral lipid content of the algal cells in comparison with salinity and alteration of the medium nitrogen sources.
- Random mutation of the algal cells using UV-C as a mutagen led to a highly significant increase in the neutral lipid content of the candidate strain.
- Fluorescence Activated Cell Sorting (FACS) technique is the most valuable tool for efficient screening of the high lipid producing cells among a complex population of cells.

6-3 Future Work

Based on the results of this study, the following future work is recommended :

- Further DNA barcodes should be targeted like the chloroplast riboulose bisphosphate large subunit gene *rbcL*, the elongation factor *tufA*, and chloroplast ribosomal subunit 23S for further confirmation of the identification of the local *D. armatus* strain.
- Compare the lipid yield obtained using NR dye with other fluorometric approaches using lipophilic fluorescent BODIPY dye, or other techniques such as Raman spectroscopy, and Fourier transform infrared spectroscopy (FTIR) to assess the optimum method of lipid quantification.
- Further investigation of the FAME properties of the local *D. armatus* strain such as Cetane number (CN), iodine value (IV), saponification value (SV), degree of unsaturation (DU) and other properties. Compare these properties with the industry standards to assess whether the local candidate species biodiesel properties can meet with the properties of the European standard (EN14214) and American standard (ASTM D6751) for biodiesel production.
- Investigate the neutral lipid profile of the UV exposed *D. armatus* cells for comparison of their content of fatty acids with the wild type strain.
- Attempt to utilise various mutagens like heavy carbon ions, or chemical mutagens such as ethyl methane sulfonate (EMS) or other mutagens to induce the lipid content of microalgae to reduce the cost of producing biodiesel from microalgae.

References

- Abou-shanab, R. A. I. *et al.* (2011) 'Characterization and identification of lipid-producing microalgae species isolated from a freshwater lake', *Biomass and Bioenergy*. Elsevier Ltd, 35(7), pp. 3079–3085. doi: 10.1016/j.biombioe.2011.04.021.
- Adams, C. *et al.* (2013) 'Bioresource Technology Understanding precision nitrogen stress to optimize the growth and lipid content tradeoff in oleaginous green microalgae', *Bioresource Technology*, 131, pp. 188–194.
- Ahmed, F. *et al.* (2014) 'Profiling of carotenoids and antioxidant capacity of microalgae from subtropical coastal and brackish waters', *FOOD CHEMISTRY*. Elsevier Ltd, 165, pp. 300–306.
- ALLAKHVERDIEV, S. I. *et al.* (1999) 'Genetic engineering of the unsaturation of fatty acids in membrane lipids alters the tolerance of *Synechocystis*', *Proc. Natl. Acad. Sci.*, 96(May), pp. 5862–5867.
- Allewalt, J. P. *et al.* (2006) 'Effect of Temperature and Light on Growth of and Photosynthesis by *Synechococcus* Isolates Typical of Those Predominating in the Octopus Spring Microbial Mat Community of Yellowstone National Park', *APPLIED AND ENVIRONMENTAL MICROBIOLOGY*, 72(1), pp. 544–550.
- Alonzo, F. and Mayzaud, P. (1999) 'Spectrofluorometric quantification of neutral and polar lipids in zooplankton using Nile red', *Marine Chemistry*, 67, pp. 289–301.
- Amaro, H. M., Guedes, A. C. and Malcata, F. X. (2011) 'Advances and perspectives in using microalgae to produce biodiesel', *Applied Energy*. Elsevier Ltd, 88(10), pp. 3402–3410.
- Amin, N. F. *et al.* (2013) 'Effect of Some Nitrogen Sources on Growth and Lipid of Microalgae *Chlorella* sp. for Biodiesel Production', *Journal of Applied Sciences Research*, 9(8), pp. 4845–4855.
- An, S. S., Friedl, T. and Hegewald, E. (1999) 'Phylogenetic Relationships of *Scenedesmus*

and Scenedesmus-like Coccoid Green Algae as Inferred from ITS-2 rDNA Sequence Comparisons', *Plant biol.*, 1, pp. 418–428.

Andresen, S. (2015) 'International Climate Negotiations: Top-down, Bottom-up or a Combination of Both?', *The International Spectator*. Routledge, 50(1), pp. 15–30. doi: 10.1080/03932729.2014.997992.

Anthony, J. *et al.* (2015) 'Ultraviolet and 5 ' Fluorodeoxyuridine Induced Random Mutagenesis in *Chlorella vulgaris* and Its Impact on Fatty Acid Profile : A New Insight on Lipid-Metabolizing Genes and Structural Characterization of Related Proteins', *Mar Biotechnol*, 17, pp. 66–80. doi: 10.1007/s10126-014-9597-5.

Araujo, K. *et al.* (2017) 'agriculture Global Biofuels at the Crossroads : An Overview of Technical , Policy , and Investment Complexities in the Sustainability of Biofuel Development', *Agriculture*, 7(32), pp. 1–22.

Arumugam, M. *et al.* (2013) 'Bioresource Technology Influence of nitrogen sources on biomass productivity of microalgae *Scenedesmus bijugatus*', *Bioresource Technology*, 131, pp. 246–249.

Balat, M. (2007) 'Global Bio-Fuel Processing and Production Trends', *Energy Exploration & Exploitation*, 25(3), pp. 195–218. doi: 10.1260/014459807782009204.

Baldauf, S. L., Manhartt, J. R. and Palmer, J. D. (1990) 'Different fates of the chloroplast *tufA* gene following its transfer to the nucleus in green algae', *Proc. Natl. Acad. Sci.*, 87(July), pp. 5317–5321.

Balduyck, L. *et al.* (2015) 'Optimization of a Nile Red method for rapid lipid determination in autotrophic , marine microalgae is species dependent', *Journal of Microbiological Methods*. Elsevier B.V., 118, pp. 152–158.

Barakat, A. *et al.* (2014) 'Eco-friendly dry chemo-mechanical pretreatments of lignocellulosic biomass : Impact on energy and yield of the enzymatic hydrolysis', *Applied Energy*. Elsevier Ltd, 113, pp. 97–105.

Bartley, M. L. *et al.* (2013) 'Effects of salinity on growth and lipid accumulation of biofuel

microalga *Nannochloropsis salina* and invading organisms', *Biomass and Bioenergy*. Elsevier Ltd, 54, pp. 83–88.

Beal, C. M. *et al.* (2010) 'Lipid analysis of *Neochloris oleoabundans* by liquid state NMR', *Biotechnology and Bioengineering*, 106(4), pp. 573–583. doi: 10.1002/bit.22701.

Bearden, D. W. (2012) *Environmental Metabolomics. In: Encyclopedia of Magnetic Resonance*. Edited by H. RK and W. R. John Wiley.

Becker, E. W. (2007) 'Micro-algae as a source of protein', *Biotechnology Advances*, 25, pp. 207–210. doi: 10.1016/j.biotechadv.2006.11.002.

Benemann, J. R. and Oswald, W. J. (1996) *Systems and economic analysis of microalgae ponds for conversion of CO₂ to biomass. Final report to Department of Energy*. doi: 10.2172/493389.

Bergmann, A., Colombo, S. and Hanley, N. (2008) 'Rural versus urban preferences for renewable energy developments ☆', *Ecological Economics*, 5, pp. 616–625.

Bertozzini, E. *et al.* (2011) 'Application of the standard addition method for the absolute quantification of neutral lipids in microalgae using Nile red', *Journal of Microbiological Methods*. Elsevier B.V., 87(1), pp. 17–23.

Betz, J. W., Aretz, W. and Hartel, W. (1984) 'Use of Flow-Cytometry in industrial microbiology for strain improvement programs', *Cytometry*, 5(2), pp. 145–150. doi: 10.1002/cyto.990050208.

Bharti, R. K. *et al.* (2017) 'ceptus t', 5075(October). doi: 10.1080/15435075.2017.1351368.

Bharti, S. K. and Roy, R. (2012) 'Quantitative H NMR spectroscopy', *Trends in Analytical Chemistry*. Elsevier Ltd, 35, pp. 5–26. doi: 10.1016/j.trac.2012.02.007.

Bigogno, C., Khozin-goldberg, I. and Cohen, Z. (2002) 'Accumulation of arachidonic acid-rich triacylglycerols in the microalga *Parietochloris incisa* (Trebuxiophyceae, Chlorophyta)', *Phytochemistry*, 60, pp. 135–143.

- Biofuels (2016) *The Fuel of the Future*. Available at: <http://www.biofuel.org.uk>.
- Borowitzka, M. A. (2013) 'High-value products from microalgae — their development and commercialisation', *J Appl Phycol*, 25, pp. 743–756. doi: 10.1007/s10811-013-9983-9.
- Borowitzka, M. A. and Borowitzka, L. J. (1988) *Microalgal biotechnology*. Cambridge: Cambridge University Press.
- Bougaran, G. *et al.* (2012) 'Enhancement of neutral lipid productivity in the microalga *Isochrysis affinis Galbana* (T-Iso) by a mutation-selection procedure', *Biotechnology and Bioengineering*, 109(11), pp. 2737–2745. doi: 10.1002/bit.24560.
- Boyer, S. L., Flechtner, V. R. and Johansen, J. R. (2001) 'Is the 16S – 23S rRNA Internal Transcribed Spacer Region a Good Tool for Use in Molecular Systematics and Population Genetics ? A Case Study in Cyanobacteria', *Mol. Biol. Evol*, 18(6), pp. 1057–1069.
- BP (2014) *BP Energy Outlook 2035*. Available at: <https://www.bp.com/content/dam/bp/pdf/energy-economics/energy-outlook-2016/bp-energy-outlook-2014.pdf>.
- BP (2017a) : *Statistical Review of World Energy*. Available at: <http://www.bp.com/en/global/corporate/energy-economics/statistical-review-of-world-energy.html>.
- BP (2017b) *BP Energy Outlook 2017 edition*. Available at: <https://www.bp.com/content/dam/bp/pdf/energy-economics/energy-outlook-2017/bp-energy-outlook-2017.pdf>.
- Breuer, G., Evers, W. A. C., *et al.* (2013) 'Analysis of Fatty Acid Content and Composition in Microalgae', *Journal of Visualized Experiments*, 5(September), pp. 1–9.
- Breuer, G., Lamers, P. P., *et al.* (2013) 'Bioresource Technology Effect of light intensity , pH , and temperature on triacylglycerol (TAG) accumulation induced by nitrogen starvation in *Scenedesmus obliquus*', *Bioresource Technology*. Elsevier Ltd, 143, pp. 1–9.

- Brower, M. *et al.* (2014) *Global Status Report*.
- Brown, L. M. and Zeiler, K. G. (1993) 'Aquatic Biomass and Carbon Dioxide Trapping', *Energy Convers. Mgmt Vol.*, 34(9), pp. 1005–1013.
- Buchheim, M. *et al.* (2011) 'Internal Transcribed Spacer 2 (nu ITS2 rRNA) Sequence-Structure Phylogenetics : Towards an Automated Reconstruction of the Green Algal Tree of Life', *PLoS ONE* |, 6(2), pp. 1–10. doi: 10.1371/journal.pone.0016931.
- Cabanelas, I. T. D. *et al.* (2016) 'Biotechnology for Biofuels Sorting cells of the microalga *Chlorococcum littorale* with increased triacylglycerol productivity', *Biotechnology for Biofuels*. BioMed Central, 9, p. 183. doi: 10.1186/s13068-016-0595-x.
- Cakmak, T. *et al.* (2012) 'Differential Effects of Nitrogen and Sulfur Deprivation on Growth and Biodiesel Feedstock Production of *Chlamydomonas reinhardtii*', 109(8), pp. 1947–1957. doi: 10.1002/bit.24474.
- Canakci, M. and Sanli, M. C. H. (2008) 'Biodiesel production from various feedstocks and their effects on the fuel properties', *J Ind Microbiol Biotechnol*, 35, pp. 431–441.
- Cao, J. *et al.* (2014) 'Bioresource Technology Significance evaluation of the effects of environmental factors on the lipid accumulation of *Chlorella minutissima* UTEX 2341 under low-nutrition heterotrophic condition', *BIORESOURCE TECHNOLOGY*. Elsevier Ltd, 152, pp. 177–184. doi: 10.1016/j.biortech.2013.10.084.
- Carlton, B. C. and Brown, B. J. (1981) (1981) *Gene mutation*. In: Gerhardt P. editor. *Manual of methods for general bacteriology*. : American Society for Microbiology. Washington DC.
- Carvalho, A. P., Meireles, A. and Malcata, F. X. (2006) 'Microalgal Reactors : A Review of Enclosed System Designs and Performances', (ii), pp. 1490–1506.
- Castell, L. L. and Mann, R. (1994) 'Optimal staining of lipids in bivalve larvae with Nile Red', *Aquaculture*, 119, pp. 89–100.
- CBOL Plant Working Group (2009) 'A DNA barcode for land plants', *PNAS*, 106, pp. 12794–12797.

Chang, J. S. *et al.* (2016) *Photobioreactors. In Current Developments in Biotechnology and Bioengineering*. The Netherlands: Elsevier: Amsterdam.

Cheban, L., Malischuk, I. and Marchenko, M. (2015) 'Cultivating *Desmodesmus armatus* (Chod .) Hegew . in recirculating aquaculture systems (RAS) waste water', *Arch. Pol. Fish.*, 23, pp. 155–162.

Cheirsilp, B. and Torpee, S. (2012) 'Bioresource Technology Enhanced growth and lipid production of microalgae under mixotrophic culture condition : Effect of light intensity , glucose concentration and fed-batch cultivation', *Bioresource Technology*. Elsevier Ltd, 110, pp. 510–516. doi: 10.1016/j.biortech.2012.01.125.

Chen, W. *et al.* (2009) 'A high throughput Nile red method for quantitative measurement of neutral lipids in microalgae', *Journal of Microbiological Methods*. Elsevier B.V., 77(1), pp. 41–47.

Chen, W., Sommerfeld, M. and Hu, Q. (2011) 'Bioresource Technology Microwave-assisted Nile red method for in vivo quantification of neutral lipids in microalgae', *Bioresource Technology*. Elsevier Ltd, 102(1), pp. 135–141. doi: 10.1016/j.biortech.2010.06.076.

Chen, X. *et al.* (2014) 'Screening of marine microalgae for biodiesel feedstock', *Advances in Microbiology*, 35(7), pp. 365–376.

Cheng, J. J. and Timilsina, G. R. (2011) 'Status and barriers of advanced biofuel technologies : A review', *Renewable Energy*. Elsevier Ltd, 36(12), pp. 3541–3549.

Chiew-yen, W. *et al.* (2004) 'Growth Response , Biochemical Composition and Fatty Acid Profiles of Four Antarctic Microalgae Subjected to UV Radiation ...', *Malaysian Journal of Science*, 23(2), pp. 103–118.

Chioccioli, M., Hankamer, B. and Ross, I. L. (2014) 'Flow Cytometry Pulse Width Data Enables Rapid and Sensitive Estimation of Biomass Dry Weight in the Microalgae *Chlamydomonas reinhardtii* and *Chlorella vulgaris*', *PLOS ONE*, 9(5), pp. 1–12. doi: 10.1371/journal.pone.0097269.

Chisti, Y. (2007) 'Biodiesel from microalgae beats bioethanol', *Biotechnology Advances*. Elsevier Inc., 25, pp. 294–306. doi: 10.1016/j.tibtech.2007.12.002.

Chisti, Y. (2008) 'Biodiesel from microalgae beats bioethanol', *Trends in Biotechnology*, 26(3), pp. 126–131. doi: 10.1016/j.tibtech.2007.12.002.

Chisti, Y. (2012) , (2012) *Raceways-based production of algal crude oil*. In: Posten, C., Walter, C.(Eds.), *Microalgal Biotechnology: Potential and Production*. de Gruyter. Berlin.

Chodat, R. (1926) 'Scenedesmus étude de génétique, de systéma- tique expérimentale et d'hydrobiologie', *Rev. Hydrobiol*, 3, pp. 71–258.

Choi, W. Y. *et al.* (2012) 'Bioethanol Production from *Ulva pertusa* Kjellman by High-temperature Liquefaction', *Chemical and Biochemical Engineering Quarterly*, 26(1), pp. 15–21. Available at: <http://connection.ebscohost.com/c/articles/75653462/bioethanol-production-fromulva-pertusa-kjellman-by-high-temperature-liquefaction>.

Christensen, T. (1964) 'The Gross Classification of Algae', in Jackson, D. F. (ed.) *Algae and Man: Based on lectures presented at the NATO Advanced Study Institute July 22 -- August 11, 1962 Louisville, Kentucky*. Boston, MA: Springer US, pp. 59–64. doi: 10.1007/978-1-4684-1719-7_3.

Cirulis, J. T. *et al.* (2012) 'Optimization of Staining Conditions for Microalgae with Three Lipophilic Dyes to Reduce Precipitation and Fluorescence Variability', *Cytometry Part A*, pp. 618–626.

Clarridge, J. E. (2004) 'Impact of 16S rRNA Gene Sequence Analysis for Identification of Bacteria on Clinical Microbiology and Infectious Diseases', *CLINICAL MICROBIOLOGY REVIEWS*, 17(4), pp. 840–862. doi: 10.1128/CMR.17.4.840.

Clerck, O. De *et al.* (2013) 'ALGAL TAXONOMY : A ROAD TO NOWHERE ? 1', *J. Phycol.*, 49(October 2012), pp. 215–225.

Confalonieri, U. *et al.* (2007) *Human health*. In M. L. Parry, O. F. Canziani, J. P. Palutikof, P. J. van der Linden, & C. E. Hanson (Eds.), *Climate change 2007: Impacts, adaptation,*

and vulnerability, contribution of working group II to the fourth assessment report of the intergovernment. Cambridge and New York: Cambridge University Press.

Converti, A. *et al.* (2009) 'Chemical Engineering and Processing : Process Intensification Effect of temperature and nitrogen concentration on the growth and lipid content of *Nannochloropsis oculata* and *Chlorella vulgaris* for biodiesel production', *Chemical Engineering and Processing*, 48, pp. 1146–1151.

Cooksey, K. E. *et al.* (1987) 'Fluorometric determination of the neutral lipid content of microalgal cells using Nile Red', *Journal of Microbiological Methods*, 6, pp. 333–345.

Cuellar-bermudez, S. P. *et al.* (2014) 'Minireview Extraction and purification of high-value metabolites from microalgae : essential lipids , astaxanthin and phycobiliproteins', *Microbial Biotechnology*, pp. 190–209. doi: 10.1111/1751-7915.12167.

Daroch, M., Geng, S. and Wang, G. (2013) 'Recent advances in liquid biofuel production from algal feedstocks', *Applied Energy*. Elsevier Ltd, 102, pp. 1371–1381.

Dashtban, M., Schraft, H. and Qin, W. (2009) 'Fungal Bioconversion of Lignocellulosic Residues ; Opportunities & Perspectives', *International Journal of Biological Sciences*, 5(6), pp. 578–595.

Davey, H. M. and Kell, D. B. (1996) 'Flow Cytometry and Cell Sorting of Heterogeneous Microbial Populations : the Importance of Single-Cell Analyses', *MICROBIOLOGICAL REVIEWS*, 60(4), pp. 641–696.

Day, J. G., Slocombe, S. P. and Stanley, M. S. (2012) 'Bioresource Technology Overcoming biological constraints to enable the exploitation of microalgae for biofuels', *Bioresource Technology*. Elsevier Ltd, 109, pp. 245–251.

Dean, A. P. *et al.* (2010) 'Bioresource Technology Using FTIR spectroscopy for rapid determination of lipid accumulation in response to nitrogen limitation in freshwater microalgae', *Bioresource Technology*. Elsevier Ltd, 101(12), pp. 4499–4507.

Demirbas, A. (2008) 'Biofuels sources , biofuel policy , biofuel economy and global biofuel projections', *Energy Conversion and Management*, 49, pp. 2106–2116.

- Demirbas, A. and Demirbas, M. F. (2011) 'Importance of algae oil as a source of biodiesel', *Energy Conversion and Management*. Elsevier Ltd, 52(1), pp. 163–170.
- Derome, A. (1987) *Modern NMR Techniques for Chemistry Research*. UK: University of Oxford.
- Doan, T. Y. and Obbard, J. P. (2011) 'Improved Nile Red staining of *Nannochloropsis* sp.', *J Appl Phyco*, 23, pp. 895–901.
- Doran, P. M. (2013) *Bioprocess engineering principles*. New York: Academic Press.
- Duong, V. T. *et al.* (2012) 'Microalgae Isolation and Selection for Prospective Biodiesel Production', *Energies*, 5, pp. 1835–1849. doi: 10.3390/en5061835.
- Easterling, W. E. *et al.* (2007) *Food, fibre and forest products*. In M. L. P.
- EIA (2016) *EIA Bioenergy countries report*. Available at: <http://www.ieabioenergy.com/wp-content/uploads/2017/04/IEA-Bioenergy-Annual-Report-2016.pdf>.
- Eland, L. E., Davenport, R. and Mota, C. R. (2012) 'Evaluation of DNA extraction methods for freshwater eukaryotic microalgae', *WR*. Elsevier, 46(16), pp. 5355–5364.
- Eroglu, E. and Melis, A. (2016) 'ScienceDirect Microalgal hydrogen production research', *International Journal of Hydrogen Energy*. Elsevier Ltd, 41(30), pp. 12772–12798.
- Erwin, J. A. (1973) *Comparative biochemistry of fatty acids in eukaryotic microorganisms*. In *Lipids and Biomembranes of Eukaryotic Microorganisms*. Erwin, J.A. New York: Academic Press.
- European Council (2014) '2030 Climate and Energy Policy Framework', *Zhurnal Eksperimental'noi i Teoreticheskoi Fiziki*, 2014(October 2014), pp. 1–10. Available at: <http://scholar.google.com/scholar?hl=en&btnG=Search&q=intitle:No+Title#0>.
- Fan, J., Andre, C. and Xu, C. (2011) 'A chloroplast pathway for the de novo biosynthesis of triacylglycerol in *Chlamydomonas reinhardtii*', *FEBS Letters*. Federation of European Biochemical Societies, 585(12), pp. 1985–1991.

FAO (2008) *The state of food and agriculture*,.

FAS (2016) (*Farming advisory system*) (2016) in *E28 Biofuels Annual 2016 – USDA Foreign Agricultural Service, June 2016*.

Fox, G. E., Pechman, K. R. and Woese, C. R. (1977) 'Comparative Cataloging of 16s Ribosomal Ribonucleic Acid: Molecular Approach to Procaryotic Systematics', *INTERNATIONAL JOURNAL OF SYSTEMATIC BACTERIOL*, 27, pp. 44–57.

Frick, A. A., Busetti, F. and Lewis, S. W. (2014) 'Aqueous Nile blue : a simple , versatile and safe reagent for the detection of latent fingerprints †', pp. 3341–3343. doi: 10.1039/c3cc49577a.

Friesner, R. A. *et al.* (2004) 'Glide : A New Approach for Rapid , Accurate Docking and Scoring . 1 . Method and Assessment of Docking Accuracy', *J. Med. Chem.*, 47, pp. 1739–1749.

Galbe, M. and Zacchi, G. (2007) 'Pretreatment of Lignocellulosic Materials for Efficient Bioethanol Production. In: Olsson L. (eds) *Biofuels. Advances in Biochemical Engineering/Biotechnology*, vol 108. Springer, Berlin, Heidelberg', *ADV. Biochem Engin/Biotechnol*, 108, pp. 41–65.

Gangadhar, K. N. *et al.* (2016) 'Assessment and comparison of the properties of biodiesel synthesized from three different types of wet microalgal biomass', *Journal of Applied Phycology*. *Journal of Applied Phycology*, 28, pp. 1571–1578. doi: 10.1007/s10811-015-0683-5.

Genicot, G. *et al.* (2005) 'The use of a fluorescent dye , Nile red , to evaluate the lipid content of single mammalian oocytes', *Theriogenology*, 63, pp. 1181–1194. doi: 10.1016/j.theriogenology.2004.06.006.

Gour, R. S. *et al.* (2016) 'Characterization and Screening of Native *Scenedesmus* sp . Isolates Suitable for Biofuel Feedstock', *PLOS ONE*, May, pp. 1–16. doi: 10.1371/journal.pone.0155321.

Govender, T. *et al.* (2012) 'Bioresource Technology BODIPY staining , an alternative to

the Nile Red fluorescence method for the evaluation of intracellular lipids in microalgae', *Bioresource Technology*. Elsevier Ltd, 114, pp. 507–511. doi: 10.1016/j.biortech.2012.03.024.

Greenspan, P., Mayer, E. P. and Fowler, S. D. (1985) 'Nile Red " A Selective Fluorescent Stain for Intracellular Lipid Droplets', *The Journal of Cell Biology*, 100(10), pp. 965–973.

Griffiths, M. J. and Harrison, S. T. L. (2009) 'Lipid productivity as a key characteristic for choosing algal species for biodiesel production', *J Appl Phycol*, 21, pp. 493–507. doi: 10.1007/s10811-008-9392-7.

Guillard, R. and Sieracki, M. (2005) *Counting Cells in Cultures with the Light Microscope*. In: Andersen RA, ed. *Algal Culturing Techniques*. Burlington, MA, USA: , . Elsevier Academic Press.

Gupta, V. K. and Tuohy, M. G. (2016) *Trends in atmospheric carbon dioxide*, National Oceanic & Atmospheric Administration, Earth System Research Laboratory (NOAA/ESRL).

Guzmán, H. M., De, A. and Valido, J. (2011) 'Analysis of interspecific variation in relative fatty acid composition : use of flow cytometry to estimate unsaturation index and relative polyunsaturated fatty acid content in microalgae', *J Appl Phycol*, 23, pp. 7–15. doi: 10.1007/s10811-010-9526-6.

Hader, D. P. (2006) *Impact of UV radiation on the aquatic environment in: environmental uv radiation: impact on ecosystem and human health and predictive models*. Netherlands: Springer.

Hadi, S. I. I. A. *et al.* (2016) 'DNA Barcoding Green Microalgae Isolated from Neotropical Inland Waters', *PLOS ONE*, February, pp. 1–18.

Halim, R. and Webley, P. A. (2015) 'Nile Red Staining for Oil Determination in Microalgal Cells : A New Insight through Statistical Modelling', 2015.

Hall, J. D. *et al.* (2010) 'An assessment of proposed DNA barcodes in freshwater green algae', *Cryptogamie Algologie*, 31(4), pp. 529–555.

Hameed, A. and Hasnain, S. (2012) 'Isolation and molecular identification of metal resistant *Synechocystis* from polluted areas Isolation and molecular identification of metal resistant *Synechocystis* from polluted areas', *African Journal of Microbiology Research*, 6(January), pp. 648–652. doi: 10.5897/AJMR11.1517.

Van Hannen, E., FinkGodhe, P. and Lurling, M. (2002) 'A revised secondary structure model for the internal transcribed spacer 2 of the green algae *Scenedesmus* and *Desmodesmus* and its implication for the phylogeny of these algae', *Eur. J. Phycol.*, 37(2), pp. 203–208. doi: 10.1017/s096702620200361x.

Hansen, J. *et al.* (2013) 'Climate sensitivity , sea level and atmospheric carbon dioxide Author for correspondence ':

Harwood, J. L. and Guschina, I. A. (2009) 'The versatility of algae and their lipid metabolism', *Biochimie*. Elsevier Masson SAS, 91(6), pp. 679–684.

Hasegawa, M., Kishino, H. and Yano, T. (1985) 'Dating of the Human-Ape Splitting by a Molecular Clock of Mitochondrial DNA', *J Mol Evol*, 22, pp. 160–174.

Hauf, W. *et al.* (2016) 'Interaction of the Nitrogen Regulatory Protein GlnB (P II) with Biotin Carboxyl Carrier Protein (BCCP) Controls Acetyl-CoA Levels in the Cyanobacterium *Synechocystis* sp . PCC 6803', *Frontiers in Microbiology*, 7(October), pp. 1–14. doi: 10.3389/fmicb.2016.01700.

Hegewald, E. (1978) 'Einu neue Unterteilung der Gattung *Scenedesmus* Meyen', *Nova Hedwigia*, 30, pp. 343–376.

Hegewald, E. and Hanagata, N. (2000) 'Phylogenetic studies on *Scenedesmaceae* (Chlorophyta)', *Algological Studies*. Stuttgart, Germany: Schweizerbart Science Publishers, 100, pp. 29–49. Available at: http://www.schweizerbart.de//papers/archiv_algolstud/detail/100/49215/Phylogentic_studies_on_Scenedesmaceae_Chlorophyta.

Hegewald, E. and Wolf, M. (2003) 'Phylogenetic relationships of *Scenedesmus* and *Acutodesmus* (Chlorophyta , Chlorophyceae) as inferred from 18S rDNA and ITS-2 sequence comparisons', *Plant Syst. Evol.*, 241, pp. 185–191.

HIRANO, A. *et al.* (1997) 'CO₂ FIXATION AND ETHANOL PRODUCTION WITH MICROALGAL PHOTOSYNTHESIS AND INTRACELLULAR ANAEROBIC FERMENTATION', *Energy*, 22(2), pp. 137–142.

Hoshina, R. *et al.* (2005) 'Genetic Evidence of ^aAmerican^o and ^aEuropean^o Type Symbiotic Algae of *Paramecium bursaria* Ehrenberg', *Plant biol.*, 7, pp. 526–532.

Hoshina, R., Kamako, S. and Imamura, N. (2004) 'Phylogenetic Position of Endosymbiotic Green Algae in *Paramecium bursaria* Ehrenberg from Japan', *Plant biol.*, 6, pp. 447–453. doi: 10.1055/s-2004-820888.

Hounslow, E. *et al.* (2016) 'The Search for a Lipid Trigger: The Effect of Salt Stress on the Lipid Profile of the Model Microalgal Species *Chlamydomonas reinhardtii* for Biofuels Production', *Current Biotechnology*, 5, pp. 305–313. doi: 10.2174/22115501056661603222344.

Hu, Q. (2004) *Environmental effects on cell composition*. In: Richmond, A. (Ed.), *Handbook of Microalgal Culture: Biotechnology and Applied Phycology*.

Hu, Q. *et al.* (2008) 'Microalgal triacylglycerols as feedstocks for biofuel production : perspectives and advances', *The Plant Journal*, 54, pp. 621–639. doi: 10.1111/j.1365-313X.2008.03492.x.

Huang, G., Chen, G. and Chen, F. (2009) 'Rapid screening method for lipid production in alga based on Nile red fluorescence', *Biomass and Bioenergy*. Elsevier Ltd, 33(10), pp. 1386–1392. doi: 10.1016/j.biombioe.2009.05.022.

Huang, L. *et al.* (2013) 'Effects of additional Mg²⁺ on the growth , lipid production , and fatty acid composition of *Monoraphidium* sp ... Effects of additional Mg²⁺ on the growth , lipid production , and fatty acid composition of *Monoraphidium* sp . FXY-10 under different cultu', *Ann Microbiol*, 64, pp. 1247–1256.

Huenteler, J. and Lee, H. (2015) (2015) *The Future of Low Carbon Road Transport; Rapporteur's Report*; Belfer Center, Kennedy School of Government, Harvard University: Cambridge, MA, USA.

Huesemann, M. H. *et al.* (2009) 'Biomass Productivities in Wild Type and Pigment Mutant of *Cyclotella* sp. (Diatom)', *Appl Biochem Biotechnol*, 157, pp. 507–526.

Hughes, K. A. (2006) 'Solar UV-B radiation, associated with ozone depletion, inhibits the Antarctic terrestrial microalga, *Stichococcus bacillaris*', *Polar Biol*, 29, pp. 327–336.

Hyka, P. *et al.* (2013) 'Flow cytometry for the development of biotechnological processes with microalgae', *Biotechnology Advances*, 31, pp. 2–16.

IEA (2016) *Annual Report 2016 IEA Bioenergy*.

IGBOKWE, J. O. and Nwaiwu, C. F. (2013) 'Effect Of Temperature On Methyl Ester (Biodiesel) Yield From Groundnut And Palm Kernel Oils', *The International Journal Of Engineering And Science*, 2(7), pp. 6–8.

Ikehata, H. and Ono, T. (2011) 'The Mechanisms of UV Mutagenesis', *J. Radiat. Res*, 52, pp. 115–125.

Innocent, D. S. *et al.* (2013) 'COMPARATIVE ANALYSIS OF BIODIESEL AND Petroleum Diesel', *International Journal of Education and Research*, 1(September), pp. 1–8.

Islam, M. A. *et al.* (2013) 'Microalgal species selection for biodiesel production based on fuel properties derived from fatty acid profiles', *Energies*, 6(11), pp. 5676–5702. doi: 10.3390/en6115676.

Izard, J. and Limberger, R. J. (2003) 'Rapid screening method for quantitation of bacterial cell lipids from whole cells', *Journal of Microbiological Methods*, 55, pp. 411–418.

James, G. O. *et al.* (2013) 'Bioresource Technology Temperature modulation of fatty acid profiles for biofuel production in nitrogen deprived *Chlamydomonas reinhardtii*', *Bioresource Technology*. Elsevier Ltd, 127, pp. 441–447. doi: 10.1016/j.biortech.2012.09.090.

Jiang, L. *et al.* (2011) 'Biomass and lipid production of marine microalgae using municipal wastewater and high concentration of CO₂', *Applied Energy*. Elsevier Ltd, 88(10), pp. 3336–3341.

Jiang, N. and Taylor, J. S. (1993) 'In Vivo Evidence That UV-Induced C → T Mutations at Dipyrimidine Sites Could Result from the Replicative Bypass of Cis-Syn Cyclobutane Dimers or Their Deamination Products', *Biochemistry*, 32(2), pp. 472–481. doi: 10.1021/bi00053a011.

Jørgensen, H., Kutter, J. org P. and Olsson, L. (2003) 'Separation and quantification of cellulases and hemicellulases by capillary electrophoresis q', *Analytical Biochemistry*, 317, pp. 85–93.

Joyard, J. *et al.* (2010) 'Progress in Lipid Research Chloroplast proteomics highlights the subcellular compartmentation of lipid metabolism', *Progress in Lipid Research*. Elsevier Ltd, 49(2), pp. 128–158. doi: 10.1016/j.plipres.2009.10.003.

Juneja, A., Ceballos, R. M. and Murthy, G. S. (2013) 'Effects of Environmental Factors and Nutrient Availability on the Biochemical Composition of Algae for Biofuels Production: A Review', *Energies*, 6, pp. 4607–4638. doi: 10.3390/en6094607.

Kaewkannetra, P., Enmak, P. and Chiu, T. (2012) 'The Effect of CO₂ and Salinity on the Cultivation of *Scenedesmus obliquus* for Biodiesel Production', *Biotechnology and Bioprocess Engineering*, 17, pp. 591–597. doi: 10.1007/s12257-011-0533-5.

Kessler, E. *et al.* (1997) 'Physiological , Biochemical , and Molecular Characters for the Taxonomy of the Subgenera of *Scenedesmus* (*C h lorococca les* , *Ch lorop hyta*)', *Bot. Acta*, 110, pp. 244–250.

Khozin-goldberg, I. and Cohen, Z. (2011) 'Biochimie Unraveling algal lipid metabolism : Recent advances in gene identi fi cation', *Biochimie*. Elsevier Masson SAS, 93(1), pp. 91–100.

Kilian, O. *et al.* (2011) 'High-efficiency homologous recombination in the oil-producing alga *Nannochloropsis sp.*', *PNAS*, 108(52), pp. 21265–21269.

Kitamoto, D. *et al.* (2009) 'Current Opinion in Colloid & Interface Science Self-assembling properties of glycolipid biosurfactants and their potential applications', *Current Opinion in Colloid & Interface Science*. Elsevier Ltd, 14(5), pp. 315–328. doi: 10.1016/j.cocis.2009.05.009.

- Knothe, G. (2008) “ Designer ” Biodiesel : Optimizing Fatty Ester Composition to Improve Fuel Properties †’, *Energy & Fuel*, 22, pp. 1358–1364.
- Kocot, K. M. and Santos, S. R. (2009) ‘Secondary structural modeling of the second internal transcribed spacer (ITS2) from Pfiesteria -like dinoflagellates (Dinophyceae)’, *Harmful Algae*, 8, pp. 441–446. doi: 10.1016/j.hal.2008.09.004.
- Kodym A., A. R. (2003) *Physical and Chemical Mutagenesis. In: Grotewold E. (eds) Plant Functional Genomics. Methods in Molecular Biology™*, vol 236. n: Grotewo. Humana Press.
- Koike, K. *et al.* (2013) ‘Parasitology International Chlorophycean parasite on a marine fish , *Sillago japonica* (Japanese sillago)’, *Parasitology International*. Elsevier Ireland Ltd, 62(6), pp. 586–589. doi: 10.1016/j.parint.2013.06.011.
- Kumar, A. *et al.* (2010) ‘Enhanced CO₂ fixation and biofuel production via microalgae : recent developments and future directions’, *Trends in Biotechnology*. Elsevier Ltd, 28(7), pp. 371–380.
- Kumar, R. *et al.* (2014) ‘Compositional Analysis of Algal Biomass in a Nuclear Magnetic Resonance (NMR) Tube’, *Journal of Algal Biomass Utilization*, 5(3), pp. 36–45.
- Kumar, S., Stecher, G. and Tamura, K. (2016) ‘MEGA7 : Molecular Evolutionary Genetics Analysis Version 7 . 0 for Bigger Datasets’, *Mol Biol Evol*, 33(7), pp. 1870–1874.
- Kumari, P., Reddy, C. R. K. and Jha, B. (2011) ‘Comparative evaluation and selection of a method for lipid and fatty acid extraction from macroalgae’, *Analytical Biochemistry*. Elsevier Inc., 415(2), pp. 134–144.
- Lakowicz, J. R. (2006) *Principles of Fluorescence Spectroscopy*. Available at: <http://nathan.instras.com/MyDocsDB/doc-800.pdf>.
- Laurens, L. M. L. *et al.* (2012) ‘Accurate and reliable quantification of total microalgal fuel potential as fatty acid methyl esters by in situ transesterification’, *Analytical and Bioanalytical Chemistry*, 403(1), pp. 167–178. doi: 10.1007/s00216-012-5814-0.
- Lavoie, J. M. *et al.* (2011) ‘World ’ s largest Science , Technology & Medicine Open Access

book publisher Biorefining Lignocellulosic Biomass via the Feedstock Impregnation Rapid and Sequential Steam Treatment', *Biofuel's Engineering Process Technology*, pp. 685–714.

Lee (2008) *Phycology*. 4th ed. Cambridge: Cambridge University.

Lee, Y. (2001) 'Microalgal mass culture systems and methods : Their limitation and potential', *Journal of Applied Phycology*, 13, pp. 307–315.

Levine, F. *et al.* (2014) 'Heats of Combustion of Fatty Acids and Fatty Acid Esters', *Appl Biochem Biotechnol* 91, pp. 235–249.

Lewis, L. A. (1997) 'Diversity and phylogenetic placement of *Bracteacoccus tereg*(Chlorophyceae, Chlorophyta) based on 18S ribosomal RNA gene sequence data.', *J. Phycol*, 3, pp. 279–285.

Li-Beisson, Y., Beisson, F. and Riekhof, W. (2015) 'Metabolism of acyl-lipids in *Chlamydomonas reinhardtii*', *The Plant Journal*, 82, pp. 504–522.

Li, K., Liu, S. and Liu, X. (2014) 'An overview of algae bioethanol production', *Int. J. Energy Res.*, 38(January), pp. 965–977.

Li, S. L. *et al.* (2002) 'An improved method for extracting fungal DNA.', *J. Yunnan. Univ*, 24, pp. 471–472.

Li, T. *et al.* (2013) 'Responses in growth, lipid accumulation, and fatty acid composition of four oleaginous microalgae to different nitrogen sources and concentrations', *Chinese Journal of Oceanology and Limnology*, 31(6), pp. 1306–1314. doi: 10.1007/s00343-013-2316-7.

Li, Y. *et al.* (2014) 'A comparative study : the impact of different lipid extraction methods on current microalgal lipid research', *Microbial Cell Factories*, 13, p. 14.

Li, Y., Fei, X. and Deng, X. (2012) 'Novel molecular insights into nitrogen starvation-induced triacylglycerols accumulation revealed by differential gene expression analysis in green algae *Micractinium pusillum*', *Biomass and Bioenergy*. Elsevier Ltd, 42, pp. 199–211.

- Lim, D. K. Y. *et al.* (2012) 'Isolation and Evaluation of Oil-Producing Microalgae from Subtropical Coastal and Brackish Waters', *PLoS ONE*, 7(7), pp. 1–13. doi: 10.1371/journal.pone.0040751.
- Lim, D. K. Y. *et al.* (2015) 'Isolation of High-Lipid *Tetraselmis suecica* Strains Following Repeated UV-C Mutagenesis, FACS, and High-Throughput Growth Selection', *BioEnergy Research*, 8(2), pp. 750–759. doi: 10.1007/s12155-014-9553-2.
- Liu, S. *et al.* (2015) 'Improving Cell Growth and Lipid Accumulation in Green Microalgae *Chlorella* sp. via UV Irradiation', *Appl Biochem Biotechnol*, 175, pp. 3507–3518.
- Lüring, M. (2003) 'Phenotypic plasticity in the green algae *Desmodesmus* and *Scenedesmus* with special reference to the induction of defensive morphology', *Ann. Limnol. - Int. J. Limn.*, 25(8), pp. 85–101. doi: 10.1093/plankt/25.8.979.
- Lv, J. *et al.* (2010) 'Bioresource Technology Enhanced lipid production of *Chlorella vulgaris* by adjustment of cultivation conditions', *Bioresource Technology*. Elsevier Ltd, 101(17), pp. 6797–6804. doi: 10.1016/j.biortech.2010.03.120.
- Madigan, M. T. (2003) *Brock, Biology of Microorganisms*. Prentice H. Upper Saddle River, N.J., Prentice Hall.
- Maity, J. P. *et al.* (2014) 'Microalgae for third generation biofuel production, mitigation of greenhouse gas emissions and wastewater treatment: Present and future perspectives e A mini review', *Energy*. Elsevier Ltd, 78, pp. 104–113. doi: 10.1016/j.energy.2014.04.003.
- Makarevi, V., Andrulevi, V. and Skorupskait, V. (2011) 'Cultivation of Microalgae *Chlorella* sp. and *Scenedesmus* sp. as a Potential Biofuel Feedstock', *Environmental Research, Engineering and Management*, 3(57), pp. 21–27.
- Manandhar-Shrestha, K. and Hildebrand, M. (2013) 'Development of flow cytometric procedures for the efficient isolation of improved lipid accumulation mutants in a *Chlorella* sp. microalga', *Journal of Applied Phycology*, 25(6), pp. 1643–1651. doi: 10.1007/s10811-013-0021-8.

Mandal, S. and Mallick, N. (2009) 'Microalga *Scenedesmus obliquus* as a potential source for biodiesel production', *Appl Microbiol Biotechnol* (2009), 84, pp. 281–291. doi: 10.1007/s00253-009-1935-6.

Mandotra, S. K. *et al.* (2016) 'Bioresource Technology Evaluation of fatty acid profile and biodiesel properties of microalga *Scenedesmus abundans* under the influence of phosphorus , pH and light intensities', *Bioresource Technology*. Elsevier Ltd, 201, pp. 222–229.

Manuelle, N. *et al.* (2009) 'Enhancement of lipid production using biochemical , genetic and transcription factor engineering approaches', *Journal of Biotechnology*, 141, pp. 31–41.

Martin, G. J. O. *et al.* (2014) 'Lipid Profile Remodeling in Response to Nitrogen Deprivation in the Microalgae *Chlorella* sp . (Trebouxiophyceae) and *Nannochloropsis* sp .', *PLOS ONE*, 9(8), pp. 1–10.

Mata, T. M., Martins, A. and Caetano, N. S. (2010) 'Microalgae for biodiesel production and other applications : A review', *Renewable and Sustainable Energy Reviewse*, 14, pp. 217–232. doi: 10.1016/j.rser.2009.07.020.

MATTOX, K. R. and STEWART, K. . (1984) *Classification of the green algae: a concept based on comparative cytology. In The Systematics of Green Algae The Systematics Association Special*. Edited by E. Irvine, D.E.G. and John, D.M. London, UK: Academic Press.

Merkley, N. and Syvitski, R. T. (2012) 'Profiling whole microalgal cells by high-resolution magic angle spinning (HR-MAS) magnetic resonance spectroscopy', *Journal of Applied Phycology*, 24(3), pp. 535–540. doi: 10.1007/s10811-011-9731-y.

Mirón, A. S. *et al.* (1999) 'Comparative evaluation of compact photobioreactors for large-scale monoculture of microalgae', *Progress in Industrial Microbiology*, 35(C), pp. 249–270. doi: 10.1016/S0079-6352(99)80119-2.

Mizuno, Y. *et al.* (2013) 'Bioresource Technology Sequential accumulation of starch and lipid induced by sulfur deficiency in *Chlorella* and *Parachlorella* species', *Bioresource*

Technology, 129, pp. 150–155.

Mohammad-ghasemnejadmaleki, H., Almassi, M. and Nasirian, N. (2014) 'Biodiesel production from microalgae and determine properties of produced fuel using standard test fuel', *Int. J. Biosci.*, 5(60), pp. 47–55.

Mondal, M. *et al.* (2017) 'Production of biodiesel from microalgae through biological carbon capture : a review', *3 Biotech.* Springer Berlin Heidelberg, 7(2), pp. 1–21.

Monshupanee, T. and Incharoensakdi, A. (2013) 'Enhanced accumulation of glycogen , lipids and polyhydroxybutyrate under optimal nutrients and light intensities in the cyanobacterium *Synechocystis sp . PCC*', *Journal of Applied Microbiology*, 116, pp. 830–838. doi: 10.1111/jam.12409.

Montero, M. F., Aristizábal, M. and García Reina, G. (2011) 'Isolation of high-lipid content strains of the marine microalga *Tetraselmis suecica* for biodiesel production by flow cytometry and single-cell sorting', *Journal of Applied Phycology*, 23(6), pp. 1053–1057. doi: 10.1007/s10811-010-9623-6.

Montoya, E. Y. O. *et al.* (2014) 'Production of *Chlorella vulgaris* as a Source of Essential Fatty Acids in a Tubular Photobioreactor Continuously Fed with Air Enriched with CO₂ at Different Concentrations', *Biotechnol. Prog.*, 30(4), pp. 916–922. doi: 10.1002/btpr.1885.

Mosier, N. *et al.* (2005) 'Features of promising technologies for pretreatment of lignocellulosic biomass', *Bioresource Technology*, 96, pp. 673–686.

MURPHY, C. W. and KENDALL, A. (2015) 'Life cycle analysis of biochemical cellulosic ethanol under multiple scenarios', *GCB Bioenergy*, 7, pp. 1019–1033. doi: 10.1111/gcbb.12204.

Mutanda, T. *et al.* (2011) 'Bioresource Technology Bioprospecting for hyper-lipid producing microalgal strains for sustainable biofuel production', *Bioresource Technology*. Elsevier Ltd, 102(1), pp. 57–70. doi: 10.1016/j.biortech.2010.06.077.

Nakayama, T. *et al.* (1996) 'The phylogenetic relationship between the

Chlamydomonadales and Chlorococcales inferred from 18SrDNA sequence data', *Phycological Research*, 44, pp. 47–55.

Nascimento, I. A. *et al.* (2013) 'Screening Microalgae Strains for Biodiesel Production: Lipid Productivity and Estimation of Fuel Quality Based on Fatty Acids Profiles as Selective Criteria', *Bioenergy Research*, 6(1), pp. 1–13. doi: 10.1007/s12155-012-9222-2.

OECD (2016) *2020 Projections of Climate Finance Towards the USD 100 Billion Goal Technical Note*. Available at: [https://www.oecd.org/environment/cc/Projecting Climate Change 2020 WEB.pdf](https://www.oecd.org/environment/cc/Projecting_Climate_Change_2020_WEB.pdf).

OECD/IEA (2008) *From 1st to 2nd generations of biofuel technologies. An overview of current industry and RDED activities*.

Osundeko, O. and Pittman, J. K. (2014) 'Bioresource Technology Implications of sludge liquor addition for wastewater-based open pond cultivation of microalgae for biofuel generation and pollutant remediation', *BIORESOURCE TECHNOLOGY*. Elsevier Ltd, 152, pp. 355–363. doi: 10.1016/j.biortech.2013.11.035.

Paik, M. *et al.* (2009) 'Separation of triacylglycerols and free fatty acids in microalgal lipids by solid-phase extraction for separate fatty acid profiling analysis by gas chromatography', *Journal of Chromatography*, 1216, pp. 5917–5923. doi: 10.1016/j.chroma.2009.06.051.

Pal, D. *et al.* (2011) 'The effect of light, salinity, and nitrogen availability on lipid production by *Nannochloropsis* sp.', *Applied Microbiology and Biotechnology*, 90(4), pp. 1429–1441. doi: 10.1007/s00253-011-3170-1.

Pancha, I. *et al.* (2014) 'Bioresource Technology Nitrogen stress triggered biochemical and morphological changes in the microalgae *Scenedesmus* sp . CCNM 1077', *BIORESOURCE TECHNOLOGY*. Elsevier Ltd, 156, pp. 146–154. doi: 10.1016/j.biortech.2014.01.025.

Phang, S. M. and Chu., W. L. (1999) *Algae culture Collection, Catalogue of Strains. Institute of Post Graduate Studies and Research*. Kuala Lumpur, Malaysia: University of

Malaysia.

Pick, U. and Rachutin-zalagin, T. (2012) 'Kinetic anomalies in the interactions of Nile red with microalgae', *Journal of Microbiological Methods*. Elsevier B.V., 88(2), pp. 189–196. doi: 10.1016/j.mimet.2011.10.008.

Posten, C. (2009) 'Design principles of photo-bioreactors for cultivation of microalgae', *Eng. Life Sci*, 9(3), pp. 165–177.

Prabakaran, P. and Ravindran, A. D. (2012) 'Scenedesmus as a potential source of biodiesel among selected microalgae', *Current Science*, 102(4), pp. 616–619.

Quintana, N. *et al.* (2011) 'Renewable energy from Cyanobacteria : energy production optimization by metabolic pathway engineering', *Appl Microbiol Biotechnol (2011)*, 91, pp. 471–490.

Radha, S. *et al.* (2013) 'Direct colony PCR for rapid identification of varied microalgae from freshwater environment Direct colony PCR for rapid identification of varied microalgae from freshwater environment', *J Appl Phycol*, 25, pp. 609–613. doi: 10.1007/s10811-012-9895-0.

Ramos, M. J. *et al.* (2009) 'Bioresource Technology Influence of fatty acid composition of raw materials on biodiesel properties', *Bioresource Technology*, 100, pp. 261–268.

Rastogi, R., Agarwal, S. and Mishra, S. K. (2015) 'Microalgae : A Promising Energy Source for Sustainable Development', *International Journal of Engineering Technology Science and Research*, 2, pp. 92–98.

Rathore, N. S. and Panwar, N. . (2007) *Renewable energy sources for sustainable development*. New Delh: ndia: New India Publishing Agency.

Rattanapoltee, P. and Kaewkannetra, P. (2013) 'Nile Red , an Alternative Fluorescence Method for Quantification of Neutral Lipids in Microalgae', *International Scholarly and Scientific Research & Innovation*, 7(9), pp. 889–893.

Reed, R. D. (1998) *Practical Skills in Biomolecular Sciences*. Harlow, Prentice Hall.

- Ren, H. *et al.* (2013) 'A new lipid-rich microalga *Scenedesmus* sp . strain R-16 isolated using Nile red staining : effects of carbon and nitrogen sources and initial pH on the biomass and lipid production', *Biotechnology for Biofuels*, 6(143), pp. 1–10.
- Ren, H. *et al.* (2014) 'Bioresource Technology Enhanced lipid accumulation of green microalga *Scenedesmus* sp . by metal ions and EDTA addition', *Bioresource Technology*. Elsevier Ltd, 169, pp. 763–767. doi: 10.1016/j.biortech.2014.06.062.
- Ren, H. *et al.* (2015) 'Improved Nile red staining of *Scenedesmus* sp . by combining ultrasonic treatment and three-dimensional excitation emission matrix fluorescence spectroscopy', *Algal Research*. Elsevier B.V., 7, pp. 11–15.
- Rezanka, T. and Sigler, K. (2009) 'Progress in Lipid Research Odd-numbered very-long-chain fatty acids from the microbial , animal and plant kingdoms', *Progress in Lipid Research*, 48, pp. 206–238. doi: 10.1016/j.plipres.2009.03.003.
- Richter, R. *et al.* (1999) 'Cyanophycinase, a peptidase degrading the cyanobacterial reserve and biochemical characterization of the purified enzyme', *European journal of biochemistry / FEBS*, 169.
- Rios, L. F. *et al.* (2015) 'Nitrogen Starvation for Lipid Accumulation in the Microalga Species *Desmodesmus* sp.', *Applied Biochemistry and Biotechnology*, 175(1), pp. 469–476. doi: 10.1007/s12010-014-1283-6.
- Rodolfi, L. *et al.* (2009) 'Microalgae for oil: Strain selection, induction of lipid synthesis and outdoor mass cultivation in a low-cost photobioreactor', *Biotechnology and Bioengineering*, 102(1), pp. 100–112. doi: 10.1002/bit.22033.
- Ruffing, A. M. (2014) 'Improved free fatty acid production in cyanobacteria with *Synechococcus* sp . PCC 7002 as host', *BIOENGINEERING AND BIOTECHNOLOGY*, 2(May), pp. 1–10. doi: 10.3389/fbioe.2014.00017.
- Rumin, J. *et al.* (2015) 'The use of fluorescent Nile red and BODIPY for lipid measurement in microalgae', *Biotechnology for Biofuels*, 8, p. 42. doi: 10.1186/s13068-015-0220-4.

SACKETT, D. L. and WOLFF, J. (1987) 'Nile Red As a Polarity-Sensitive Fluorescent of Hydrophobic Protein Surfaces', *Analytical Biochemistry*, 167, pp. 228–234.

Salama, E.-S. *et al.* (2013) 'Biomass, lipid content, and fatty acid composition of freshwater *Chlamydomonas mexicana* and *Scenedesmus obliquus* grown under salt stress', *Bioprocess and Biosystems Engineering*, 36(6), pp. 827–833. doi: 10.1007/s00449-013-0919-1.

Sandgren, M. *et al.* (2001) 'The X-ray Crystal Structure of the *Trichoderma reesei* Family 12 Endoglucanase 3 , Cel12A , at Å Resolution', *J. Mol. Biol.*, 308, pp. 295–310. doi: 10.1006/jmbi.2001.4583.

Sarkar, N. *et al.* (2012) 'Bioethanol production from agricultural wastes : An overview', *Renewable Energy*. Elsevier Ltd, 37, pp. 19–27. doi: 10.1016/j.renene.2011.06.045.

Sarpal, A. *et al.* (2016) 'Journal of Biotechnology & Biomaterials', *Journal of Biotechnology & Biomaterials*, 6(1), pp. 1–15. doi: 10.4172/2155-952X.1000220.

Sarpal, A. S. *et al.* (2015) 'Determination of lipid content of oleaginous microalgal biomass by NMR spectroscopic and GC--MS techniques', *Analytical and Bioanalytical Chemistry*, 407(13), pp. 3799–3816. doi: 10.1007/s00216-015-8613-6.

Sathya, S. and Srisudha, S. (2013) 'RESEARCH ARTICLE ISOLATION AND IDENTIFICATION OF FRESHWATER MICROALGAL STRAINS – POTENTIAL FOR BIOFUEL PRODUCTION', *International Journal of Recent Scientific Research*, 4, pp. 1432–1437.

Sato, A. *et al.* (2014) 'Responsibility of regulatory gene expression and repressed protein synthesis for triacylglycerol accumulation on sulfur-starvation in *Chlamydomonas reinhardtii*', *ORIGINAL RESEARCH ARTICLE*, 5(September), pp. 1–12.

Sato, N. *et al.* (1995) 'Isolation and characterization of mutants affected in lipid metabolism of *Chlamydomonas reinhardtii*', *Eur. J. Biochem*, 230, pp. 987–993.

Satpati, G. G., Gorain, P. C. and Pal, R. (2016) 'Efficacy of EDTA and Phosphorous on Biomass Yield and Total Lipid Accumulation in Two Green Microalgae with Special Emphasis on Neutral Lipid Detection by Flow Cytometry', *Advances in Biology*, 2016, pp.

1–12.

Satpati, G. G. and Pal, R. (2014) 'Rapid detection of neutral lipid in green microalgae by flow cytometry in combination with Nile red staining — an improved ... Rapid detection of neutral lipid in green microalgae by flow cytometry in combination with Nile red staining — an improved techn', *Ann Microbio*, 65(2), pp. 937–949. doi: 10.1007/s13213-014-0937-5.

Satpati, G. G. and Pal, R. (2015) 'Rapid detection of neutral lipid in green microalgae by flow cytometry in combination with Nile red staining---an improved technique', *Annals of Microbiology*, 65(2), pp. 937–949. doi: 10.1007/s13213-014-0937-5.

Scharlemann, J. P. W. and Laurance, W. F. (2008) 'How Green Are Biofuels?', *SCIENCE*, 319(January), pp. 43–45.

Scott, S. A. *et al.* (2010) 'Biodiesel from algae : challenges and prospects', *Current Opinion in Biotechnology*. Elsevier Ltd, 21(3), pp. 277–286. doi: 10.1016/j.copbio.2010.03.005.

Selvarajan, R. *et al.* (2015) 'Screening and Evaluation of Some Green Algal Strains (Chlorophyceae) Isolated from Freshwater and Soda Lakes for Biofuel Production', *Energies*, 8, pp. 7502–7521. doi: 10.3390/en8077502.

Sforza, E. *et al.* (2012) 'Adjusted Light and Dark Cycles Can Optimize Photosynthetic Efficiency in Algae Growing in Photobioreactors', *PLOS ONE*, 7(6), pp. 1–10. doi: 10.1371/journal.pone.0038975.

Sharma, K. K. *et al.* (2012) 'High Lipid Induction in Microalgae for Biodiesel Production', *Energies*, 5, pp. 1532–1553.

Sharma, K., Li, Y. and Schenk, P. M. (2014) 'UV-C-mediated lipid induction and settling, a step change towards economical microalgal biodiesel production', *Green Chem*, pp. 3539–3548. doi: 10.1039/c4gc00552j.

Shelly, K. *et al.* (2005) 'Interactions between UV-B exposure and phosphorus nutrition. I. Effects on growth, phosphate uptake, and chlorophyll fluorescence', *Journal of*

Phycology, 41(6), pp. 1204–1211. doi: 10.1111/j.1529-8817.2005.00148.x.

Sheng, J., Vannela, R. and Rittmann, B. E. (2011) 'Bioresource Technology Evaluation of methods to extract and quantify lipids from *Synechocystis* PCC 6803', *Bioresource Technology*. Elsevier Ltd, 102(2), pp. 1697–1703. doi: 10.1016/j.biortech.2010.08.007.

Show, P. L. *et al.* (2017) 'A Holistic Approach to Managing Microalgae for Biofuel Applications', *Int. J. Mol. Sci.*, 18, pp. 1–34.

Sibi, G., Shetty, V. and Mokashi, K. (2016) 'Enhanced lipid productivity approaches in microalgae as an alternate for fossil fuels e A review', *Journal of the Energy Institute*. Elsevier Ltd, 89(3), pp. 330–334. doi: 10.1016/j.joei.2015.03.008.

Siegler, H. D. la H. *et al.* (2012) 'Improving the reliability of fluorescence-based neutral lipid content measurements in microalgal cultures', *Algal Research*. Elsevier B.V., 1(2), pp. 176–184.

Singh, R. N. and Sharma, S. (2012) 'Development of suitable photobioreactor for algae production – A review', *Renewable and Sustainable Energy Reviews*. Elsevier Ltd, 16(4), pp. 2347–2353. doi: 10.1016/j.rser.2012.01.026.

Sitepu, I. R. *et al.* (2012) 'An improved high-throughput Nile red fluorescence assay for estimating intracellular lipids in a variety of yeast species', *Journal of Microbiological Methods*. Elsevier B.V., 91(2), pp. 321–328. doi: 10.1016/j.mimet.2012.09.001.

Sitz, T. and Schmidt, R. R. (1973) 'Purification of *Synechococcus lividus* by Equilibrium Centrifugation and Its Synchronization by Differential Centrifugation', *JOURNAL OF BACTERIOLOGY*, 115(1), pp. 43–46.

Skoog, D. A., Holler, F. J. and Crouch, S. R. (2007) *Principles of Instrumental Analysis*. , Belmont, C.A., Thomson/Brooks-Cole. 6th Editio.

Songruk, N., Incharoensakdi, A. and Jantaro, S. (2015) 'Effect of salt stress on fatty acid and lipid levels in cyanobacterium *Synechocystis* sp . PCC 6803', *Burapha University International Conference*, 66(0), pp. 798–804.

Stackebrandt, E. and Goodfellow, M. (1991) *In Nucleic Acid Techniques in bacterial*

systematics. Wiley, 1991.

Storms, Z. J. *et al.* (2014) 'A Simple and Rapid Protocol for Measuring Neutral Lipids in Algal Cells Using Fluorescence 1 . Isolation of Dry Algal Biomass to be Used as Standards for Fluorescence Readings 2 . Gravimetric Quantification of Neutral Lipids by Hexane Extraction (Adapted', *Journal of Visualized Experiments*, 87(May), pp. 1–7. doi: 10.3791/51441.

Tabatabaei, M. *et al.* (2011) 'Biodiesel production from genetically engineered microalgae : Future of bioenergy in Iran', *Renewable and Sustainable Energy Reviews*. Elsevier Ltd, 15(4), pp. 1918–1927.

Takagi, M. and Yoshida, T. (2006) 'Effect of Salt Concentration on Intracellular Accumulation of Lipids and Triacylglyceride in Marine Microalgae *Dunaliella* Cells', *Journal of Bioscience and Bioengineering*, 101(3), pp. 223–226.

TALEBI, A. F. *et al.* (2013) 'Comparative Salt Stress Study on Intracellular Ion Concentration in Marine and Salt-adapted Freshwater Strains of ... Comparative Salt Stress Study on Intracellular Ion Concentration in Marine and Salt-adapted Freshwater Strains of Microalgae', *Not Sci Biol*, 5(3), pp. 309–315.

Tan, Y. and Lin, J. (2011) 'Bioresource Technology Biomass production and fatty acid profile of a *Scenedesmus rubescens* -like microalga', *Bioresource Technology*. Elsevier Ltd, 102(21), pp. 10131–10135. doi: 10.1016/j.biortech.2011.07.091.

Tang, D. *et al.* (2011) 'Bioresource Technology CO₂ biofixation and fatty acid composition of *Scenedesmus obliquus* and *Chlorella pyrenoidosa* in response to different CO₂ levels', *Bioresource Technology*. Elsevier Ltd, 102(3), pp. 3071–3076.

Terashima, M. *et al.* (2015) 'A fluorescence-activated cell sorting-based strategy for rapid isolation of high-lipid *Chlamydomonas* mutants', *The Plant Journal*, 81, pp. 147–159.

Thai, T., Doan, Y. and Obbard, J. P. (2012) 'Enhanced intracellular lipid in *Nannochloropsis* sp . via random mutagenesis and flow cytometric cell sorting', *Algal Research*. Elsevier B.V., 1(1), pp. 17–21. doi: 10.1016/j.algal.2012.03.001.

Ting, H. *et al.* (2017) 'Progress in microalgae cultivation photobioreactors and applications in wastewater treatment : A review', *Int J Agric & Biol Eng*, 10(1), pp. 1–29. doi: 10.3965/j.ijabe.20171001.2705.

Tredici, M. R. (2004) *Mass production of microalgae: Photobioreactors. In:), Handbook of microalgal culture: biotechnology and applied phycology.* Richmond,.

Ugwu, C. U., Aoyagi, H. and Uchiyama, H. (2008) 'Photobioreactors for mass cultivation of algae', *Bioresource Technology*, 99, pp. 4021–4028. doi: 10.1016/j.biortech.2007.01.046.

Vanormelingen, P. *et al.* (2007) 'The systematics of a small spineless *Desmodesmus* species, *D. Costato-granulatus* (Sphaeropleales, Chlorophyceae), based on its2 rDNA sequence analyses and cellwall morphology', *Journal of Phycology*, 43(2), pp. 378–396. doi: 10.1111/j.1529-8817.2007.00325.x.

Velmurugan, N. *et al.* (2013) 'Bioresource Technology Evaluation of intracellular lipid bodies in *Chlamydomonas reinhardtii* strains by flow cytometry', *Bioresource Technology*. Elsevier Ltd, 138, pp. 30–37. doi: 10.1016/j.biortech.2013.03.078.

Vieira, H. H. *et al.* (2016) 'tuf A gene as molecular marker for freshwater Chlorophyceae', *Algae*, 31(2), pp. 155–165.

Vigeolas, H. *et al.* (2012) 'Isolation and partial characterization of mutants with elevated lipid content in *Chlorella sorokiniana* and *Scenedesmus obliquus*', *Journal of Biotechnology*. Elsevier B.V., 162(1), pp. 3–12. doi: 10.1016/j.jbiotec.2012.03.017.

Wang, B. *et al.* (2008) 'CO₂ bio-mitigation using microalgae', *Applied Microbiology and Biotechnology*, 79(5), pp. 707–718. doi: 10.1007/s00253-008-1518-y.

Wang, Q. *et al.* (2011) 'Potential Approaches to Improving Biodegradation of Hydrocarbons for Bioremediation of Crude Oil Pollution', *Journal of Environmental Protection*, 2(1), pp. 47–55.

Ward, A. J., Lewis, D. M. and Green, F. B. (2014) 'Anaerobic digestion of algae biomass : A review', *Algal Research*. Elsevier B.V., 5, pp. 204–214.

Wi, S. G. *et al.* (2015) 'Biotechnology for Biofuels Lignocellulose conversion for biofuel : a new pretreatment greatly improves downstream biocatalytic hydrolysis of various lignocellulosic materials', *Biotechnology for Biofuels*. BioMed Central, 8, p. 228. doi: 10.1186/s13068-015-0419-4.

Williams, P. J. B. and Laurens, L. M. L. (2010) 'Microalgae as biodiesel & biomass feedstocks : Review & analysis of the biochemistry , energetics & economics †', *Energy Environ. Sci.*, 3(i), pp. 554–590. doi: 10.1039/b924978h.

Woese, C. R. (1987) 'Bacterial Evolution Background,', *MICROBIOLOGICAL REVIEWS*, 51(2), pp. 221–271.

Wong, C. Y. *et al.* (2007) 'Comparing the response of Antarctic, tropical and temperate microalgae to ultraviolet radiation (UVR) stress', *Journal of Applied Phycology*, 19(6), pp. 689–699. doi: 10.1007/s10811-007-9214-3.

Wong, D. M., Nguyen, T. T. N. and Franz, A. K. (2014) 'Ethylenediaminetetraacetic acid (EDTA) enhances intracellular lipid staining with Nile red in microalgae *Tetraselmis suecica*', *Algal Research*. Elsevier B.V., 5, pp. 158–163. doi: 10.1016/j.algal.2014.08.002.

Wu, S. *et al.* (2014) 'Detection of intracellular neutral lipid content in the marine microalgae *Prorocentrum micans* and *Phaeodactylum tricornutum* using Nile red and BODIPY 505/515', *Journal of Applied Phycology*, 26(4), pp. 1659–1668. doi: 10.1007/s10811-013-0223-0.

Van Wychen, S. and Laurens, L. M. L. (2013) *Determination of Total Lipids as Fatty Acid Methyl Esters (FAME) by in situ Transesterification*. Laboratory Analytical Procedure (LAP) NREL/TP-5100-60958. Golden, CO, USA: National Renewable Energy Laboratory,.

Xia, L., Song, S. and Hu, C. (2016) 'High temperature enhances lipid accumulation in nitrogen-deprived *Scenedesmus obtusus* XJ-15', *Journal of Applied Phycology*, 28(2), pp. 831–837. doi: 10.1007/s10811-015-0636-z.

Xia, S. *et al.* (2013) 'marine drugs', *Mar. Drugs*, 11, pp. 2667–2681.

Xie, B. *et al.* (2014) 'High-throughput fluorescence-activated cell sorting for lipid

hyperaccumulating *Chlamydomonas reinhardtii* mutants', *Plant Biotechnology Journal*, 12, pp. 872–882.

Xin, L. *et al.* (2010) 'Bioresource Technology Effects of different nitrogen and phosphorus concentrations on the growth, nutrient uptake, and lipid accumulation of a freshwater microalga *Scenedesmus* sp.', *Bioresource Technology*. Elsevier Ltd, 101(14), pp. 5494–5500.

Xin, L., Hong-ying, H. and Yu-ping, Z. (2011) 'Bioresource Technology Growth and lipid accumulation properties of a freshwater microalga *Scenedesmus* sp. under different cultivation temperature', *Bioresource Technology*. Elsevier Ltd, 102(3), pp. 3098–3102. doi: 10.1016/j.biortech.2010.10.055.

Xu, D. *et al.* (2013) 'Bioresource Technology Detection and quantitation of lipid in the microalga *Tetraselmis subcordiformis* (Wille) Butcher with BODIPY 505 / 515 staining', *BIORESOURCE TECHNOLOGY*. Elsevier Ltd, 127, pp. 386–390. doi: 10.1016/j.biortech.2012.09.068.

Yeesang, C. and Cheirsilp, B. (2011) 'Bioresource Technology Effect of nitrogen, salt, and iron content in the growth medium and light intensity on lipid production by microalgae isolated from freshwater sources in Thailand', *Bioresource Technology*. Elsevier Ltd, 102(3), pp. 3034–3040.

Yilancioglu, K., Tekin, H. O. and Cetiner, S. (2016) 'Nitrogen Source, an Important Determinant of Fatty Acid Accumulation and Profile in *Scenedesmus obliquus*', *ACTA PHYSICA POLONICA A*, 130(1), pp. 428–433. doi: 10.12693/APhysPolA.130.428.

Ying, K., Gilmour, D. J. and Zimmerman, W. B. (2014) 'Microbial & Biochemical Technology Effects of CO₂ and pH on Growth of the Microalga *Dunaliella salina*', *Microbial & Biochemical Technology*, 6(1), pp. 167–173. doi: 10.4172/1948-5948.1000138.

Zabawinski, C. *et al.* (2001) 'Starchless Mutants of *Chlamydomonas reinhardtii* Lack the Small Subunit of a Heterotetrameric ADP-Glucose Pyrophosphorylase', *JOURNAL OF BACTERIOLOGY*, 183(3), pp. 1069–1077. doi: 10.1128/JB.183.3.1069.

Zakhidov, R. A. (2008) 'Central Asian countries energy system and role of renewable energy sources', *Applied Solar Energy*, 44(3), pp. 218–223. doi: 10.3103/S0003701X08030201.

Zaslavskaja, L. A. *et al.* (2000) 'TRANSFORMATION OF THE DIATOM PHAEODACTYLUM TRICORNUTUM (BACILLARIOPHYCEAE) WITH A VARIETY OF SELECTABLE MARKER AND REPORTER GENES 1 and', *J. Phycol.*, 36, pp. 379–386.

Zhang, Y. *et al.* (2013) 'Nitrogen Starvation Induced Oxidative Stress in an Oil- Producing Green Alga *Chlorella sorokiniana* C3', *PLOS ONE*, 8(7), pp. 1–12. doi: 10.1371/journal.pone.0069225.

Zhou, G.-J. *et al.* (2012) 'Biosorption of zinc and copper from aqueous solutions by two freshwater green microalgae *Chlorella pyrenoidosa* and *Scenedesmus obliquus*', *Environmental Science and Pollution Research*, 19(7), pp. 2918–2929. doi: 10.1007/s11356-012-0800-9.

Zhu, L. D., Li, Z. H. and Hiltunen, E. (2016) 'Review Article Strategies for Lipid Production Improvement in Microalgae as a Biodiesel Feedstock', 2016, pp. 1–8.

APPENDIX

Appendix A

Forward 16S rDNA sequence read of *Synechocystis* PCC603 958 bp

AGCTACACATGCAGTCGACGGAGTTCTTCGGACTTAGTGCGGACGGGTGAGTAACACGTGAGAACC
TACCTTCAGAATGGGGACAACAGTTGGAAACGACTGCTAATACCCAATGTGCCGAAAGGTGAAAGATT
TATCGTCTGAAGATGGGCTCGCGTCTGATTAGCTAGATGGTGGGGTAAGAGCCTACCATGGCAACGAT
CAGTAGCTGGTCTGAGAGGATGAGCAGCCACACTGGGACTGAGACACGGCCCAGACTCCTACGGGAG
GCAGCAGTGGGGAATTTCCGCAATGGGCGAAAGCCTGACGGAGCAATACCGCGTGAGGGAGGAAG
GTCCTTGATTGTAAACCTCTTTTATCAGGGAAGAAGTTCTGACGGTACCTGATGAATAAGCATCGGCT
AACTCCGTGCCAGCAGCCGCGGTAATACGGAGGATGCAAGCGTTATCCGGAATTATTGGGCGTAAAG
CGTCCGTAGGTGGTTATGCAAGTCTGCCGTTAAGAATGGAGCTTAACTCCATAGGAGCGGTGGA AAC
TGCAAGACTAGAGTACAGTAGGGGTAGCAGGAATCCAGTGTAGCGGTGAAATGCGTAGATATTGG
GAAGAACATCGGTGGCGAAAGCGTGCTACTGGGCTGAAACTGACACTGAGGGACGAAAGCTAGGGT
AGCGAAAGGGATTAGATACCCCTGTAGTCCTAGCCGTAAACGATGGATACTAGGCGTGGCTTGTATCG
ACCCGAGCCGTGCCGAAGCTAACGCGTTAAGTATCCCGCCTGGGGAGTACGCACGCAAGTGTGAAAC
TCAAAGGAATTGACGGGGGCCCGCACAAGCGGTGGAGTATGTGGTTAATTTCGATGCAACGCGAAGA
ACCTTACCAAGGCTTGACATCCCTGGAATCCTGCGGAAACGTGGGAGTGCCTTAGGGAGCCAGGAGA
CAGGT.

Reverse 16S rDNA sequence read of *Synechocystis* PCC603 959 bp

CTTCGGCGCCCTCCTCCCTAGGTTAGAGTAACGACTTCGGGCGTGACCAGCTCCCATGGTGTG
ACGGGCGGTGTGTACAAGGCCCGGGAACGAATTCACCGCAGTATTCTGACCTGCGATTACTA
GCGATTCCCTCCTTCATGCAGGCGAGTTGCAGCCTGCAATCTGAACTGAGGCCGGGTTTGATG
GGATTGCTTACTCTCGCGAGCTCGCTGCCCGTTGTCCCGACCATTGTAGTACGTGTGTAGCC
CAAGGCGTAAGGGGCATGATGACTTGACGTCATCCCCACCTTCCTCCGGTTTGTCACCGGCAG
TCTCTCTAGAGTGCCCAACTTAATGATGGCAACTAAAACGAGGGTTGCGCTCGTTGCGGGA
CTTAACCCAACATCTCACGACACGAGCTGACGACAGCCATGCACCACCTGTCTCCTGGCTCCC
TAAGGCACTCCCACGTTTCCGCAGGATTCCAGGGATGTCAAGCCTTGGTAAGGTTCTTCGCGT
TGCATCGAATTAACACATACTCCACCGCTTGTGCGGGCCCCCGTCAATTCCTTTGAGTTTCA
CACTTGCGTGCGTACTCCCCAGGCGGGATACTTAACGCGTTAGCTTCGGCACGGCTCGGGTC
GATACAAGCCACGCCTAGTATCATCGTTTACGGCTAGGACTACAGGGGTATCTAATCCCTTTC
GCTACCCTAGCTTTTCGTCCTCAGTGTGAGTTTCAGCCCAGTAGCACGCTTTTCGCCACCGATGT
TCTTCCCAATATCTACGCATTTACCGCTACACTGGGAATTCCTGCTACCCCTACTGTACTCTAG
TCTTGCAGTTTCCACCGCTCCTATGGAGTTAAGCTCCATTCTTTAACGGCAGACTTGCATAACC
ACCTACGGACGCTTACGCCCAATAATTCCGGATAACGCTTGCATCCTCCGTATTACCGCGGCT
G

Appendix B

Forward 18S rDNA sequence read of undefined Pond water samples (later defined as *Desmodemus armatus*) 512 bp

```
CAGTTAAAGCTCGTAGTTGGATTTCCGGTGGGTTCTAGCGGTCCGCCTATGGTGAGTACT
GCTATGGCCTTCCTTTCTGTCCGGGACGGGCTTCTGGGCTTCACTGTCCGGGACTCGGAG
TCGACGTGGTTACTTTGAGTAAATTAGAGTGTTCAAAGCAGGCTTACGCCAGAATACTTT
AGCATGGAATAACACGATAGGACTCTGGCCTATCTTGTTGGTCTGTAGGACCGGAGTAAT
GATTAAGAGGGACAGTCGGGGGCATTTCGTATTTTCATTGTCAGAGGTGAAATTCTTGGATT
TATGAAAGACGAACTACTGCGAAAGCATTTGCCAAGGATGTTTTTTCATTAATCAAGAACGA
AAGTTGGGGGCTCGAAGACGATTAGATAACGTCGTAGTCTCAACCATAAACGATGCCGAC
TAGGGATTGGCGAATGTTTTTTTAATGACTTCGCCAGCACCTTATGAGAAATCAAAGTTT
TTGGGTTGCGGGGAAGTAT
```

Reverse 18S rDNA sequence read of undefined Pond water samples (later defined as *Desmodemus armatus*) 509 bp

```
TAGGGCTGGCGAGTCATTAACAAAAACATTCGCCAATCCCTAGTCGGCATCGTTTATGGTT
GAGACTACGACGGTATCTAATCGTCTTCGAGCCCCAACTTTCGTTCTTGATTAATGAAA
ACATCCTTGGCAAATGCTTTCGCAGTAGTTCGTCTTTCATAAATCCAAGAATTTACCTC
TGACAATGAAATACGAATGCCCCGACTGTCCCTCTTAATCATTACTCCGGTCCTACAGA
CCAACAAGATAGGCCAGAGTCCTATCGTGTTATTCCATGCTAAAGTATTCTGGCGTAAGC
CTGCTTTGAACACTCTAATTTACTCAAAGTAACCACGTGCGACTCCGAGTCCCGGACAGTG
AAGCCCAGAAGCCCGTCCCCGACAGAAAGGAAGGCCATAGCAGTACTCACCATAGGCGGA
CCGCTAGAACCCACCCGAAATCCAACACTACGAGCTTTTTAACTGCAACAACCTAAATATAC
GCTATTGGAGTGAAATTT
```

Appendix C

Forward ITS1 sequence read of undefined Pond water samples (later defined as *Desmodesmus armatus*) 996 bp

```
TAGCCATGCATGTCTAAGTATAAACTGCTTATACTGTGAAACTGCGAATGGCTCATTAAA
TCAGTTATAGTTTATTTGGTGGTACCTTCTTACTCGGAATAACCGTAAGAAATTTAGAGC
TAATACGTGCGTAAATCCCGACTTCTGGAAGGGACGTATATATTAGATAAAAAGGCCGACC
GGGCTCTGCCGACCCGCGGTGAATCATGATATCTTACGAAGCGCATGGCCTTGTGCCG
GCGCTGTTCCATTCAAATTTCTGCCCTATCAACTTTCGATGGTAGGATAGAGGCCTACCA
TGGTGGTAACGGGTGACGGAGGATTAGGGTTCGATTCCGGAGAGGGAGCCTGAGAAACGG
CTACCACATCCAAGGAAGGCAGCAGGCGCGCAAATTACCCAATCCTGATACGGGGAGGTA
GTGACAATAAATAACAATACCGGGCATTTCATGTCTGGTAATTGGAATGAGTACAATCTA
AATCCCTTAACGAGGATCCATTGGAGGGCAAGTCTGGTGCCAGCAGCCGCGGTAATTCCA
GCTCCAATAGCGTATATTTAAGTTGTTGCAGTTAAAAAGCTCGTAGTTGGATTTCCGGGTG
GGTTTCAGCGGTCCGCCTATGGTGAGTACTGCTGTGGCCTTCCTTACTGTTGGGGACCTG
CTTCTGGGCTTCATTGTCCGGGACAGGGATTACGCATGGTTACTTTGAGTAAATTGGAGT
GTTCAAAGCAGGCTTACGCCGTGAACATTTTAGCATGGAATAACATGATAGGACTCTGCC
CTATTCTGTTGGCCTGTAGGAGTGGAGTAATGATTAAGAGGAACAGTCGGGGGCATTTCGT
ATTTCAATTGTCAGAGGTGAAATTCCTGGATTTATGAAAGACGAACTACTGCGAAAGCATT
TGCCAAGGATGTTTTCATTAATCAAGAACGAAAGTTGGGGGCTCGAAGACGATTAGATAC
CGTCGTAGTCTCAACCA
```

Reverse ITS1 sequence read of undefined Pond water samples (later defined as *Desmodemus armatus*) 919 bp.

TCATCCTTCCTATGTCTGGACCTGGTAAGTTTTCCCGTGTTGAGTCAAATTAAGCCGCAG
GCTCCACGCCTGGTGGTGCCCTTCCGTCAATTCCTTTAAGTTTTCAGCCTTGCGACCATAC
TCCCCCGGAACCCAAAACTTTGATTTCTCTCAAGGTGCTGACGGAGTCATGCAAAAAC
GTCCGCAATCCCTAGTCGGCATCGTTTATGGTTGAGACTACGACGGTATCTAATCGTCT
TCGAGCCCCAACTTTCGTTCTTGATTAATGAAAACATCCTTGGCAAATGCTTTCGCAGT
AGTTCGTCTTTCATAAATCCAAGAATTCACCTCTGACAATGAAATACGAATGCCCCGA
CTGTTCTCTTAATCATTACTCCACTCCTACAGGCCAACAGAATAGGGCAGAGTCCTATC
ATGTTATTCCATGCTAAAATGTTACGGCGTAAGCCTGCTTTGAACACTCCAATTTACTC
AAAGTAACCATGCTGAATCCCTGTCCCGGACAATGAAGCCCAGAAGCAGGTCCCCAACAG
TAAGGAAGGCCACAGCAGTACTCACCATAGGCGGACCGCTGAAACCCACCCGAAATCCAA
CTACGAGCTTTTTAACTGCAACAACCTAAATATACGCTATTGGAGCTGGAATTACCGCGG
CTGCTGGCACCAGACTTGCCCTCCAATGGATCCTCGTTAAGGGATTTAGATTGTAATCAT
TCCAATTACCAGACATGAAATGCCCGGTATTGTTATTTATTGCACTACCTCCCCGTATC
AGGATTGGGTAATTTGCGCGCCTGCTGCCTTCCTTGGATGTGGTAGCCGTTTCTCAGGCT
CCCTCTCCGGAATCGAACCCCTATTCTCCGTCACCCGTTACCACCATGGTAGG

Appendix D

Forward ITS2 sequence read of undefined Pond water samples (later defined as *Desmodesmus armatus*) 950 bp

GAGAGTTCATTAAACCCTCCCACCTAGAGGAAGGAGAAGTCGTAACAAGGTTTCCGTAGC
CATGCGGATGTCAGTCTTAAAAGGACTGGCAAGTGGGAACGAATGTATATTCTTTCCTGC
AAGACTGTCAAATTGCCGGAACATCCTGTTAGGCCACTGGTACCGCCCTCTCTAGGAAAC
TAGGTTGTGGCACCGTAGGGAACTTGCGGGTATGGTAAAAATCCAGTGGATAGGGACAA
TCGGCAGCCAAGCCCTAAGGGTAAGCAATTACCTACGGGTGCAGTTCACAGACTAAATGG
CAGTCGGCTGGCCTGACGGCTGGCTTAAGATATAGTCGGGCCCTACCGAGAGGTAGCCTA
TAAGAGGACGGCACTTGTGCTTGAGAGCTTATAGGAGGTTGGGTAATACTTATTGCCGTA
AGGCATTAAGGGCTGCTGAACAGTGGCCTCAAACCTGGAGTAACCGAGGTGAACCTGCGG
AAGGATCATTGAATATGCAAACCACAACACGCACTCTTTTATTTGTGTACCGACGTTAGG
TCATAACCTTAACCCGGTTTGGCCTACTAACCTACACACACCATTGACCAACCATTGATT
AAACCAAACCTCTGAAGTTTCGGCTGCTGTTAATCGGCAGTTTTAACGAAAACAACCTCTCA
ACAACGGATATCTTGCTCTCGCAACGATGAAGAACGCAGCGAAATGCGATACGTAGTGT
GAATTGCAGAATTCCGTGAACCATCGAATCTTTGAACGCATATTGCGCTCGACTCCTCGG
AGAAGAGCATGTCTGCCTCAGCGTCGGTTTACACCCTCACCCCTCTTCTTTTCAAGGAA
GCTTGTCTGCTTGCTCAAGCCGGCATCAGGGGTGGATCTGGCCCTCCCAATCGGATTCA
CTTTCAGTTGGGTTGGCTGAAACACA

Reverse IT2 sequence read of undefined Pond water samples (later defined as *Desmodesmus armatus*) 1058 bp

TAAGCGCGAGCTTACGGGGTTCTCACCCCTCTGACGCCCTTTCCAGGAGACTTTAGCT
CGGCCCGTTGCAGAGGGTACTTCTATAGACTACAATTCTCCAAGGGAGATTTACAAGTTG
GGCTTTGCGCGGTTTCGCTCGCCGTTACTAAGCGCATCCTTGTTAGTTTCTTTTCTCCGC
TTAGTGATATGCTTAAGTTCAGCGGGTAGCCTTGCCTGAGCTCAGGTCTGAATACAGAGAT
ACGCGCCAGAGACGCGTTTCTGCTTGGCTCCTAACCGGTCTCAGACACAACCTTCGTG
TAGGCACCCGAGGGTGTGCTACCTATCCAGTTGAGCCCGAATCGGGTCCCAGTTTAAAGC
CTCTGTGCTTCAGCCAACCCAACCGAAAGTGAATCCGATTGGGAGGGCCAGATCCACCCC
TGATGCCGGCTTGAGCAAGCACGACAAGCTTCTTGAAAAGGAAGAGGGGTGAGGGTGTA
AACCGACGCTGAGGCAGACATGCTCTTCTCCGAGGAGTCGAGCGCAATATGCGTTCAAAG
ATTCGATGGTTCACGGAATTCTGCAATTCACACTACGTATCGCATTTGCTGCGTTCTTC
ATCGTTGCGAGAGCCAAGATATCCGTTGTTGAGAGTTGTTTTCGTTAAAACCTGCCGATTA

ACAGCAGCCGAAACTTCAGAGTTTGGTTTAATCAATGGTTGGTCAATGGTGTGTGTAGGT
TAGTAGGCCAAACCGGGTTAAGGTTATGACCTAACGTCGGTACACAAATAAAAGAGTGCG
TGTTGTGGTTTGCATATTCAATGATCCTTCCGCAGGTTACCTCGGTACTCCAGGTTTG
AGGCCACTGTTTCAGCAGCCCTTAATGCCTTACGGCAATAAGTATTACCCAACCTCCTATA
AGCTCTAAGCACAAGTGCCAGTCCTTATAGGCTACCTCTCGGTAGGGCCCGACTATA
TCTTAAGCCAGCCGTCAGGCCAGCCGACTGCCATTTAGTCTGTGAACTGCACCCGTAGGT
AATTGCTTACCCTTAGGGCT

Appendix E

Forward 5.8S rDNA sequence read of undefined Pond water samples (later defined as *Desmodesmus armatus*) 868 bp

```
GACGCATTTGCCAAGGATGTTTTCATTAATCAAGAACGAAAGTTGGGGGCTCGAAGACGA
TTAGATACCGTCGTAGTCTCAACCATAAACGATGCCGACTAGGGATTGGCGGACGTTTTT
GCATGACTCCGTCAGCACCTTGAGAGAAATCAAAGTTTTTGGGTTCCGGGGGGAGTATGG
TCGCAAGGCTGAAACTTAAAGGAATTGACGGAAGGGCACCACCAGGCGTGGAGCCTGCGG
CTTAATTTGACTCAACACGGGAAAACCTACCAGGTCCAGACATAGGAAGGATTGACAGAT
TGAGAGCTCTTTCTTGATTCTATGGGTGGTGGTGCATGGCCGTTCTTAGTTGGTGGGTTG
TCTTGTCAGGTTGATTCCGGTAACGAACGAGACCTCAGCCTTTAAATAGTCACGGTCGCT
TTTTGCGGTTGGTTTGACTTCTTAGAGGGACAGTTGGCGTTTAGTCAACGGAAGTATGAG
GCAATAACAGGTCTGTGATGCCCTTAGATGTTCTGGGCCGCACGCGCGCTACACTGATGC
ATTCAACAAGCCTATCCCTAGCCGAAAGGCTCGGGTAATCTTTGAAACTGCATCGTGATG
GGGATAGATTATTGCAATTATTAGTCTTCAACGAGGAATGCCTAGTAAGCGCAATTCATC
AGATTGCGTTGATTACGTCCCTGCCCTTTGTACACACCCGCCGTCGCTCCTACCGATTGG
GTGTGCTGGTGAAGTGTTTCGGATTGGCAATTATCGGTGGCAACACTGTCGATTGCCGAGA
AGTTCATTAACCCCTCCCACCTAGAGGAAGGAGAAGTCGTAACAAGGTTTCCGTAGCCAT
GCGGATGCCAGTC
```

Reverse 5.8S rDNA sequence read of undefined Pond water samples (later defined as *Desmodemus armatus*) 990 bp

GCACTGTT CAGCAGCCCTTAATGCCTTACGGCAATAAGTATTACCCAACCTCCTATAAGC
TCTCAAGCACAAAGTGCCGTCCTCTTATAGGCTACCTCTCGGTAGGGCCCGACTATATCTT
AAGCCAGCCGTCAGGCCAGCCGACTGCCATTTAGTCTGTGAACTGCACCCGTAGGTAATT
GCTTACCCTTAGGGCTTGGCTGCCGATTGTCCCTATCCACTGGATTTTTACCATACCCGC
AAGTTTCCCTACGGTGCCACAACCTAGTTTCTAGAGAGGGCGGTACCAGTGGCCTAACA
GGATGTTCCGGCAATTTGACAGTCTTGACAGGAAAGAATATACATTCGTTCCCACTTGCCA
GTCCTTTTAAGACTGACATCCGCATGGCTACGGAAACCTTGTTACGACTTCTCCTTCCTC
TAGGTGGGAGGGTTTAATGAACTTCTCGGCAATCGACAGTGTTGCCACCGATAATTGCCA
ATCCGAACACTTCACCAGCACACCCAATCGGTAGGAGCGACGGGCGGTGTGTACAAAGGG
CAGGGACGTAATCAACGCAATCTGATGAATTGCGCTTACTAGGCATTCTCGTTGAAGAC
TAATAATTGCAATAATCTATCCCCATCACGATGCAGTTTCAAAGATTACCCGAGCCTTTC
GGCTAGGGATAGGCTTGTTGAATGCATCAGTGTAGCGCGCGTGCGGCCCAGAACATCTAA
GGGCATCACAGACCTGTTATTGCCTCATACTTCCGTTGACTAAACGCCAACTGTCCCTCT
AAGAAGTCAAACCAACCGCAAAAAGCGACCGTGACTATTTAAAGGCTGAGGTCTCGTTCCG
TACGGGGAATCAACCTGACAAGACAACCCACCAACTAAGAACGGCCATGCACCACCACCC
ATAGAATCAAGAAAGAGCTCTCAATCTGTCAATCCTTCCTATGTCTGGACCTGGTAAGTT
TTCCCGTGTTGAG